ACTIVATION OF THE SARS-CoV-2 SPIKE PROTEIN BY *CRYPTOCOCCUS NEOFORMANS* SECRETED PROTEASES

---

by

Nozethu Mjokane

Submitted **i**n **a**ccordance **w**ith **t**he **r**equirements **f**or **t**he **d**egree

Doctor of **P**hilosophy

Department of **M**icrobiology and **B**iochemistry

Faculty of **N**atural and **A**gricultural **S**ciences

University of the **F**ree State

Bloemfontein

South Africa

Promotor**: P**rof **O.M. S**ebolai

Co-promotors: **P**rof. **C.H. P**ohl; **P**rof **J. A**lbertyn; **D**r **O.M.N. G**cilitshana

DECLARATION

I, Nozethu Mjokane, declare that this doctoral degree research thesis or publishable, interrelated articles, that I herewith submit for the doctoral degree qualification at the University of the Free State is my independent work and that I have not previously submitted it for a qualification at another institution of higher education.

I, Nozethu Mjokane, hereby declare that I am aware that the copyright is invested in the University of the Free State.

I, Nozethu Mjokane, hereby declare that all royalties as regards intellectual property that was developed during the course of and/or in connection with the study at the University of the Free State will accrue to the University.

I, Nozethu Mjokane, hereby declare that I am aware that this research may only be published with the dean's approval.

_____ **27 November 2023**

Signature **Date**

DEDICATION

This work is dedicated to my family: my mother, Mrs Mjokane; late dad, Mr Mjokane; sisters; nieces and nephews. Thank you!

ACKNOWLEDGEMENTS

In full appreciation, I would like to thank:

- **Prof Sebolai,** for his constant support, guidance, patience, and constructive criticism throughout my PhD study.
- **Prof Pohl,** for tireless support and constant input during my studies.
- **Prof Albertyn** for guidance and valuable input during my studies.
- **Dr Gcilitshana,** for your support and believing in me throughout the study.
- **Prof Sabiu,** for helping me with the computational programme HADDOCK for protein-to-protein interactions.
- **Dr Akintemi,** for helping me with the computational programme HADDOCK for protein-to-protein interactions.
- **Prof Matsabisa,** for the kind donation of the HEK-293T cells.
- **Ms Schoeman,** for helping me with the cultivation and maintenance of HEK-293T cells.
- **Mr Collett**, for his help with capturing and editing the digital images used in this study
- **Dr Ogundeji,** for her kind support throughout this journey.
- **Dr Folorunso,** for valuable input during my studies.
- **Dr Nyaga,** for allowing me to use the facilities for my molecular work in the Next Generation Sequencing Unit, Department of Medical Virology, University of the Free State
- **Dr G. Marais,** for granting me access to his laboratory so I can grow a culture of *Aspergillus fumigatus.*

- **The University of the Free State,** for accepting me as a student and granting me access to central facilities so I could fulfil my dream of obtaining this degree.
- ***Cryptococcus* Laboratory members,** for their unconditional support.
- **Pathogenic Yeast Research Group members,** including the rest of the department, for accepting me and for constant encouragement and support.
- **National Research Foundation,** for financial assistance.
- Outmost gratitude to **my family and friends** for showing so much love and support throughout my journey.

TABLE OF CONTENTS

CHAPTER 1:

LITERATURE REVIEW

CHAPTER 2:

THE DETECTION OF CRYPTOCOCCAL PROTEASES IN THE SUPERNATANT AND EVIDENCE OF THEIR THEORETICAL ACTIVATION OF THE SARS-COV-2 SPIKE PROTEIN

CHAPTER 3:

ENZYMATIC EVIDENCE OF CRYPTOCOCCAL SUPERNATANT PROTEOLYTICALLY ACTIVATING THE SARS-COV-2 SPIKE PROTEIN

CHAPTER 4:

GENERAL DISCUSSION AND CONCLUSIONS

ADDENDUM NO. 1:

***ASPERGILLUS FUMIGATUS* SECRETES A PROTEASE(S) THAT DISPLAYS *IN SILICO* BINDING AFFINITY TOWARDS THE SARS-COV-2 SPIKE PROTEIN AND MEDIATES SARS-COV-2 PSEUDOVIRION ENTRY INTO HEK 293T CELLS**

ADDENDUM NO. 2:

THE USE OF THE SOUTH AFRICAN-BASED MEDICINAL PLANT, *ARTEMISIA AFRA*, IN LIMITING THE ACTIVATION OF THE MIMETIC SARS-COV-2 SPIKE PROTEIN

THESIS SUMMARY

The thesis is not structured in a classical way. As such, it is composed of a literature review section (Chapter 1) and two research chapters (Chapters 2 and 3). A general discussion section (Chapter 4) and addendums are also included. As some chapters are in a publication format, repetition of essential information could not be avoided.

Chapter 1 reviews the emergence of SARS-CoV-2 and its impact. In particular, it considers the co-infection of this virus with respiratory fungal pathogens, which are major independent risk factors that complicate COVID-19 by causing a more severe infection resulting in higher mortality than that of either infection on its own. These fungal pathogens secreted furin-like proteases to further their virulence during host invasion. In this context, the thesis argues that it is foreseeable that the virus could also access these fungal furin-like proteases and pervert them in order to activate its latent spike protein. Therefore, this set up a number of questions, which are addressed in the thesis concerning the possible activation of the viral latent spike protein by fungal furin-like proteases.

In Chapter 2, it was sought to characterise *Cryptococcus* (*C.*) *neoformans* proteases and assess if they could theoretically bind to the SARS-CoV-2 spike protein. To be specific, previous papers reporting on cryptococcal serine proteases were perused, and this made it possible to select a number of proteases, namely cryptococcal serine carboxypeptidase (CNBF4600), cryptococcal cerevisin (CNBJ2870) and cryptococcal peptidase (CNBA1340), cryptococcal peptidase (CNAG_00150) and cryptococcal cerevisin (CNAG_04625). By designing specific primers, it was possible to show that these serine

proteases were expressed in *Cryptococcus neoformans* H99, the prototypical cryptococcal strain used in this thesis. Therefore, the expressed gene products were expected to be secreted into the culture media. This was important for the work that follows in Chapter 3. Through using the computational programme, High Ambiguity Driven protein-protein DOCKing (HADDOCK), it was possible to show that some of the selected cryptococcal serine proteases could interact with the coronavirus spike protein and yield a binding affinity greater than and comparable to furin.

However, as HADDOCK is a computational programme, the predicted binding affinities might not correlate with the experimental binding affinities in solution, more so since the used *Cryptococcus neoformans* proteases structures were predicted and not solved. To account for this, Chapter 3 sought to provide enzymatic evidence using the collected culture media – in the form of supernatant. To do this, a mimetic fluorogenic peptide of the SARS-CoV-2 spike protein was designed and modified to have intra-molecular fluorescence quenching capability using 7-methoxycoumarin-4-yl acetyl (MCA) at the N-terminus and N-2,4-dinitrophenyl (DNP) at the C-terminus. The assay was performed using the cryptococcal supernatant. For reference, recombinant furin was included as this is the serine protease present in humans that catalyses the activation of the spike protein. Here, it was determined that cryptococcal serine proteases present in the supernatant could cleave the mimetic spike protein at S1/S2 site with biochemical efficiency comparable to furin. To test the veracity of these data, SARS-CoV-2 pseudovirion containing a full-length spike protein was used. It was possible to show that the

pseudovirion could be transduced into HEK-293T cells in the presence of the cryptococcal supernatant.

Chapter 4 takes into account the obtained results and provides a summary of the major observations. Of note, the thesis theorises that yeast kexin proteases are responsible for the observed activity. This is because there is a functional homology between yeast kexin proteases and furin (both are convertases); thus, it is reasonable that the supernatant (which contains yeast kexin proteases) could activate the latent SARS-CoV-2 spike protein. The thesis further proves that other respiratory fungal pathogens have yeast kexin proteases that activate the spike protein. This evidence is documented in Addendum no. 1. All things considered, the findings point to the regulation of protease activity as a viable approach to control the activation of the spike protein by either mammalian protease or fungal proteases. To this end, protease inhibitors could be used to control unwanted proteolysis. Addendum no. 2 attempted to show this. Here, it was possible to show that the South African-based medicinal plant *Artemisia* tea infusion extract and its active compound artemisinin could control the activation of the mimetic SARS-CoV-2 spike protein by furin but not the supernatant. The latter highlights the need to purify the supernatant and isolate yeast kexin proteases. The idea of exploring the control of unwanted proteolysis is also an interventional measure considered by Pfizer, the pharmaceutical company. This American multinational pharmaceutical and biotechnology corporation successfully piloted Paxlovid to control SARS-CoV-2. This drug contains an anti-protease (PF-07321332) that inhibits the protease (SARS-CoV-2 3CLp) responsible for viral replication.

CHAPTER 1:

LITERATURE REVIEW

Parts of this chapter have been published.

Publication: Mjokane et al. The possible role of microbial proteases in facilitating SARS-CoV-2 brain invasion. *Biology*, 2021; 10: 966.

Author contribution: Conceptualisation, writing of original draft manuscript, and subsequent review and editing.

1.1 ABSTRACT

SARS-CoV-2 has been shown to display proclivity towards organs bearing angiotensin-converting enzyme (ACE2) expression cells. Of interest herein is the ability of the virus to exhibit neurotropism. However, there is limited information on how this virus invades the brain. This contribution explores how, in the context of a microbial co-infection (using a cryptococcal co-infection as a model), SARS-CoV-2 could reach the brain. It was theorised that the secretion of proteases by disseminated fungal cells might also activate the viral spike glycoprotein for membrane fusion with brain endothelial cells, leading to endocytosis. Understanding this potential invasion mechanism could lead to better SARS-CoV-2 intervention measures, which may also be applicable in instances of co-infection, especially with protease-secreting pathogens.

Keywords: *Cryptococcus*, Co-infection, Neurotropism, Protease, SARS-CoV-2.

1.2 INTRODUCTION

The respiratory failure caused by the novel coronavirus was first reported in December 2019 in Wuhan, China (Zhu et al., 2020). Today, this novel virus has been classified as a severe acute respiratory syndrome coronavirus-2 (SARS-CoV-2; commonly known as COVID-19). The virus targets the human pulmonary system with frequent detection in the nasopharyngeal swab and saliva swab either with antibody-antigen immunoassay or real-time polymerase chain reaction (RT-PCR) diagnosis (Bruce et al., 2020; Iwasaki and Yang, 2020; Procop et al., 2020; Wyllie et al., 2020; Zhen et al., 2020; Lambert-Niclot et al., 2021). When inhaled, the virus could reach the lung space and inflame the alveoli, increasing levels of pro-inflammatory cytokines leading to the infiltration of mononuclear cells (such as lymphocytes, monocytes, and macrophages) and accumulation of fluid in the lungs (Routley, 2021). Further work showed that signalling pathways involving G-protein coupled receptors (GPCR) are usually arrested during pulmonary SARS-CoV-2 infection. This leads to perturbation of epithelial transport processes and homeostasis surface secretion involving cystic fibrosis transmembrane conductance regulator (CFCR) protein kinase A coupled Cl^- channel and epithelial Na^+ channel (Hameid et al., 2021).

This speculates that accumulated fluid from incontinence secretion from pneumocytes may be due to epithelial surfactant degradation and dysfunctional endothelial cells from impaired nitric oxide bioavailability caused by this infection. This consequently results in a pneumonia-like disease with difficulties in gas exchange, making it hard to receive enough oxygen and expel carbon dioxide. The symptoms of pneumonia can range from

mild to severe, including cough, loss of appetite, shortness of breath, fever, and chest pain (Zaki et al., 2012; Chen et al., 2020; Huang et al., 2020). However, severe cases can lead to acute respiratory distress syndrome (ARDS) and, subsequently, multiple organ failure in the lungs, heart, brain, kidney, and others (Chu et al., 2020; Lescure et al., 2020; Macchi et al., 2020; Wang et al., 2020).

SARS-CoV-2 is the current seventh member of the *Coronaviridae* family (genus: *β-coronavirus*), exclusively infecting humans (Zhu et al., 2020), but some wild animals are considered to be the carriers of this virus, especially bats Lau et al. (2020) and Malayan pangolins (Lam et al., 2020; Xiao et al., 2020). Inarguably, SARS-CoV-2 infection is generally acquired from a contaminated environment, and it is rapidly transmitted via person-to-person contact (Chan et al., 2020; Li et al., 2020; Phan et al., 2020; Wang et al., 2020). SARS-CoV-2 is assigned a basic reproduction rate between 2.2–2.5 (Li et al., 2020; Petersen et al., 2020), which means every potential carrier, usually asymptomatic/atypical symptomatic, could have spread the infection to more than two people in their immediate environment. Significantly, SARS-CoV-2 transmission is driven by the family cluster more than the community spread (WHO, 2020).

A large proportion of the mortality comes from patients with underlying diseases. By assessing the risk factors associated with adult COVID-19 patients in various studies, hypertension, diabetes, chronic obstructive pulmonary disease (COPD), cardiovascular or cerebrovascular disease, hepatic dysfunction, obesity, renal failure, and cancer have become the dominant comorbidities with the highest mortality rate (Bhatraju et al., 2020;

COVID-19 Response Team et al., 2020; Ejaz et al., 2020; Guan et al., 2020; Li et al., 2020; Simonnet et al., 2020; Wang et al., 2020; Yang et al., 2020; Zheng et al., 2020). An interesting disease aspect is the manifestation of SARS-CoV-2 pneumonia in the presence of other invasive, pneumonia-causing bacteria and fungi. However, research into the existence of such co-infections lags far behind that of non-infectious diseases (**Table 1.1**). In Jiangsu, China, early assessment of COVID-19 patients for microbial co-infections (i.e., within one to four days of SARS-CoV-2 infection) showed that over 90% of such patients were infected with other respiratory pathogens, more so bacterial pathogens (Zhu et al., 2020). More importantly, the proportion of mixed co-infections was also confirmed to increase with SARS-CoV-2 severity. The above study is critical as it shows how such co-infections may hamper the vaccine response.

Therefore, there is an urgent need to research how SARS-CoV-2 pneumonia differs from other types of pneumonia. Moreover, such studies could potentially assist in understanding how SARS-CoV-2 may disseminate to invade other organ systems. Herein, it is speculated that patients infected with SARS-CoV-2 would also be at a greater risk of co-developing the opportunistic cryptococcal pulmonary infection. More importantly, cryptococcal infection is used as a possible model to explain how SARS-CoV-2 could invade the brain. This organism is endowed with a pool of extracellular hydrolytic proteases that may modulate SARS-CoV-2 proteolytic activation or degrading the cellular gap junction extracellular matrix to promote transcellular migration.

Table 1.1 The disproportionate reports concerning the co-occurrence of SARS-CoV-2 with non-infectious compared with infectious conditions.

The Co-Occurrence of SARS-CoV-2 with Other Infections					
Non-Infectious Conditions			**Aetiological Agents**		
	Scopus	**PubMed**		**Scopus**	**PubMed**
			Meningitis-causing agents		
Cancer	42,719	12,180	*M. tuberculosis*	8440	1206
Diabetes	26,288	6663	*S. pneumoniae*	1065	122
Hypertension	16,623	4393	*P. aeruginosa*	1773	107
Obesity	14,643	2923	*H. capsulatum*	49	8
Cerebrovascular disease	4351	1628	*C. neoformans*	160	11
Asthma	8238	1358	*Mucoralean* spp.	4	26
			Non-meningitis-causing agents		
Renal failure	6098	1656	*A. fumigatus*	435	44
*COPD	4613	779	*Ca. albicans*	840	36
Hepatic dysfunction	1698	1956	*Ca. auris*	187	107

*COPD = Chronic obstructive pulmonary disease. The data was generated by searching Scopus (period: 2020–2021) and Pubmed (period: 2020–2021) using “SARS-CoV-2” and a “specific non-infectious condition” or a “specific aetiological agent”. M. = *Mycobacterium*; S. = *Streptococcus*; P. = *Pseudomonas*; A. = *Aspergillus*; Ca. = *Candida*; C. = *Cryptococcus*; H. = *Histoplasma.*

One such example is the action of cryptococcal serine proteases, metalloproteases and aspartyl peptidases, capable of compromising the cell gap junction and enhancing the intracranial invasion of viral particles. This paper examined the pathogenesis of SARS-CoV-2 and proposed a possible role of *Cryptococcus neoformans* serine proteases, metalloproteases (fungalysin, Mpr1) and aspartyl peptidases (Major aspartyl peptidase 1, May1) in enhancing SARS-CoV-2 brain invasion. We, thus, re-iterated the need to consider the microbial co-infection with SARS-CoV-2 in the management of the COVID-19 pandemic.

1.3 SARS-CoV-2: CURRENT UNDERSTANDING OF ITS POSSIBLE BRAIN INVASION

The route of viral dissemination into the brain region remains an enigma; however, neurological dysfunctions associated with brain and central nervous system (CNS) invasion by SARS-CoV-2 has been emphasised (Hung et al., 2003; Gu et al., 2005; Saad et al., 2014; Helms et al., 2020; Mao et al., 2020; Moriguchi et al., 2020; Zhou et al., 2020). In the earlier report of SARS-CoV-1 brain invasion in human angiotensin-converting enzyme (hACE2) transgenic mice, brain invasion occurred via the olfactory bulb with a rapid infection that spreads transneuronally, resulting in a significant neuropathy in the cardiorespiratory region of the medulla, causing death (Netland et al., 2008). This report demonstrates the significance of angiotensin-converting enzyme-2 (ACE-2) in the neuronal and glial cells viral invasion in the human CNS. For this reason,

it has been speculated that SARS-CoV-2 may invade the human brain parenchyma, causing neuronal dysfunction; however, little is known about how SARS-CoV-2 reaches the brain. The extrapulmonary dissemination of SARS-CoV-2 via the blood and lymphatic vessels is established, and the tendency to invade and infect other organs of the human body is very high. This is because almost all the vital organs of the body possess ACE2-expressing cells, including the vascular endothelial cells and arterial smooth muscle cells (Hamming et al., 2004). A few investigations on the systemic spreading and organ invasion of SARS-CoV-2 have shown that this virus may spread into the brain via hematogenous dissemination, synaptic end junction via a neural pathway, and retrograde/anterograde neurones (Netland et al., 2008; Li et al., 2020; Wu et al., 2020; Zhou et al., 2020). The neuropathic effect of SARS-CoV-2 is caused via the invasion of the meningeal endothelial layer within the blood-brain barrier (BBB), which makes the virus associate with the ACE2 receptor-expressing neuroglial cells in the medulla region of the brain.

As described in **Figure 1.1,** SARS-CoV-2 approaches hACE2 through the S2 domain of the spike glycoprotein. To reveal the fusion peptide, furin targets the amino acid motif P**R**RA**R**^{685}↓ at the interface of the S1/S2 site, including the paired dibasic motif with a single **KR**^{815}↓ motif at the S2 site **(Figure 1.2).** However, the S2 site has an additional furin-like cleavage site that can be processed by other proteases, such as the transmembrane serine protease 2 and cathepsin L (Gioia et al., 2020). The same is true for other human coronavirus spike proteins, SARS-CoV and Middle East respiratory

syndrome coronavirus (MERS-CoV), as they have a similar overall organisation of the spike protein as SARS-CoV-2 as well as furin-like sites.

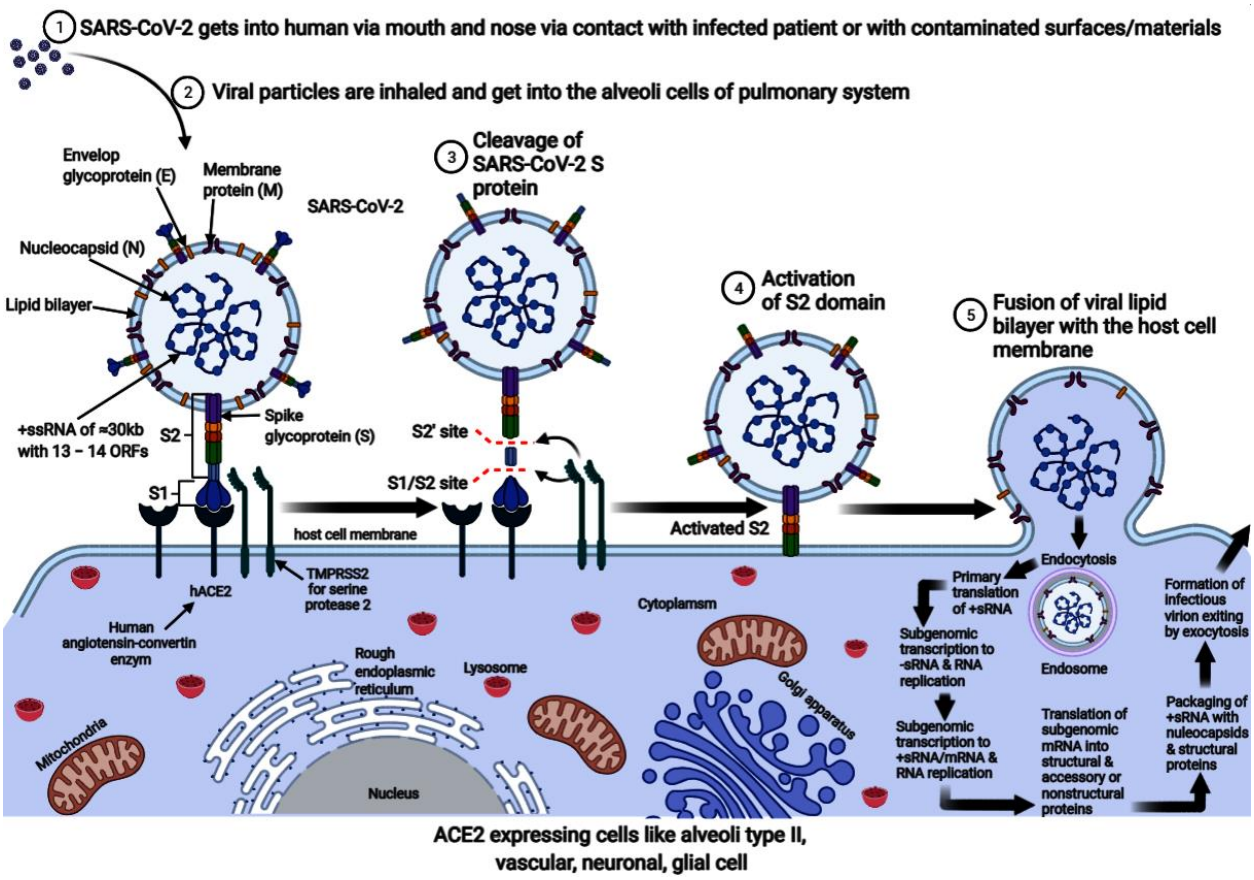

Figure 1.1 Mechanism of SARS-CoV-2 viral entry, endocytosis, translation, replication, viral packaging, and exocytosis in ACE2-expressing cells. A complete infectious SARS-CoV-2 is +ssRNA enclosed nucleocapsid surrounded by a lipid bilayer that harbours envelop glycoprotein, a membrane protein with protruding crownlike spike protein, which binds the membrane-located ACE2 enzyme that facilitates proteolytic cleavage of S-protein on the viral particle (2–3). Activated S-protein induces invagination of the host cell membrane leading to endocytic movement of the viral particle (4–5). The endosome is degraded with the help of lysosomal cathepsin L/B to release the viral genome for primary

translation to produce the RNA-dependent RNA polymerase (RdRp complex). The polymerase transcribes the +sRNA to sub-genomic s–RNA and subsequently full-length +sRNA and some sub-genomic mRNAs that are translated by the host cell ribosomal machinery into nucleocapsid structural and accessory protein. Successful translation, transcription, and RNA replication lead to viral packaging, and the infectious virion can leave the cell by exocytosis to infect the next cell. The image was drawn using BioRender.com.

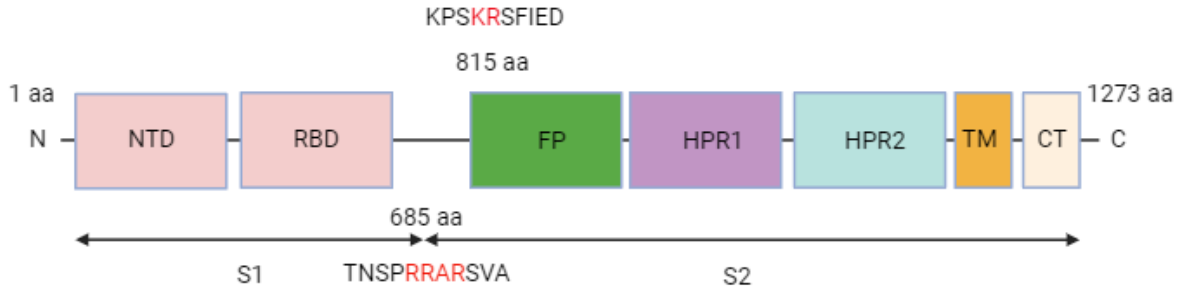

Figure 1.2 The schematic representation of SARS-CoV-2 spike protein. The spike protein has two subunits, namely the S1 and S2. The S1 has the N Terminal Domain (NTD), Receptor Binding Domain (RBD) while the S2 has the Fusion peptide (FP), Heptad repeat 1 (HR1), Heptad repeat 2 (HR2), Transmembrane domain (TM), and Cytoplasmic Tail (CT). The amino acid sequences in red show the multibasic motifs of the preferred consensus sequence for furin and furin-like proteases. The image was drawn using BioRender.com.

After successful activation of the spike protein (as detailed above), it is expected that endocytosis would follow, leading to an infection (Andersen et al., 2020; Hartenian et al., 2020; Wrobel et al., 2020). The resultant infection may lead to an infected individual

experiencing loss of smell and taste, anxiety, dizziness, depression, aggression, confusion, ataxia, seizures, Guillain-Barré syndrome, meningoencephalitis, acute ischemia, haemorrhagic stroke, and respiratory failure (Al Saiegh et al., 2020; Baig et al., 2020; Chen et al., 2020; Chen et al., 2020; Chen et al., 2020; Duong et al., 2020; Eliezer et al., 2020; Li et al., 2020; Oxley et al., 2020; Rogers et al., 2020; Wang et al., 2020; Zhao et al., 2020).

It is also plausible that macrophages could carry the virus across the BBB. Here, the virus could attack the endothelial cells causing the BBB damage via the intracranial cytokine storm/infiltration (Mehta et al., 2020; Poyiadji et al., 2020). The cytokine storm comes from systemic inflammation or direct attack on the T-lymphocytes and macrophages (Grifoni et al., 2020; Zhang et al., 2020). The subgroups of macrophages express ACE2, such as the cluster of differentiation 68 ($CD68^{+}$) and $CD169^{+}$, which may act as Trojan horses carrying the viral particles across the BBB via transcytosis. This event has been linked to the viral spread, tissue inflammation, and lymphopenia experienced during COVID-19 infection (Park, 2020). The evidence of the virus in the cerebrospinal fluid (CSF) and the brain region showed that viral invasion is possible; therefore, inter-synaptic CNS viral invasion cannot be ruled out.

1.4 POSSIBLE ROLE OF CRYPTOCOCCAL PROTEASES IN PROMOTING VIRAL INVASION ON THE CONTEXT OF CO-INFECTION WITH SARS-CoV-2

Proteases perform multiple roles in the normal immune response to tissue injury or microbial colonisation. For example, host-derived proteases assist in the recruitment of immune cells to infection sites by deteriorating the basement of membranes (Table 1.2) (Elkington et al., 2005). In the priming event of membrane-bound viral glycoproteins, e.g., influenza A haemagglutinin, HIV-1 glycoprotein-160, measles virus F0, Newcastle disease virus F0, among others, posttranslational proteolytic cleavage has been shown to be a fundamental biochemical process essential for syncytium generation, (Rajah et al., 2022). Several mammalian proteases have emerged as important for activating these latent precursors into biologically active products (Bassi et al., 2000). For example, the subtilisin-like endopeptidase furin, which is also a member of the S8 family (Dufour et al., 1998; Gitlin-Domagalska et al., 2023). This protease is enriched in the *trans*-Golgi network and cycles to the cell surface (Mayer et al., 2004; Schapiro et al., 2004). Furin is said to process precursors with the canonical basic amino acid target sequence **R**-X-**R** or **R**-X-**K**↓, where X can be any amino acid residue (Papa et al., 2021). In the case of SARS-CoV-2, the spike protein is also a suitable precursor that is processed by furin.

Furin, the prototypical mammalian serine endopeptidase critical for SARS-CoV-2 activation, belongs to the evolutionary ancient family of proprotein convertases (Parvaz, and Jalali, 2021). The yeast kexin protease (Kex2p), first identified by Fuller and co-workers, belongs to the same family and is the fungal homologue of furin (Fuller et al.,

1990). These two convertases (furin and yeast kexin protease) were shown to share 50% gene sequence similarity Fuller et al. (1989); Tanaka, (2003) that translates into significant functional homology (Bresnahan et al., 1990). The latter is reflected in the ability of the yeast kexin protease to recognise the same furin cleavage sites, i.e., the multibasic motifs of the preferred consensus sequence **R**-X-**R** or **R**-X-**K**↓. Therefore, by implication, it is reasonable to foresee fungal kexin proteases processing mammalian and viral substrates that are typically cleaved by mammalian furin. To illustrate this, Bresnahan and co-workers showed that yeast kexin could process a precursor of the mouse nerve growth factor into a competent protein that is documented to regulate sensory neuron growth and development (Bresnahan et al., 1990; Seidah et al., 1996). Foster and co-workers reported that the Kex2p could process the human protein C precursor into a mature protein C that regulates anticoagulation and inflammation, among others (Foster et al., 1991). Concerning viral precursors, Moulard and co-workers reported that Kex2p could cleave both the HIV-1 envelope glycoprotein (gp) precursor and a synthetic peptide mimicking the cleavage site of HIV-1 gp160 at the dibasic site (Moulard et al., 1994). This led these authors to conclude that there is a functional analogy between yeast Kex2p and the cellular protease responsible for the maturation of HIV-1 envelope glycoproteins in infected human cells. In another study, Mjokane et al. showed that an uncharacterised *Cryptococcus neoformans* furin-like protease present in the culture media could process a mimetic S1/S2 site of a SARS-CoV-2 spike protein with the motif P**R**RA**R**^{685}↓ with the biochemical efficiency that was comparable to furin (Mjokane et al., 2022). Taken together, these reports highlight that during fungi-viral co-

infections, viruses would have access to a broad pool of mammalian and microbial furin-like proteases that could be exploited to ensure their host invasion.

In fungi, the yeast kexin proteases are essential for cellular growth and development, including virulence. For example, in *Saccharomyces cerevisiae*, the *KEX-2* gene product processes the precursor of killer toxins (Bader et al., 2008). This toxin kills cells of the same or related species, thus helping the organism to appropriate environmental advantage over susceptible cells. Furthermore, this subtilisin-like serine protease can process alpha-factor pheromone substrates, which is crucial for initiating fungal mating (Naider and Becker, 2004). In *Cryptococcus neoformans*, a subtilisin-like serine protease that belongs to the kexin family is also reported to be involved in melanin production, although the exact mechanism is unknown (Clarke et al., 2016; Gutierrez-Gongora and Geddes-McAlister, 2022). In *Aspergillus fumigatus*, the disruption of the kexin protease gene results in retarded growth, reduced conidia, and defects in cell wall integrity (Wang et al., 2005).

Table 1.2 Properties of some proteases of interest that may facilitate SARS-CoV-2 brain invasion.

Sequence	Type	Source	MW (kDa)	pH	Catalytic Residue	Zinc Chelating	Traditional Function	Purported Function in the Context of SARS-CoV-2 Infection	References
1	Furin (serine-based)	*Homo sapiens* (Human)	104	5–8	Asp, His, Ser	No (calcium-chelating)	Activates functionally important protein precursors	Activates the viral S protein for membrane fusion into cells	(Creemers et al., 1993; Cieplik and Klenk, 1998; Solovyeva et al., 2016)

Table 1.2 (continued). Properties of some proteases of interest that may facilitate SARS-CoV-2 brain invasion.

Sequence	Type	Source	MW (kDa)	pH	Catalytic Residue	Zinc Chelating	Traditional Function	Purported Function in the Context of SARS-CoV-2 Infection	References
2	Serine-based protease (uncharacterised)	*Cryptococcus neoformans*	75	7.2	Ser	No	Promotes fungal brain invasion	May activate the viral S protein or promote viral transcellular migration	(Strickland and Shi, 2021; Rodrigues et al., 2003; Vu et al., 2014)

Table 1.2 (continued). Properties of some proteases of interest that may facilitate SARS-CoV-2 brain invasion.

Sequence	Type	Source	MW (kDa)	pH	Catalytic Residue	Traditional Function	Purported Function in the Context of SARS-CoV-2 Infection	References
3	Serine carboxypeptidase (CNBF4600) (serine-based)	*Cryptococcus neoformans*	Uncharacterised	Uncharacterised	Asp, His, Ser	Promote tissue invasion by cleaving basement membrane component	Activates the viral S protein for membrane fusion into cells	(Eigenheer et al., 2007)

Table 1.2 (continued). Properties of some proteases of interest that may facilitate SARS-CoV-2 brain invasion.

Sequence	Type	Source	MW (kDa)	pH	Catalytic Residue	Traditional Function	Purported Function in the Context of SARS-CoV-2 Infection	References
4	Peptidase (CNBA1340) (serine-based)	*Cryptococcus neoformans*	Uncharacterised	Uncharacterised	Asp, His, Ser	Promote tissue invasion by cleaving basement membrane component	Activates the viral S protein for membrane fusion into cells	(Eigenheer et al., 2007)

Table 1.2 (continued). Properties of some proteases of interest that may facilitate SARS-CoV-2 brain invasion.

Sequence	Type	Source	MW (kDa)	pH	Catalytic Residue	Traditional Function	Purported Function in the Context of SARS-CoV-2 Infection	References
5	Peptidase (CNAG_00150) (serine-based)	*Cryptococcus neoformans*	100.9	Uncharacterised	Asp, His, Ser	Quorum sensing	Activates the viral S protein for membrane fusion into cells	(Gutierrez-Gongora & Geddes-McAlister, 2022)

Table 1.2 (continued). Properties of some proteases of interest that may facilitate SARS-CoV-2 brain invasion.

Sequence	Type	Source	MW (kDa)	pH	Catalytic Residue	Traditional Function	Purported Function in the Context of SARS-CoV-2 Infection	References
6	Cerevisin (CNAG_04625) (serine-based)	*Cryptococcus neoformans*	53.6	Uncharacterised	Asp, His, Ser	Melanin synthesis	Activates the viral S protein for membrane fusion into cells	(Gutierrez-Gongora & Geddes-McAlister, 2022)

Table 1.2 (continued). Properties of some proteases of interest that may facilitate SARS-CoV-2 brain invasion.

Sequence	Type	Source	MW (kDa)	pH	Catalytic Residue	Traditional Function	Purported Function in the Context of SARS-CoV-2 Infection	References
7	Cerevisin (CNBJ2870) (serine-based)	*Cryptococcus neoformans*	Uncharacterised	Uncharacterised	Asp, His, Ser	Promote tissue invasion by cleaving basement membrane component	Activates the viral S protein for membrane fusion into cells	(Eigenheer et al., 2007)

Like other enzymes in living systems, the action of proteases is also tightly controlled by inhibitors, which can arrest their catalytic activity. Animal (vertebrate) protease inhibitors are localised in tissues as secretory proteins that block the activity of endogenous and exogenous proteases to prevent unwanted proteolysis (Marathe et al., 2019). Commercial sources of serine-based protease inhibitors, some of which are biologically extracted and purified, showing specificity towards mammalian serine proteases, may be useful in this regard. In addition to this, the papain-like cysteine protease inhibitors such as leupeptin, E64, E64d, E64c, and cystatin can modify the thiol group at the active site of this enzyme to block its activity. The potencies of these protease inhibitors have been demonstrated to reduce viral antigen titre by targeting cathepsin L (CatL) (Chandran et al., 2005; Barrientos and Rollin, 2007). A vast majority of these inhibitors against the serine, threonine, and cysteine-protease activities and their biological applications have been well documented (Otto and Schirmeister, 1997; Powers et al., 2002).

Concerning SARS-CoV-2, there is evidence that shows that specific protease inhibitors could block the viral cellular entry. In a cell model viral entry system, a commercially available serine protease inhibitor, camostat mesylate, partially blocked the SARS-CoV viral entry (Kawase et al., 2012; Hoffmann et al., 2020). However, total inhibition of entry was observed when combined with cathepsin B/H/L cysteine inhibitor, E-64d (known under different names such as aloxistatin/loxistatin/(2S,3S)-trans-Epoxysuccinyl-L-leucylamido-3-methylbutane ethyl ester/(1S,2S)-2-(((S)-1-((4-Guanidinobutyl)amino)-4-methyl-1-oxopentan-2-yl)carbamoyl) cyclopropanecarboxylic acid) (Djomkam et al., 2020; Hoffmann et al., 2020).

This E64d is the ethyl ester derivate of E64c, which has gained a lot of attention as a therapeutic agent both in animal and human studies to correct physiological dysfunction, regulated enzyme formation and prevent viral activation (Kim et al., 1995; Powers et al., 2002). To show the diversity of protease inhibitors, caspases are cysteine-aspartyl-dependent proteases whose activity are not inhibited by the epoxysuccinate derivates of E64. However, this enzyme, together with other cysteine proteases such as papain, calpains, caspases, cathepsin B, H, and L, is inhibited by peptidylchloromethylketones – except cathepsin G, which is slowly inhibited (Powers et al., 2002). As much as protease inhibitors hold promising therapeutic effects, thorough care should be put in place to weigh the physiological and disease-preventing effects of these inhibitors when applied clinically. For example, the E64 family of derivatives are potent inhibitors of cysteine proteases (cathepsin B, H, L, and calpain), reducing muscular dystrophy, improving locomotor activity, protecting proteoglycan degradation, preventing lesion and apoptosis, attenuating parathyroid hormonal effect on calpain, preventing viral replication and coronavirus protein processing and other biological effects; however, it is associated with hepatic injury, teratogenesis, and attenuated myofibril assembly (Powers et al., 2002). The use of protease inhibitors in the treatment of other viral pathogens, such as HIV and hepatitis C, is already established. Unfortunately, treatment can also induce metabolic syndromes such as dyslipidemia (Lv et al., 2015). At the moment, Pfizer is exploring the use of a protease inhibitor viz. SARS-CoV-2-3CL, to inhibit viral entry (Marzi et al., 2022). The drug is reported to have potent in vitro anti-viral activity against SARS-CoV-2 (Pfizer Inc.). It will be interesting to observe if the therapeutic benefits of this drug will outweigh its side-effects.

1.5 CONCLUSIONS

Understanding how the spike protein is primed is fundamental to understanding viral pathogenesis. We speculate that the regulation of protease levels via inhibiting the growth of protease-secreting microbes (this may affect both the resident and invading microbes) may contribute to the impairment of host invasion by SARS-CoV-2. Therefore, there is a need to accurately diagnose and resolve underlying microbial infections, which may exogenously avail proteases within an afflicted host – and unintentionally promote SARS-CoV-2 invasion. The latter is also applicable to all infectious members of the *β-coronavirus* genus that could cause pathological conditions in people with underlying microbial infections.

1.6 PURPOSE OF STUDY

The emergence of the novel SARS-CoV-2 in 2019 threatened the world with its rapid spreading and how the ancestral Wuhan strain was extremely potent. As a result, this infectious agent has attracted significant research targeted at vaccine and drug development to attenuate the disease COVID-19. However, to compound matters, pneumonia-causing fungi have been shown to, unfortunately, complicate COVID-19. The presented literature herein infers that during SARS-CoV-2 and pneumonia-causing fungi co-infection, fungal furin-like proteases could activate the SARS-CoV-2 viral glycoprotein.

This may be true as fungal furin-like proteases share some level of amino acid homology with the host furin proteases.

Therefore, this work aims to shed more light on the SARS-CoV-2-*Cryptococcus neoformans* interactions by focusing on a critical disease aspect related to the activation of SARS-CoV-2 spike protein by proteases secreted by *Cryptococcus neoformans*. To address this disease aspect, several research objectives were set out. These included:

1. To conduct a scan of the literature to identify serine proteases secreted by *Cryptococcus neoformans.*
2. To assess if *Cryptococcus neoformans* H99 can express the selected serine proteases through using qPCR.
3. To determine if the *Cryptococcus neoformans* H99 culture (in the form of supernatant) has proteolytic activity using a Pierce colorimetric protease assay kit.
4. To conduct an *in-silico* study using the HADDOCK server to determine if the selected cryptococcal proteases can bind to the coronavirus spike protein.
5. To determine if the cryptococcal supernatant proteolytic activity is sufficient to process a memetic peptide based on the SARS-CoV-2 spike protein as well as SARS-CoV-2 pseudovirions that contain the full-length spike protein.

It is envisaged that the successful execution of these objectives could yield insight into SARS-CoV-2 activation, entry into a host cell and how entry could potentially be controlled.

1.7 REFERENCES

1. Andersen, K. G., Rambaut, A., Lipkin, W. I., Holmes, E. C. and Garry, R. F. (2020). The proximal origin of SARS-CoV-2. *Nat Med.* 26, 450–452. DOI:10.1038/s41591-020-0820-9
2. Bader, O., Krauke, Y. and Hube, B (2008). Processing of predicted substrates of fungal Kex2 proteinases from *Candida albicans*, *C. glabrata, Saccharomyces cerevisiae* and *Pichia pastoris. BMC Microbiol.* 8, 116. DOI:10.1186/1471-2180-8-116
3. Baig, A. M., Khaleeq, A., Ali, U. and Syeda, H. (2020). Evidence of the COVID-19 virus targeting the CNS: tissue distribution, host–virus interaction, and proposed neurotropic mechanisms. *ACS Chem Neurosci.* 11, 995–998. DOI:10.1021/acschemneuro.0c00122
4. Barrientos, L. G. and Rollin, P. E. (2007). Release of cellular proteases into the acidic extracellular milieu exacerbates Ebola virus-induced cell damage. *Virol.* 358, 1–9. DOI: 10.1016/j.virol.2006.08.018
5. Bassi, D. E., Mahloogi, H. and Klein-Szanto, A. J. (2000). The proprotein convertases furin and PACE4 play a significant role in tumor progression. *Mol Carcinog.* 28, 63-69. DOI:10.1002/1098-2744(200006)28:2<3C63::AID-MC1>3E3.0.CO;2-C

6. Bhatraju, P. K., Ghassemieh, B. J., Nichols, M., Kim, R., Jerome, K. R., Nalla, A. K., Greninger, A. L., Pipavath, S., Wurfel, M. M., Evans, L., Kritek, P. A., West, T. E., Luks A., Gerbino A., Dale C. R., Goldman J. D., O'Mahony S. and Mikacenic C. (2020). Covid-19 in critically ill patients in the Seattle region—Case series. *N Engl J Med*. 382, 2012–2022. DOI:10.1056/nejmoa2004500

7. Bobofchak K. M., Pineda A. O., Mathews F. S. and Di Cera E. (2005). Energetic and structural consequences of perturbing Gly-193 in the oxyanion hole of serine proteases. *J Biol Chem.* 280, 25644–25650. DOI:10.1074/jbc.m503499200

8. Bresnahan, P. A., Leduc, R., Thomas, L., Thorner, J., Gibson, H. L., Brake, A. J., Barr, P. J. and Thomas, G. (1990). Human fur gene encodes a yeast KEX2-like endoprotease that cleaves pro-beta-NGF *in vivo. J Cell Biol*. 111, 2851-9. DOI:10.1083/jcb.111.6.2851

9. Bruce, E. A., Huang, M. L., Perchetti, G. A., Tighe, S., Laaguiby, P., Hoffman, J. J., Gerrard, D. L., Nalla, A. K., Wei, Y., Greninger, A. L., Diehl, S. A., Shirley, D. J., Leonard, D. G. B., Huston, C. D., Kirkpatrick, B. D., Dragon, J. A., Crothers, J. W., Jerome, K. R. and Botten, J. W. (2020). Direct RT-qPCR detection of SARS-CoV-2 RNA from patient nasopharyngeal swabs without an RNA extraction step. *PLoS Biol*. 18, e3000896. DOI: 10.1371/journal.pbio.3000896

10. Chan, J. F., Kok, K. H., Zhu, Z., Chu, H., To, K. K., Yuan, S., Yuen, K. Y. (2020). Genomic characterisation of the 2019 novel human pathogenic coronavirus isolated from a patient with atypical pneumonia after visiting Wuhan. *Emerg Microbes Infect.* 9, 221–236. DOI:10.1080/22221751.2020.1719902

11. Chandran, K., Sullivan, N. J., Felbor, U., Whelan, S. P. and Cunningham, J. M. (2005). Endosomal proteolysis of the Ebola virus glycoprotein is necessary for infection. *Science.* 308, 1643–1645. DOI:10.1126/science.1110656

12. Chen, J., Qi, T., Liu, L., Ling, Y., Qian, Z., Li, T., Li, F., Xu, Q., Zhang, Y., Xu, S., Song, Z., Zeng, Y., Shen, Y., Shi, Y., Zhu, T., and Lu, H. (2020). Clinical progression of patients with COVID-19 in Shanghai, China*. J Infect*. 80, e1–e6. DOI: 10.1016/j.jinf.2020.03.004

13. Chen, T., Wu, D., Chen, H., Yan, W., Yang, D., Chen, G., Ma, K., Xu, D., Yu, H., Wang, H., Wang, T., Guo, W., Chen, J., Ding, C., Zhang, X., Huang, J., Han, M., Li, S., Luo, X. and Zhao, J. (2020). Clinical characteristics of 113 deceased patients with coronavirus disease 2019: retrospective study. *BMJ*. 368, 1-12. DOI:10.1136/bmj.m1091

14. Chen, N., Zhou, M., Dong, X., Qu, J., Gong, F., Han, Y., Qiu, Y., Wang, J., Liu, Y., Wei, Y., Xia, J., Yu, T., Zhang, X. and Zhang, L. (2020). Epidemiological and clinical characteristics of 99 cases of 2019 novel coronavirus pneumonia in Wuhan, China: A descriptive study. *Lancet.* 395, 507–513. DOI:10.1016/s0140-6736(20)30211-7

15. Chu, D. K. W., Pan, Y., Cheng, S. M. S., Hui, K. P. Y., Krishnan, P., Liu, Y., Ng, D. Y. M., Wan, C. K. C., Yang, P., Wang, Q., Peiris, M. and Poon, L. L. M. (2020). Molecular diagnosis of a novel coronavirus (2019-nCoV) causing an outbreak of pneumonia. *Clin Chem.* 66, 549–555. DOI:10.1093/clinchem/hvaa029

16. Clarke, S. C., Dumesic, P. A., Homer, C. M., O'Donoghue, A. J., La Greca, F., Pallova, L., Majer, P., Madhani, H. D. and Craik, C. S. (2016). Integrated activity and genetic profiling of secreted peptidases in *Cryptococcus neoformans* reveals an aspartyl peptidase required for low pH survival and virulence. *PLoS pathog*. 12, e1006051. DOI: 10.1371/journal.ppat.1006051

17. COVID, C., Team, R., Chow, N., Fleming-Dutra, K., Gierke, R., Hall, A. and Ussery, E. (2020). Preliminary estimates of the prevalence of selected underlying health conditions among patients with coronavirus disease 2019—United States, February 12–March 28, 2020. *MMWR Morb Mortal Wkly Rep.* 69, 382–386. DOI:10.15585/mmwr.mm6913e2

18. Creemers, J. W. M., Siezen, R. J., Roebroek, A. J. M., Ayoubi, T. A. Y., Huylebroeck, D. and Van de Ven, W. J. M. (1993). Modulation of furin mediated proprotein processing activity by site-directed mutagenesis. *J Biol Chem.* 268, 21826–21834. DOI:10.1016/S0021-9258(20)80616-4

19. Cieplik, M. and Klenk, H. W. G. (1998). Identification and characterisation of *Spodoptera frugiperda* furin: A thermostable subtilisin-like endopeptidase. *Biol Chem.* 379, 1433–1440. DOI:10.1515/bchm.1998.379.12.1433

20. Di Cera, E. (2009). Serine proteases. *IUBMB Life.* 61, 510-515. DOI:10.1002/2iub.186

21. Djomkam, A. L. Z., Olwal, C. O., Sala, T. B. and Paemka, L. (2020). Commentary: SARS-CoV-2 cell entry depends on ACE2 and TMPRSS2 and is blocked by a clinically proven protease inhibitor. *Front Oncol*. 10, e1448. DOI:10.3389/fonc.2020.01448

22. Dufour, E. K., Denault, J. B., Hopkins, P. C. and Leduc, R. (1998). Serpin-like properties of α1-antitrypsin Portland towards furin convertase. *FEBS Lett.* 426, 41-46. DOI:10.1016/s0014-5793(98)00307-x

23. Duong, L., Xu, P., Liu, A. (2020). Meningoencephalitis without respiratory failure in a young female patient with COVID-19 infection in downtown Los Angeles, early April 2020. *Brain Behav Immun*. 87, 1–33. DOI: 10.1016%2Fj.bbi.2020.04.024

24. Eigenheer, R. A., Lee, Y. J., Blumwald, E., Phinney, B. S. and Gelli, A. (2007). Extracellular glycosylphosphatidylinositol-anchored mannoproteins and proteases of *Cryptococcus neoformans. FEMS Yeast Res.* 7, 499-510. DOI:10.1111/j.1567-1364.2006. 00198.x

25. Eliezer, M., Hautefort, C., Hamel, A.-L., Verillaud, B., Herman, P., Houdart, E. and Eloit, C. (2020). Sudden and complete olfactory loss of function as a possible symptom of COVID-19. *JAMA Otolaryngol Neck Surg*. 146, 674–675. DOI:10.1001/jamaoto.2020.0832

26. Ejaz, H., Alsrhani, A., Zafar, A., Javed, H., Junaid, K., Abdalla, A. E., Abosalif, K. O. A., Ahmed, Z. and Younas, S. (2020). COVID-19 and comorbidities: Deleterious impact on infected patients. *J. Infect Public Health.* 13, 1833–1839. DOI: 10.1016/j.jiph.2020.07.014

27. Elkington, P. T. G., O'kane, C.M. and Friedland, J. S. (2005). The paradox of matrix metalloproteinases in infectious disease. *Clin Exp Immunol*. 142, 12–20. DOI:10.1111/j.1365-2249.2005. 02840.x

28. Foster, D. C., Holly, R. D., Sprecher, C. A., Walker, K. M. and Kumar, A. (1991). Endoproteolytic processing of the human protein C precursor by the yeast Kex2 endopeptidase coexpressed in mammalian cells. *Biochemistry.* 30, 367–372. DOI:10.1021/bi00216a009

29. Fuller, R. S., Brake, A. J. and Thorner, J. (1989). Intracellular targeting and structural conservation of a prohormone-processing endoprotease. *Science.* 246, 482-486.DOI:10.1126/science.2683070

30. Gioia, M., Ciaccio, C., Calligari, P., De Simone, G., Sbardella, D., Tundo, G., Fasciglione, G. F., Di Masi, A., Di Pierro, D., Bocedi, A., Ascenzi, P. and Coletta, M. (2020). Role of proteolytic enzymes in the COVID-19 infection and promising therapeutic approaches. *Biochem Pharmacol*. 182, 114225. DOI: 10.1016/j.bcp.2020.114225

31. Gitlin-Domagalska, A., Dębowski, D., Maciejewska, A., Samsonov, S., Maszota-Zieleniak, M., Ptaszynska, N., Łęgowska, A. and Rolka, K. (2023). Cyclic peptidic furin inhibitors developed by combinatorial chemistry. *ACS Med Chem Lett*. 14, 458-465. DOI:10.1021/acsmedchemlett.3c00008

32. Grifoni, A., Weiskopf, D., Ramirez, S. I., Mateus, J., Dan, J. M., Moderbacher, C. R., Rawlings, S. A., Sutherland, A., Premkumar, L. and Jadi, R. S. (2020). Targets of T cell responses to SARS-CoV-2 coronavirus in humans with COVID-19 disease and unexposed individuals. *Cell.* 181, 1489–1501. DOI: 10.1016/j.cell.2020.05.015

33. Gu, J., Gong, E., Zhang, B., Zheng, J., Gao, Z., Zhong, Y., Zou, W., Zhan, J., Wang, S., Xie, Z., et al. (2005). Multiple organ infection and the pathogenesis of SARS. *J Exp Med.* 202, 415–424. DOI:10.1084%2Fjem.20050828

34. Guan, W.-J., Ni, Z.-Y., Hu, Y., Liang, W.-H., Ou, C.-Q., He, J.-X., Liu, L., Shan, H., Lei, C.-L., Hui, D.S., et al. (2020). Clinical characteristics of coronavirus disease 2019 in China. *N Engl J Med.* 382, 1708–1720. DOI:10.1056/nejmoa2002032

35. Gutierrez-Gongora, D. and Geddes-McAlister, J. (2022). Peptidases: promising antifungal targets of the human fungal pathogen, *Cryptococcus neoformans*. *FACETS.* 7, 319-342. DOI:10.1139/facets-2021-0157

36. Hameid, R. A., Cormet-Boyaka, E., Kuebler, W. M., Uddin, M. and Berdiev, B. K. (2021). SARS-CoV-2 may hijack GPCR signaling pathways to dysregulate lung ion and fluid transport. *Am J Physiol Lung Cell Mol Physiol*. 320, L430–L435. DOI:10.1152/ajplung.00499.2020

37. Hamming, I., Timens, W., Bulthuis, M. L. C., Lely, A. T., Navis, G. J., van Goor, H. (2004). Tissue distribution of ACE2 protein, the functional receptor for SARS coronavirus. A first step in understanding SARS pathogenesis. *J Pathol.* 203, 631–637. DOI:10.1002/path.1570

38. Hartenian, E., Nandakumar, D., Lari, A., Ly, M., Tucker, J. M. and Glaunsinger, B. A. (2020). The molecular virology of coronaviruses. *J Biol Chem.* 295, 12910–12934. DOI:10.1074%2Fjbc.REV120.013930

39. Hedstrom, L. (2002). Serine protease mechanism and specificity. *Chem Rev.* 102, 4501-4524. DOI:10.1021/cr000033x

40. Helms, J., Kremer, S., Merdji, H., Clere-Jehl, R., Schenck, M., Kummerlen, C., Collange, O., Boulay, C., Fafi-Kremer, S., Ohana, M., Anheim, M.and Meziani, F. (2020). Neurologic features in severe SARS-CoV-2 infection. *N Engl J Med.* 382, 2268–2270. DOI:10.1056/nejmc2008597

41. Hoffmann, M., Kleine-Weber, H., Schroeder, S., Krüger, N., Herrler, T., Erichsen, S., Erichsen, S., Schiergens, T. S., Herrler, G. and Wu, N. H. l. (2020). SARS-CoV-2 cell entry depends on ACE2 and TMPRSS2 and is blocked by a clinically proven protease inhibitor. *Cell.* 181, 271–280.e8. DOI: 10.1016/j.cell.2020.02.052

42. Huang, A., Lu, M., Ling, E., Li, P. and Wang, C. (2020). A M35 family metalloprotease is required for fungal virulence against insects by inactivating host prophenoloxidases and beyond. *Virulence*. 11, 222–237. DOI:10.1080%2F21505594.2020.1731126

43. Hung, E. C. W., Chim, S. S. C., Chan, P. K. S., Tong, Y. K., Ng, E. K. O., Chiu, R. W. K., Leung, C. B., Sung, J. J. Y., Tam, J. S. and Lo, Y. M. D. (2003). Detection of SARS coronavirus RNA in the cerebrospinal fluid of a patient with severe acute respiratory syndrome. *Clin Chem.* 49, 2108–2109. DOI:10.1373/clinchem.2003.025437

44. Iwasaki, A. and Yang, Y. (2020). The potential danger of suboptimal antibody responses in COVID-19. *Nat Rev Immunol*. 20, 339–341. DOI:10.1038/s41577-020-0321-6

45. Kawase, M., Shirato, K., van der Hoek, L., Taguchi, F. and Matsuyama, S. (2012). Simultaneous treatment of human bronchial epithelial cells with serine and cysteine protease inhibitors prevents severe acute respiratory syndrome coronavirus entry. *J Virol.* 86, 6537–6545. DOI:10.1128/jvi.00094-12

46. Kim, J. C., Spence, R. A., Currier, P. F., Lu, X. and Denison, M. R. (1995). Coronavirus protein processing and RNA synthesis is inhibited by the cysteine proteinase inhibitor E64d. *Virology*. 208, 1–8. DOI:10.1006/viro.1995.1123

47. Lam, T. T. Y., Jia, N., Zhang, Y. W., Shum, M. H. H., Jiang, J. F., Zhu, H. C., Tong, Y. G., Shi, Y. X., Ni, X. B., Liao, Y. S., et al. (2020). Identifying SARS-CoV-2-related coronaviruses in Malayan pangolins. *Nature*. 583, 282–285. DOI:10.1038/s41586-020-2169-0

48. Lambert-Niclot, S., Cuffel, A., Le Pape, S., Vauloup-Fellous, C., Morand-Joubert, L., Roque-Afonso, A. M., Le Goff, J. and Delaugerre, C. (2021). Evaluation of a rapid diagnostic assay for detection of SARS-CoV-2 antigen in nasopharyngeal swabs. *J Clin Microbiol*. 58, 1814–1820. DOI:10.1128/jcm.00977-20

49. Lau, S. K. P., Luk, H. K. H., Wong, A. C. P., Li, K. S. M., Zhu, L., He, Z., Fung, J., Chan, T. T. Y., Fung, K. S. C. and Woo, P. C. Y. (2020). Possible bat origin of severe acute respiratory syndrome coronavirus 2. *Emerg Infect Dis.* 26, 1542–1547. DOI:10.3201/eid2607.200092

50. Lescure, F. X., Bouadma, L., Nguyen, D., Parisey, M., Wicky, P. H., Behillil, S., Gaymard, A., Bouscambert-Duchamp, M., Donati, F., Le, H. Q., et al. (2020). Clinical and virological data of the first cases of COVID-19 in Europe: A case series. *Lancet Infect Dis.* 20, 697–706. DOI:10.1016/s1473-3099(20)30200-0

51. Li, Q., Guan, X., Wu, P., Wang, X., Zhou, L., Tong, Y., Ren, R., Leung, K. S. M., Lau, E. H. Y., Wong, J. Y. et al. (2020). Early Transmission Dynamics in Wuhan, China, of Novel Coronavirus–Infected Pneumonia. *N Engl J Med.* 382, 1199–1207. DOI:10.1056/nejmoa2001316

52. Li, Y., Bai, W., Hashikawa, T. (2020). The neuroinvasive potential of SARS-CoV2 may play a role in the respiratory failure of COVID-19 patients. *J Med Virol.* 92, 552–555. DOI:10.1002/jmv.25728

53. Li, Z., Wu, M., Yao, J., Guo, J., Liao, X., Song, S., Li, J., Duan, G., Zhou, Y., Wu, X., Zhou, Z., Wang, T., Hu, M., Chen, X., Fu, Y., Lei, C., et al. (2020). Caution on kidney dysfunctions of COVID-19 patients. *Int J Mol Sci*. 1–25. DOI:10.1101/2020.02.08.20021212

54. Lv, Z., Chu, Y. and Wang, Y. (2015). HIV protease inhibitors: A review of molecular selectivity and toxicity. *HIV AIDS (Auckl).* 7, 95–104. DOI:10.2147%2FHIV.S79956

55. Machhi, J., Herskovitz, J., Senan, A. M., Dutta, D., Nath, B., Oleynikov, M. D., Blomberg, W. R., Meigs, D. D., Hasan, M., Patel, M., et al. (2020). The natural history, pathobiology, and clinical manifestations of SARS-CoV-2 infections. *J Neuroimmune Pharmacol.* 15, 359–386. DOI:10.1007%2Fs11481-020-09944-5

56. Malik, Y. S., Kumar, P., Ansari, M. I., Hemida, M. G., El Zowalaty, M. E., Abdel-Moneim, A. S., Ganesh, B., Salajegheh, S., Natesan, S., Sircar, S. and Safdar, M., et al. (2021). SARS-CoV-2 spike protein extrapolation for COVID diagnosis and vaccine development. *Front Mol Biosci.* 8, 607886. DOI:10.3389/fmolb.2021.607886

57. Mao, L., Jin, H., Wang, M., Hu, Y., Chen, S., He, Q., Chang, J., Hong, C., Zhou, Y. D., Wang, X. M., Miao, X., Li, Y., Hu, B. (2019). Neurologic manifestations of hospitalised patients with coronavirus disease 2019 in Wuhan, China. *JAMA Neurol*. 77, 683–690. DOI:10.1001%2Fjamaneurol.2020.1127

58. Marathe, K. R., Patil, R. H., Vishwakarma, K. S., Chaudhari, A. B. and Maheshwari, V. L. (2019). Protease inhibitors and their applications: An overview. S*tud in Nat Products Chem.* 62, 211-242. DOI:10.1007/s00441-004-0866-x

59. Marzi, M., Vakil, M.K., Bahmanyar, M., Zarenezhad, E. (2022). Paxlovid: Mechanism of action, synthesis, and *in silico* study. *Biomed Res Int*. 2022, 1-16. DOI:10.1155/2022/7341493

60. Mayer, G., Boileau, G. and Bendayan, M. (2004). The proprotein convertase furin colocalizes with caveolin-1 in the Golgi apparatus and endosomes of hepatocytes. *Cell Tissue Res.* 316, 55-63. DOI:10.1007/s00441-004-0866-x

61. Mehta, P., McAuley, D. F., Brown, M., Sanchez, E., Tattersall, R. S. and Manson, J. J. (2020). COVID-19: Consider cytokine storm syndromes and immunosuppression. *Lancet*. 395, 1033–1034. DOI:10.1016/S0140-6736(20)30628-0

62. Moriguchi, T., Harii, N., Goto, J., Harada, D., Sugawara, H., Takamino, J., Ueno, M., Sakata, H., Kondo, K., Myose, N., et al. (2020). A first case of meningitis/encephalitis associated with SARS-Coronavirus-2. *Int J Infect Dis*. 94, 55–58. DOI: 10.1016/j.ijid.2020.03.062

63. Moulard M., Achstetter T., Kieny M. P., Montagnier L. and Bahraoui E (1994). Kex2p: a model for cellular endoprotease processing human immunodeficiency virus type 1 envelope glycoprotein precursor. *Eur J Biochem*. 225, 565-72. DOI:10.1111/j.1432-1033.1994. 00565.x

64. Mjokane, N., Maliehe, M., Folorunso, O. S., Ogundeji, A. O., Gcilitshana, O. M., Albertyn, J., Pohl, C. H. and Sebolai, O. M. (2022). Cryptococcal protease (s) and the activation of SARS-CoV-2 spike (S) protein. *Cells.* 11, 437. DOI:10.3390/cells11030437

65. Naider F. and Becker J. M. (2004). The alpha-factor mating pheromone of Saccharomyces cerevisiae: a model for studying the interaction of peptide hormones and G protein-coupled receptors. *Peptides.* 225, 565–572. DOI: 10.1016/j.peptides.2003.11.028

66. Netland, J., Meyerholz, D. K., Moore, S., Cassell, M. and Perlman, S. (2008). Severe acute respiratory syndrome coronavirus infection causes neuronal death in the absence of encephalitis in mice transgenic for human ACE2. *J Virol.* 82, 7264–7275. DOI:10.1128/jvi.00737-08

67. Otto, H. H. and Schirmeister, T. (1997). Cysteine proteases and their inhibitors. *Chem Rev.* 97, 133–172. DOI:10.1021/cr950025u

68. Oxley, T. J., Mocco, J., Majidi, S., Kellner, C. P., Shoirah, H., Singh, I. P., De Leacy, R. A., Shigematsu, T., Ladner, T. R., Yaeger, K. A., Skliut, M., Weinberger, J., Dangayach, N. S., Bederson, J. B., Tuhrim, S. and Fifi, J. T. (2020). Large-vessel stroke as a presenting feature of Covid-19 in the young. *N Engl J Med*. 382, e60(1)-e60(3). DOI:10.1056/nejmc2009787

69. Park, M.D. (2020). Macrophages: A Trojan horse in COVID-19? *Nat Rev Immunol*. 20, 351. DOI:10.1038%2Fs41577-020-0317-2

70. Papa, G., Mallery, D. L., Albecka, A., Welch, L.G., Cattin-Ortolá, J., Luptak, J., Paul, D., McMahon, H. T., Goodfellow, I. G., Carter, A., Munro, S. and James, L. C. (2021). Furin cleavage of SARS-CoV-2 Spike promotes but is not essential for infection and cell-cell fusion. *PLoS Pathog*. 17, e1009246. DOI: 10.1371/journal.ppat.1009246

71. Parvaz, N. and Jalali, Z. (2021). Molecular evolution of PCSK family: Analysis of natural selection rate and gene loss. *PLoS One*. 16, e0259085. DOI:10.1371%2Fjournal.pone.0259085

72. Pfizer Inc. Available online: https://www.pfizer.com/news/press-release/press-release-detail/pfizer-initiates-phase-1-studynovel-oral-antiviral (accessed on 7 September 2021).

73. Phan, L. T., Nguyen, T. V., Luong, Q. C., Nguyen, T. V., Nguyen, H. T., Le, H. Q., Nguyen, T. T., Cao, T. M. and Pham, Q. D. (2020). Importation and human-to-human transmission of a novel coronavirus in Vietnam. *N Engl J Med.* 382, 872–874. DOI: DOI:10.1056/nejmc2001272

74. Petersen, E., Koopmans, M., Go, U., Hamer, D.H., Petrosillo, N., Castelli, F., Storgaard, M., Al Khalili, S. and Simonsen, L. (2020). Comparing SARS-CoV-2 with SARS-CoV and influenza pandemics. *Lancet Infect Dis*. 20, e238–e244. DOI:10.1016/S1473-3099(20)30484-9

75. Procop, G. W., Shrestha, N. K., Vogel, S., van Sickle, K., Harrington, S., Rhoads, D. D., Rubin, B. P. and Terpeluk, P. (2020). A direct comparison of enhanced saliva to nasopharyngeal swab for the detection of SARS-CoV-2 in symptomatic patients. *J Clin Microbiol.* 58, 1–6. DOI:10.1148/radiol.2020201187

76. Poyiadji, N., Shahin, G., Noujaim, D., Stone, M., Patel, S. and Griffith, B. (2020). COVID-19–associated acute hemorrhagic necrotizing encephalopathy: imaging features. *Radiology*. 296, E119–E120. DOI:10.1148/radiol.2020201187

77. Powers, J. C., Asgian, J. L., Ekici, O. D. and James, K. E. (2002). Irreversible inhibitors of serine, cysteine, and threonine proteases. *Chem Rev.* 102, 4639–4750. DOI:10.1021/cr010182v

78. Rajah, M. M., Bernier, A., Buchrieser, J. and Schwartz, O. (2021). The Mechanism and consequences of SARS-CoV-2 spike-mediated fusion and syncytia formation. *J Mol Biol*. 434, 167280. DOI:10.1016/s0882-4010(02)00195-x

79. Rodrigues, M. L., Dos, R. F. C. G., Puccia, R., Travassos, L. R. and Alviano, C. S. (2003). Cleavage of human fibronectin and other basement membrane-associated proteins by a *Cryptococcus neoformans* serine proteinase*. Microb Pathog.* 34, 65–71. DOI:10.1016/s0882-4010(02)00195-x

80. Rogers, J. P., Chesney, E., Oliver, D., Pollak, T. A., McGuire, P., Fusar-Poli, P., Zandi, M. S., Lewis, G. and David, A. S. (2020). Psychiatric and neuropsychiatric presentations associated with severe coronavirus infections: A systematic review and meta-analysis with comparison to the COVID-19 pandemic. *Lancet Psychiatry*. 7, 611–627. DOI:10.1016/S2215-0366(20)30203-0

81. Routley, N. (2021). Visualizing what COVID-19 does to your body. Available online: https://www.visualcapitalist.com/visualizingwhat-covid-19-does-to-your-body/ (accessed on 26 June 2021)

82. Saad, M., Omrani, A. S., Baig, K., Bahloul, A., Elzein, F., Matin, M. A., Selim, M. A. A., Al Mutairi, M., Al Nakhli, D., Al Aidaroos, A. Y., et al. (2014). Clinical aspects and outcomes of 70 patients with Middle East respiratory syndrome coronavirus infection: A single-center experience in Saudi Arabia. *Int J Infect Dis.* 29, 301–306. DOI: 10.1016/j.ijid.2014.09.003

83. Simonnet, A., Chetboun, M., Poissy, J., Raverdy, V., Noulette, J., Duhamel, A., Labreuche, J., Mathieu, D., Pattou, F., Jourdain, M. (2020). High prevalence of obesity in severe acute respiratory syndrome coronavirus-2 (SARS-CoV-2) requiring invasive mechanical ventilation. *Obesity*. 28, 1195–1199. DOI:10.1002/oby.22831

84. Steitz, T. A., and Shulman, R. G., (1982). Crystallographic and NMR studies of the serine proteases. *Annu Rev Biophys Bioeng.* 11, 419-444. DOI:10.1146/annurev.bb.11.060182.002223

85. Saiegh, F. A., Ghosh, R., Leibold, A., Avery, M. B., Schmidt, R. F., Theofanis, T., Mouchtouris, N., Philipp, L., Peiper, S. C., Wang, Z.-X., Rincon, F., Tjoumakaris, S. I., Jabbour, P., Rosenwasser, R. H. and Gooch, M. R. (2020). Status of SARS-CoV-2 in cerebrospinal fluid of patients with COVID-19 and stroke. *J Neurol Neurosurg Psychiatry.* 91, 846-848. DOI:10.1136/jnnp-2020-323522

86. Schapiro, F. B., Soe, T. T., Mallet, W. G. and Maxfield, F. R. (2004). Role of cytoplasmic domain serines in intracellular trafficking of furin. *Mol Biol Cell.* 15, 2884-2894. DOI:10.1091%2Fmbc.E03-09-0653

87. Seidah, N. G., Benjannet, S., Sangeeta Pareek, Savaria, D., Hamelin, J., Goulet, B., Jacynthe Laliberté, Lazure, C., Chrétien, M. and Murphy, R. F. (1996). Cellular processing of the nerve growth factor precursor by the mammalian pro-protein convertases. *Biochem J.* 15, :951-60. DOI:10.1042%2Fbj3140951

88. Solovyeva, N. I., Gureeva, T. A., Timoshenko, O. S., Moskvitina, T. A. and Kugaevskaya, E. V. (2016). Furin as proprotein convertase and its role in normal and pathological biological processes. *Biomed Khim*. 11, 609–621. DOI:10.18097/pbmc20166206609

89. Strickland, A. B., Shi, M. (2021). Mechanisms of fungal dissemination. *Cell Mol Life Sci*. 78, 3219–3238. DOI:10.1007%2Fs00018-020-03736-z

90. Tanaka, S. (2003). Comparative aspects of intracellular proteolytic processing of peptide hormone precursors: studies of proopiomelanocortin processing. *Zoolog Sci.* 20, 1183-1198. DOI:10.2108/zsj.20.1183

91. Vu, K., Tham, R., Uhrig, J. P., Thompson, G. R., Pombejra, S. N., Jamklang, M., Bautos, J. M. and Gelli, A. (2014). Invasion of the central nervous system by *Cryptococcus neoformans* requires a secreted fungal metalloprotease. *mBio.* 5, 1–13. DOI:10.1128/mbio.01101-14

92. Wang, J., Zhou, H., Lu, H., Du, T., Luo, Y., Wilson and Jin, C. (2015). Kexin-like endoprotease KexB is required for N-glycan processing, morphogenesis and virulence in *Aspergillus fumigatus*. *Fungal Genet Biol.* 76, 57–69. DOI: 10.1016/2Fj.fgb.2015.02.006

93. Wang, T., Du, Z., Zhu, F., Cao, Z., An, Y., Gao, Y. and Jiang, B. (2020). Comorbidities and multi-organ injuries in the treatment of COVID-19. *Lancet.* 395, e52. DOI:10.1016/s0140-6736(20)30558-4

94. WHO. (2020). Report of the WHO-China Joint Mission on Coronavirus Disease 2019 (COVID-19)—16–24 Feburary 2020. Available online: https://www.who.int/docs/default-source/coronaviruse/who-china-joint-mission-on-covid-19-final-report.pdf (accessed on 24 May 2021).

95. Wrobel, A. G., Benton, D. J., Xu, P., Roustan, C., Martin, S. R., Rosenthal, P. B., Skehel, J. J. and Gamblin, S. J. (2020). SARS-CoV-2 and bat RaTG13 spike glycoprotein structures inform on virus evolution and furin-cleavage effects. *Nat Struct Mol Biol.* 27, 763–767. DOI:10.1038/s41594-020-0509-2

96. Wu, Y., Xu, X., Chen, Z., Duan, J., Hashimoto, K., Yang, L., Liu, C. and Yang, C. (2020). Nervous system involvement after infection with COVID-19 and other coronaviruses. *Brain Behav. Immun*. 87, 18–22. DOI: 10.1016/j.bbi.2020.03.031

97. Wyllie, A. L., Fournier, J., Casanovas-Massana, A., Campbell, M., Tokuyama, M., Vijayakumar, P., Geng, B., Muenker, M. C., Moore, A. J. and Vogels, C. B. F. (2020). Saliva is more sensitive for SARS-CoV-2 detection in COVID-19 patients than nasopharyngeal swabs. *N Engl J Med*: DOI:10.1101/2020.04.16.20067835

98. Xiao, K., Zhai, J., Feng, Y., Zhou, N., Zhang, X., Zou, J. J., Li, N., Guo, Y., Li, X., Shen, X. Zhang, Z., Shu, F., Huang, W., Li, Y., et al. (2020). Isolation of SARS-CoV-2-related coronavirus from Malayan pangolins. *Nature.* 583, 286–289. DOI:10.1038/s41586-020-2313-x

99. Yang, X., Yu, Y., Xu, J., Shu, H., Liu, H., Wu, Y., Zhang, L., Yu, Z., Fang, M., Yu, T., Wang, Y., Pan, S., et al. (2020). Clinical course and outcomes of critically ill patients with SARS-CoV-2 pneumonia in Wuhan, China: A single-centered, retrospective, observational study. *Lancet Respir. Med*. 8, 475–481. DOI:10.1016/s2213-2600(20)30079-5

100. Zaki, A. M., van Boheemen, S., Bestebroer, T. M., Osterhaus, A. D. M. E. and Fouchier, R. A. M. (2012). Isolation of a novel coronavirus from a man with pneumonia in Saudi Arabia. *N Engl J Med*. 367, 1814–1820. DOI:10.1056/nejmoa1211721

101. Zhao, H., Shen, D., Zhou, H., Liu, J. and Chen, S. (2020). Guillain-Barré syndrome associated with SARS-CoV-2 infection: Causality or coincidence? *Lancet Neurol*. 19, 383–384. DOI:10.1016/s1474-4422(20)30109-5

102. Zhang, H., Kang, Z., Gong, H., Xu, D., Wang, J., Li, Z., Cui, X., Xiao, J., Meng, T. and Zhou, W. (2020). The digestive system is a potential route of 2019-nCov infection: A bioinformatics analysis based on single-cell transcriptomes. *BioRxiv* 1–20. DO:10.1101/2020.01.30.927806

103. Zhen, W., Manji, R., Smith, E. and Berry, G. J. (2020). Comparison of four molecular *in vitro* diagnostic assays for the detection of SARS-CoV-2 in nasopharyngeal specimens. *J Clin Microbiol*. 58, 1–8. DOI:10.1128/jcm.00743-20

104. Zheng, Y. Y., Ma, Y. T., Zhang, J. Y. and Xie, X. (2020). COVID-19 and the cardiovascular system. *Nat Rev Cardiol*. 17, 259–260. DOI:10.1038/s41569-020-0360-5

105. Zhou, L., Zhang, M., Wang, J., Gao, J. (2020). SARS-CoV-2: Underestimated damage to nervous system. *Travel Med Infect*. 36, 101642. DOI: 10.1016/j.tmaid.2020.101642

106. Zhou, P., Yang, X. L., Wang, X. G., Hu, B., Zhang, L., Zhang, W., Si, H. R., Zhu, Y., Li, B., Huang, C. L., et al. (2020). A pneumonia outbreak associated with a new coronavirus of probable bat origin. *Nature*. 579, 270–273. DOI:10.1038/s41586-020-2012-7

107. Zhu, N., Zang, D., Wang, W., Li, X., Yang, B., Song, J., Zhao, X., Huang, B., Shi, W., Lu, R., Niu, P., Zhan, F., Ma, X., Wang, D., Xu, W., Wu, G., Gao, G. F. and Tan, W. (2020). A Novel Coronavirus from patients with pneumonia in China, 2019. *N Engl J Med.* 382, 727–733. DOI:10.1056/nejmoa2001017

108. Zhu, X., Ge, Y., Wu, T., Zhao, K., Chen, Y., Wu, B., Zhu, F., Zhu, B. and Cui, L. (2020). Co-infection with respiratory pathogens among COVID-2019 cases. *Virus Res.* 285, 1–6. DOI: 10.1016/j.virusres.2020.198005

CHAPTER 2:

THE DETECTION OF CRYPTOCOCCAL PROTEASES IN THE SUPERNATANT AND EVIDENCE OF THEIR THEORETICAL ACTIVATION OF THE CORONAVIRUS SPIKE PROTEIN

Parts of this chapter have been published.

Publication: Mjokane et al. Cryptococcal Protease(s) and the Activation of SARS-CoV-2 Spike (S) Protein. *Cells,* 2022; 11: 437.

Author contribution: Conceptualisation, methodology, software, formal analysis, writing original draft preparation, writing review and editing.

2.1 ABSTRACT

Several studies show that COVID-19 can co-manifest in a patient with other respiratory fungal pathogens, such as *Cryptococcus (C.) neoformans*. In this context, it is plausible that a fungal furin-like protease could also be accessed and distorted by SARS-CoV-2 to participate in the activation of its latent spike glycoprotein. In this contribution, it was sought to determine if: 1) *Cryptococcus neoformans* expressed a number of genes encoding for serine proteases, *viz*. cryptococcal serine carboxypeptidase *(CNBF4600),* cryptococcal peptidase *(CNBA1340),* cryptococcal peptidase *(CNAG_00150),* cryptococcal cerevisin *(CNAG_04625),* and cryptococcal cerevisin *(CNBJ2870)*, 2) the supernatant (obtained from the culture media used to grow cryptococcal cells) had proteolytic activity, and 3) the selected proteases could theoretically bind to the coronavirus spike protein through using a computer-based tool, HADDOCK. It was noted that cells expressed the selected protease genes, whose products may be secreted into the supernatant. Thus, these products may partly be responsible for the observed proteolytic activity recorded after 36 h of cultivation. Importantly, these selected proteases could interact with the spike protein, and some had a better or comparable binding affinity to the spike protein than furin protease – a serine protease found in human cells that typically activates the coronavirus spike protein, following an *in silico* comparative analysis of the molecular docking parameters. Taken together, the data suggests that cryptococcal supernatant contains serine proteases that may activate the spike protein.

Key words: *Cryptococcus neoformans,* Docking, Furin, Gene expression, HADDOCK, Proteolysis, SARS-CoV-2, Serine proteases, Spike protein, Supernatant.

2.2 INTRODUCTION

Cryptococcus (C.) neoformans is a terrestrial organism that can successfully lodge in alveoli of the human lungs to cause life-threatening infections (Crabtree et al., 2012). Key to its success is the ability to deploy its virulence factors, among these are proteases which are enzymes that catalyses the hydrolysis of peptide bonds (López-Otín and Bond, 2008). During infection, proteases are essential for pathogen translocation. In *Cryptococcus*, these proteins have been documented to play a role in the damaging of host allowing dissemination of *Cryptococcus neoformans* to the lung parenchyma from the alveolar space (Eigenheer et al., 2007).

In general, serine proteases are defined by serine as the nucleophilic amino acid and have the canonical catalytic triad made up of Ser-His-Asp (Ekici et al., 2009). To hydrolyse a substrate, these proteases recognise specific amino acid sequences which are regarded as cleavage sites (Ekici et al., 2009). For example, furin (which is a human serine-based protease) hydrolyses the SARS-CoV-2 spike protein at the S1/S2 site wherein it recognises the basic amino acid target sequence **R**-X-**R** or **R**-X-**K**↓, where X can be any amino acid residue (Bestle et al., 2020; Papa et al., 2021; Peacock et al., 2021). As proteases evolved, they maintained their characteristic features, mechanistic action for processing their substrates. Is it reasonable to foresee cryptococcal proteases hydrolysing the same furin cleavage site on the coronavirus spike protein? To test this, a simulation programme, HADDOCK was used. HADDOCK (High Ambiguity Driven protein-protein DOCKing) is a computational tool used to model protein-to-protein

interactions. It predicts complexes by calculating structure complementarity, energy stabilities which include electrostatic interactions, root- mean-square deviation (RMSD), Van der Waals energy, desolvation energy, restraints violation energy, and buried surface area (van Dijk et al., 2006). However, it is a prediction that needs further confirmation, for example by performing enzymatic studies.

2.3 MATERIALS AND METHODS

2.3.1 Cultivation of *Cryptococcus neoformans* and collection of the supernatant

The standard cryptococcal reference strain *viz*. *Cryptococcus neoformans* H99, was used in the study. This strain was plated on yeast–malt extract (YM) agar (3 g/L yeast extract, 3 g/L malt extract, 5 g/L peptone, 10 g/L glucose, 16 g/L agar (Merck, South Africa)). The plate was incubated for 24 h at 30°C. Next, a loopful of fungal colonies was scooped and inoculated into a 250 mL conical flask that contained 100 mL of fresh, sterile YNB (6.7 g/L; Thermo Fisher Scientific, South Africa) broth that was supplemented with glucose (4%; w/v; Merk, South Africa). The flask was then incubated at 30°C for 36 h while agitated at 160 rpm on an orbital shaker (Lasec, South Africa).

To collect the supernatant, 1 mL of the culture media (containing cryptococcal cells) was dispensed into a 2 mL plastic tube. The tube was centrifuged at 1000 × *g* for 5 min at

30°C to pellet the cells and to aspirate the supernatant, which contained the cryptococcal proteases.

2.3.2 Detecting the gene expression levels of selected cryptococcal protease(s)

Before assessing if the cryptococcal strain H99 transcribed certain serine proteases, a literature search was done to scour for reports of cryptococcal serine proteases. Information about these proteases is summarised in **Table 2.1**. To prepare cells for the real-time qPCR experiment, the cryptococcal cells were incubated for 6 h and 24 h. Thereafter, the culture media was centrifuged at 1000 × *g* for 5 min at 30°C to pellet the cells. The pellet was washed twice with a physiological buffer saline (Sigma-Aldrich, South Africa). To lyse the cells, 350 µL of the GTC (guanidium thiocyanate) lysis buffer (prepared using 20 µL of 14.3 M 2-mercaptoethanol (Merck, South Africa)) was added to the washed pellet. To this, glass beads (5 mm) were added, and the contents were vortex mixed for 5 min at room temperature. To ensure capsule and cell wall breakage, the cells were disrupted using a sonicator (Bendelin Electronic, Germany) set at 0.64 Hz for 5 cycles during a 15 min period at 4°C. The total RNA was extracted from the lysate following the E.Z.N.A. protocol (Omega Bio-Tek, United States). The nanodrop was used to ensure quality control and quantification of the extracted total RNA. The cDNA for real-time PCR was generated using Invitrogen™ SuperScript™ VILO™ cDNA synthesis kit.

Table 2.1 Furin and cryptococcal proteases and their proposed function in the context of COVID-19 development.

Protease	**Type of protease**	**Source**	**Function(s) in source organism**	**Function in the context of SARS-CoV-2 infection**
Furin protease (PDB ID: 5JXH)	Serine-based	*Homo sapiens*	Activates proprotein substrates (Villoutreix et al., 2022)	Proteolytic cleavage of the viral S1/S2 site (Jaimes et al., 2019; 2020)
Cryptococcal serine carboxypeptidase (PDB ID: CNBF4600)	Serine-based	*Cryptococcus neoformans*	Tissue invasion by cleaving basement membrane components (Eigenheer et al., 2007)	Suggested to act on the furin cleavage site within the S1/S2 site (Mjokane et al., 2022)
Cryptococcal peptidase (PDB ID: CNBA1340)	Serine-based	*Cryptococcus neoformans*	Tissue invasion by cleaving basement membrane components (Eigenheer et al., 2007)	Suggested to act on the furin cleavage site within the S1/S2 site (Mjokane et al., 2022)

Table 2.1 (continued). Furin and cryptococcal proteases and their proposed function in the context of COVID-19 development.

Protease	Type of protease	Source	Function(s) in source organism	Function in the context of SARS-CoV-2 infection
Cryptococcal peptidase (PDB ID: CNAG_00150)	Serine-based	*Cryptococcus neoformans*	Quorum-sensing (Gutierrez-Gongora and Geddes-McAlister, 2022)	Suggested to act on the furin cleavage site within the S1/S2 site (Mjokane et al., 2022)
Cryptococcal cerevisin (PDB ID: CNAG_04625)	Serine-based	*Cryptococcus neoformans*	Melanin synthesis (Gutierrez-Gongora and Geddes-McAlister, 2022)	Suggested to act on the furin cleavage site within the S1/S2 site (Mjokane et al., 2022).
Cryptococcal cerevisin (PDB ID: CNBJ2870)	Serine-based	*Cryptococcus neoformans*	Tissue invasion by cleaving basement membrane components (Eigenheer et al., 2007)	Suggested to act on the furin cleavage site within the S1/S2 site (Mjokane et al., 2022).

A volume of 25 µL for each real-time qPCR reaction was prepared using 12.5 µL 2x One-Step-SYBR Green Master Mix, 1.5 µL (84.4 ng/µL template RNA, 2.5 µL (10 µM) for the forward and reverse primers (**Table 2.2**), 5.75 µL of RNase-free water and 0.25 µL of Rotor-Gene RT Mix.

Table 2.2. Primer sequences.

Primer	**Sequence (5' – 3 ')**
GAPDH	F- TGAAGCAGGCATCTGAGGG
	R- CGAAGGTGGAAGAGTGGGAG
Beta Actin	F- TGTACAATGGTATTGCCGACC
	R- CTGGTCCCTCAATCGTCCAC
CNBF4600	F- TTGATGAACCGGGAGGTCCG
	R- GAAGGACGAGACGGGGACTG
CNBA1340	F- ACTGCTCAGCAACTTCCCGT
	R- AATGTCGGCGACGGCATAGA
CNAG_00150	F- GGTCCCCTACATGGGTGTCG
	R- AGCGGGCGAATTCATACCGA
CNAG_04625	F- TTCACTGACGACGGCCAAGT
	R- GCCGGCATAACCGAAGAAGC
CNBJ2870	F- CCGAGGTGGCCTATGTCGAG
	R- AAATACGGGCGAGACCCCAG

With the beta-actin and GAPDH (glyceraldehyde-3-phosphate dehydrogenase) as internal controls, the qPCR was carried out with a Quantabio Q cycler (Whitehead Scientific, South Africa) with initial incubation step at 95°C for 2 min. Two-step cycling was performed with 40 cycles. Each step consisted of 2 steps: 95°C for 5 seconds (denaturation step) and 62°C for 20 seconds (annealing/extension step). In the end, the changes in steady-state mRNA levels of the selected genes were quantified relative to the levels of the internal controls (i.e., beta-actin and GAPDH). The selected protease genes were: cryptococcal serine carboxypeptidase *(CNBF4600)*, cryptococcal peptidase *(CNBA1340),* cryptococcal peptidase *(CNAG_00150)*, cryptococcal cerevisin *(CNAG_04625),* and cryptococcal cerevisin *(CNBJ2870)*.

2.3.3 Protease assay

To confirm the mobilisation of cryptococcal protease(s) into the supernatant, the supernatant was tested with a Pierce™ Colorimetric Protease Assay Kit in accordance with the manufacturer's protocol. This kit measures total protease activity in samples. It contains the universally accepted reference for hydrolysis, viz. trypsin as the standard protease for cleaving succinylated casein, which is the provided substrate. A negative control, i.e., blank control without the protease and the peptide, was included. Moreover, a peptide control without the protease was also included. In the end, the background signal of these negative controls was used for normalisation. Three independent experiments were carried out.

2.3.4 Molecular docking studies: protein acquisition, preparation and molecular docking

The X-ray crystal structures of the 1) solved coronavirus spike glycoprotein (PDB ID: 2AJF), 2) solved homo sapiens furin protease (PDB ID: 5JXH), 3) predicted cryptococcal serine carboxypeptidase (PDB ID: CNBF4600), 4) predicted cryptococcal peptidase (PDB ID: CNBA1340), 5) predicted cryptococcal peptidase (PDB ID: CNAG_00150), 6) predicted cryptococcal cerevisin (PDB ID: CNAG_04625), and 7) predicted cryptococcal cerevisin (PDB ID: CNBJ2870) were obtained from the Research Collaboratory for Structural Bioinformatics (RCSB) Protein Data Bank (PDB) (https://www.rcsb.org) and Uniprot Protein Data Bank (https://www.uniprot.org). Information about these cryptococcal proteases was obtained from literature wherein they were reported to be crucial for the survival of *Cryptococcus neoformans* (**Table 2.1**).

The obtained structures were optimised *in silico* by removing water molecules and non-standard naming protein residue connectivity (Aribisala et al., 2022). Molecular docking of the crystal structures of the coronavirus spike protein (target) and the selected proteases/peptides (ligands) were executed using the high ambiguity driven protein-protein docking (HADDOCK) server (https://haddock.science.uu.nl) (Dominguez et al., 2003). This open-source computational tool was used to analyse the protein-protein interactions through the HADDOCK score, root-mean-square deviation (RMSD), Van der Waals energy, electrostatic energy, desolvation energy, restraints violation energy, and buried surface area.

2.3.5 Statistical analysis

Three biological replicates were included for each independent experiment. The GraphPad Prism software version 8.3.1 for Windows (GraphPad Software, San Diego, CA, USA; www.graphpad.com) was used to calculate mean values and the standard error of the means (SEM). Where appropriate, the same programme was used to perform the multiple comparison test using Tukey's test as an option.

2.4 RESULTS

2.4.1 *Cryptococcus neoformans* showed expression of selected proteases

The gene expression profile of the selected genes is summarised in **Figure 2.1.** It was observed that all the selected proteases were expressed. More to this, the levels of cryptococcal serine carboxypeptidase *(CNBF4600)* significantly decreased ($p < 0.05$) at 24 h when compared to 6 h, while the levels of two other cryptococcal peptidases *(CNBA1340* and *CNAG_00150),* and two other cryptococcal cerevisins *(CNAG_04625* and *CNBJ2870)* remained relatively similar ($p > 0.05$) at 6 and 24 h. The latter shows the presence and potential activity of these proteases in *Cryptococcus neoformans*.

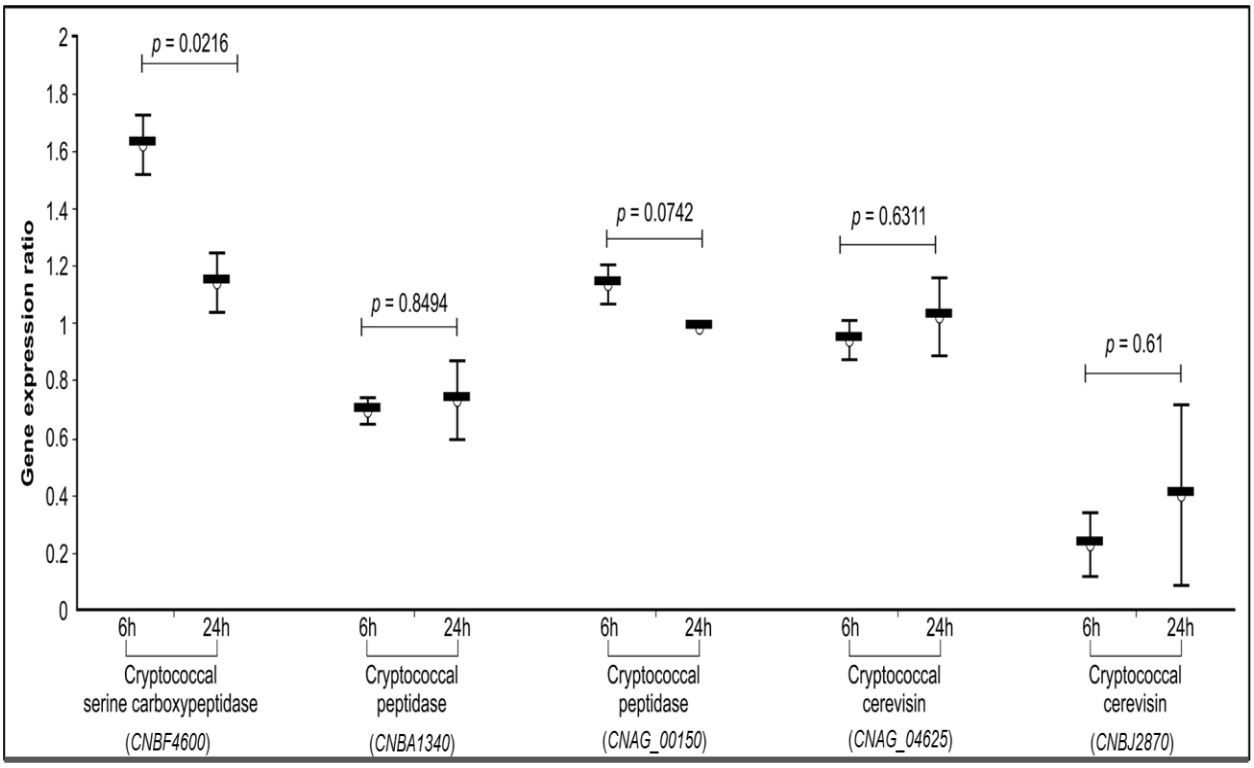

Figure 2.1. The transcriptional levels of the selected cryptococcal protease genes following cultivation for 6 and 24 h. The changes in steady-state mRNA levels of the selected genes were quantified relative to the levels of the internal controls.

2.4.2 The cryptococcal supernatant contains protease(s)

Figure 2.2 summarises the analysis results of the supernatant for the detection of cryptococcal proteases. The supernatant was collected from cells that had reached a cell density of 6.65×10^6 cells/mL (SEM = 7.51×10^5) after 36 h. The cryptococcal supernatant showed proteolytic activity comparable to the trypsin standard.

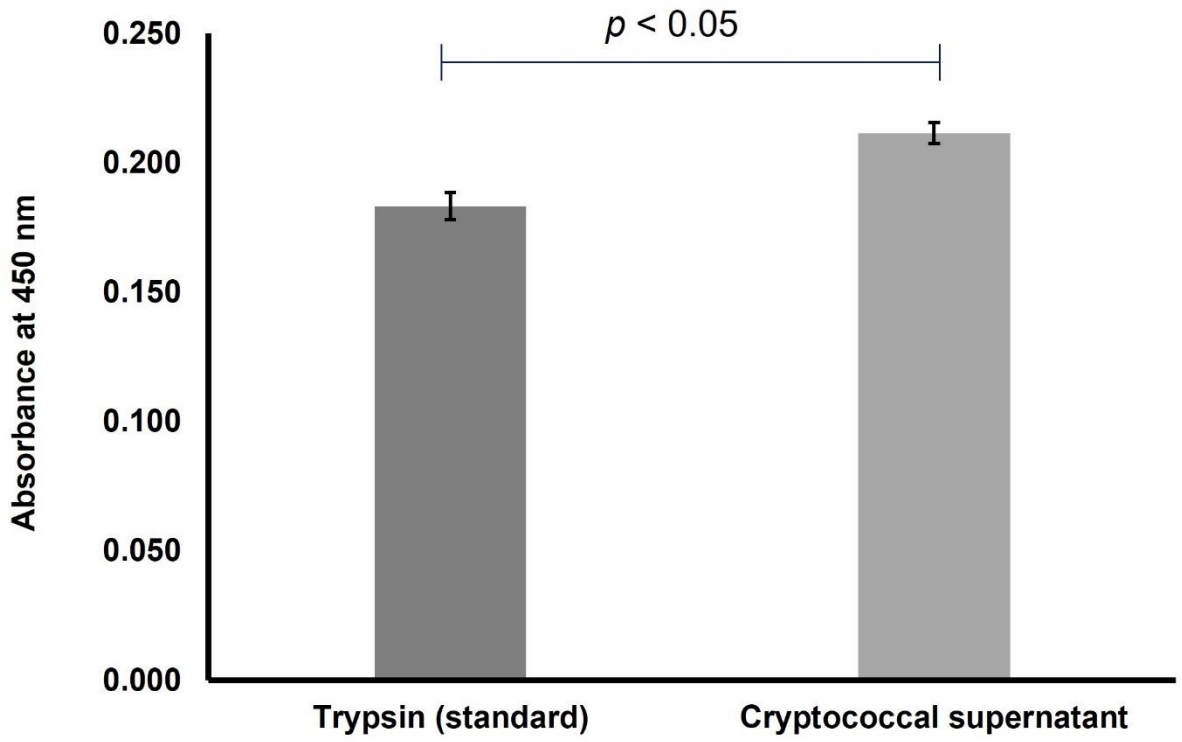

Figure 2.2. The detection of cryptococcal protease(s) in the supernatant obtained from cryptococcal cultivation media, i.e., YNB broth. The depicted cryptococcal data were obtained from three independent experiments.

2.4.3 Some cryptococcal proteases show better or comparable binding affinity to SARS-CoV-2 spike protein than furin protease

The *in silico* comparative analysis data of the docking parameters of coronavirus spike protein with furin protease or cryptococcal proteases is detailed in **Table 2.2** Furin protease was used as a reference protease as it cleaves the S1/S2 site within the SARS-CoV-2 spike protein in an infected host and thus, it was compared to the cryptococcal proteases. It was noted that docking between furin protease-coronavirus spike protein

gave a HADDOCK score of -83.8 ± 2.5. Interestingly, docking of cryptococcal serine carboxypeptidase (PDB ID: CNBF4600) against coronavirus spike protein yielded a significantly greater negative score of -129.4± 6.6 ($p = 0.0231$) than that of furin protease, while one of the cryptococcal peptidase (CNBA1340), had a comparable score of -81.7± 6.2 to the furin protease ($p > 0.05$). The cryptococcal cerevisin (PDB ID: CNBJ2870), cerevisin (PDB ID: CNAG_04625) and the other peptidase (PDB ID: CNAG_00150) all had scores higher than -80. The average RMSD value of furin protease in complex with coronavirus spike protein was 12.8 ± 0.1 Å, which was higher compared to 0.5 ± 0.3 Å and 0.6 ± 0.4 Å observed with cryptococcal serine carboxypeptidase (PDB ID: CNBF4600) and cryptococcal peptidase (PDB ID: CNBA1340), respectively (**Table 2.2**). The Van der Waals energy and electrostatic energy that contribute to the binding strength for each complex were calculated. For the furin protease-coronavirus spike protein complex, the Van der Waals and electrostatic energy values were -154.3 ± 36.6 kcal/mol and -64.8 ± 3.8 kcal/mol, respectively.

Compared to these, the cryptococcal serine carboxypeptidase-coronavirus spike protein complex had scores of -77.8 ± 6.0 kcal/mol (Van der Waals energy) and -272.8 ± 20.7 kcal/mol (electrostatic energy) while the cryptococcal peptidase-coronavirus spike protein complex yielded scores of -68.7 ± 2.3 kcal/mol (Van der Waals energy) and -62.2 ± 3.6 kcal/mol (electrostatic energy). It was noted that Van der Waals energy dominated the furin protease-coronavirus spike protein complex and cryptococcal peptidase-coronavirus spike protein complex protein-protein interactions.

Table 2.3 The intermolecular binding energies of the docked furin-coronavirus spike protein complex and cryptococcal proteases-coronavirus spike protein.

Protease	**RMSD (Å)**	**HADDOCK score**	**Van der Waals energy (kcal/mol)**	**Electrostatic energy (kcal/mol)**	**Desolvation energy (kcal/mol)**	**Restraints violation energy (kcal/mol)**	**Buried surface area (Å²)**
Furin protease (PDB ID: 5JXH)	12.8 ± 0.1	-83.8 ± 2.5	-154.3 ± 36.6	-64.8 ± 3.8	-29.3 ± 2.3	412.6 ± 54.9	1880.5 ± 81.1
Cryptococcal serine carboxypeptidase (PDB ID: CNBF4600)	0.5 ± 0.3	-129.4 ± 6.6	-77.8 ± 6.0	-272.8 ± 20.7	-29.1 ± 5.2	321.1 ± 42.62	424.3 ± 48.0
Cryptococcal peptidase (PDB ID: CNBA1340)	0.6 ± 0.4	-81.7 ± 6.2	-68.7 ± 2.3	-62.2 ± 3.6	-29.7 ± 1.4	291.3 ± 40.5	1533.4 ± 33.5

Table 2.3 The intermolecular binding energies of the docked furin-coronavirus spike protein complex and cryptococcal proteases-coronavirus spike protein.

Protease	**RMSD (Å)**	**HADDOCK score**	**Van der Waals energy (kcal/mol)**	**Electrostatic energy (kcal/mol)**	**Desolvation energy (kcal/mol)**	**Restraints violation energy (kcal/mol)**	**Buried surface area (Å^2)**
Cryptococcal peptidase (PDB ID: CNAG_00150)	31.0 ± 0.1	-78.4 ± 5.5	-68.6 ± 7.6	-78.7 ± 7.0	-19.7 ± 1.8	255.8 ± 23.6	2044.9 ± 96.7
Cryptococcal cerevisin (PDB ID: CNAG_04625)	19.4 ± 0.3	-76.4 ± 4.9	-53.0 ± 3.3	-189.7 ± 7.2	-12.4 ± 2.6	269.3 ± 53.5	1817.6 ± 114.9

Table 2.3 The intermolecular binding energies of the docked furin-coronavirus spike protein complex and cryptococcal proteases-coronavirus spike protein.

Protease	**RMSD (Å)**	**HADDOCK score**	**Van der Waals energy (kcal/mol)**	**Electrostatic energy (kcal/mol)**	**Desolvation energy (kcal/mol)**	**Restraints violation energy (kcal/mol)**	**Buried surface area (Å^2)**
Cryptococcal cerevisin (PDB ID: CNBJ2870)	0.8 ± 0.4	-71.7± 6.4	-57.8 ± 5.3	-156.0 ± 25.5	-13.6 ± 2.8	309.0 ± 54.1	1486.5 ± 63.3

In contrast, electrostatic energy dominated the protein-protein interaction of the cryptococcal serine carboxypeptidase-coronavirus spike protein complex. The buried surface area, i.e., the amount of protein surface not in contact with water upon complexation, data was calculated and analysed. Here, it was noted that the docked proteases had scores in the order cryptococcal serine carboxypeptidase at 424.3 ± 48.0 $Å^2$ > furin protease at 1880.5 ± 81.1 $Å^2$ > cryptococcal peptidase at 1533.4 ± 33.5 $Å^2$. When considering the furin protease's desolvation energy (-29.3 ± 2.3 kcal/mol) and restraint violation energy (412.6 ± 54.9 kcal/mol), these were observed to be far less than the buried surface area score (1880.5 ± 81.1 $Å^2$). A similar observation was made for the cryptococcal peptidase. On the other hand, the cryptococcal serine carboxypeptidase gave a high-quality association with its HADDOCK score as its desolvation energy was (-29.1 ± 5.2 kcal/mol) and restraint violation energy (321.1 ± 42.62 kcal/mol) were closer to its buried surface area score (424.3 ± 48.0 $Å^2$).

While **Figure 2.3** shows the surface representation of the docked complexes (furin protease-coronavirus spike protein, cryptococcal serine carboxypeptidase-coronavirus spike protein, and cryptococcal peptidase-coronavirus spike protein) at their respective optimal orientation, the characteristic amino acid residues for each protease that were poised to interact with the spike protein cleavage site in the docked complex structure are shown in **Figure 2.4.**

Proteases	Surface representation of interaction between spike protein and proteases
Furin protease (F5JXH)	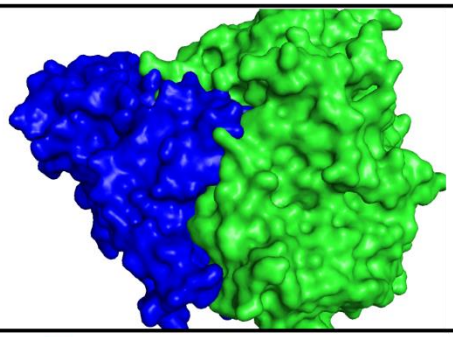
Cryptococcal serine carboxypeptidase (CNBF4600)	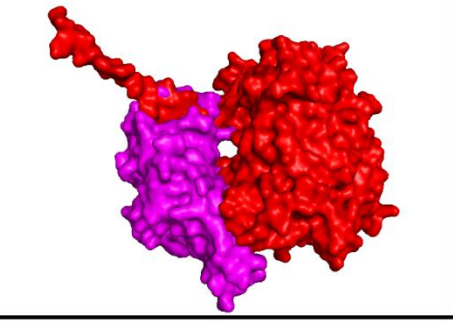
Cryptococcal peptidase (CNBA1340)	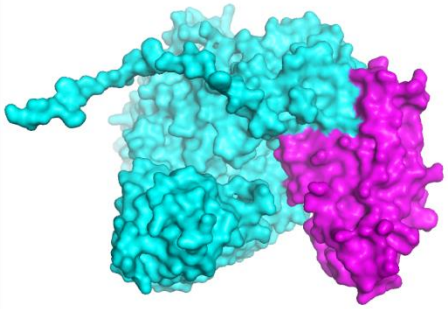

Figure 2.3. The surface representation of the docked furin protease-coronavirus spike protein complex and cryptococcal proteases-coronavirus spike protein complexes. The Chimera programme (v21.1) was used for the interactive visualisation and analysis of the molecular structures.

Proteases	Interactions	Amino acid residues interacting with SARS-CoV-2 spike protein
Furin protease (F5JXH)	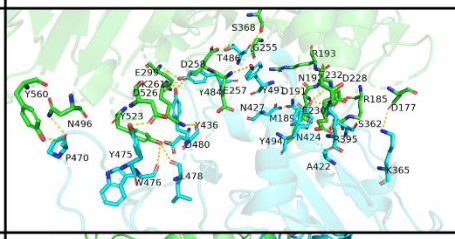	Y560,N496, P470, E299, K261, D526, Y523, Y475, W476, Y436, D480, L478, D258, Y484, E257, S368, G255, T486, Y49, N427, R193, T232, N192, D191, E230, M189, N424, Y494, D228,R185, D177, S362, R395, A422, K365
Cryptococcal serine carboxypeptidase (CNBF4600)	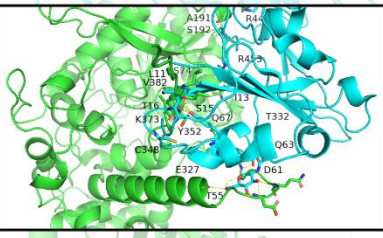	A191, S192, S74, L11, V382, T16, K353, S15, Y352, C348, E327, T55, R44, R453, Q67, T332, Q63, D61
Cryptococcal peptidase (CNBA1340)	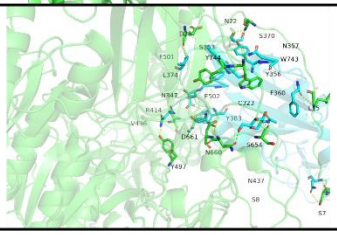	D28, F501, L374, N347, R414, V436, S353, Y744, E502, D661, N660, Y497, N22, S370, N357, W743, Y356, F360, L15, C323, Y383, S654, N437, S8, S7

Figure 2.4. The intermolecular interactions of the docked furin protease-coronavirus spike protein complex and cryptococcal proteases-coronavirus spike protein showing the amino acid residues of each protease that interacts with the spike protein. The Chimera programme (v21.1) was used for the interactive visualisation and analysis of the molecular structures.

Specifically, furin protease interacted with Y560, N496, P470, E299, K261, D526, Y523, Y475, W476, Y436, D480, L478 D258, Y484, E257, S368, G255, T486, Y49, N427, R193, T232, N192, D191, E230, M189, N424, Y494, D228, R185, D177, S362, R395, A422 and K365 at the binding pocket of the spike protein. On the other hand, cryptococcal serine carboxypeptidase interacted with A191, S192, S74, L11, V382, T16, K353, S15, Y352, C348, E327, T55, R44, R453, Q67, T332, Q63 and D61 while cryptococcal peptidase

with D28, F501, L374, N347, R414, V436, S353, Y744, E502, D661, N660, Y497, N22, S370, N357, W743, Y356, F360, L15, C323, Y383, S654, N437, S8 and S7. Similarly, the number of hydrogen bonds linking the coronavirus spike protein to the respective proteases is presented in **Figure 2.5**, with the spike protein complexation with furin, cryptococcal serine carboxypeptidase and cryptococcal peptidase (PDB ID: CNBA1340) having 7, 9 and 6 bonds, respectively.

Proteases	Interactions	H-Bonds
Furin protease (F5JXH)	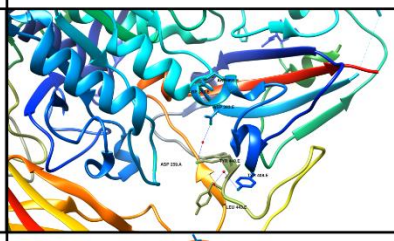	7
Cryptococcal peptidase S28 (CNBF4600)	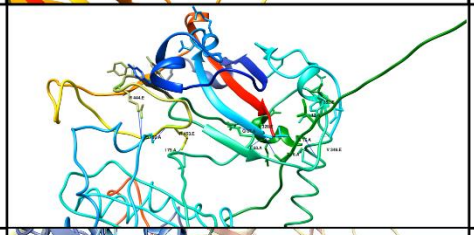	9
Cryptococcal peptidase (CNBA1340)	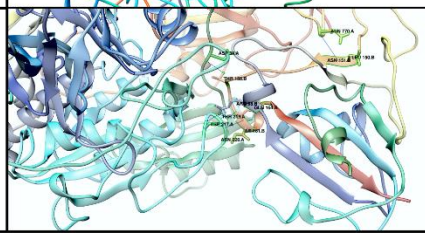	6

Figure 2.5 The intermolecular interaction of the docked furin protease-coronavirus spike protein complex and cryptococcal proteases-coronavirus spike protein showing the H-bonds for each protease and the coronavirus spike protein. The Chimera programme (v21.1) was used for the interactive visualisation and analysis of the molecular structures.

2.5 DISCUSSION

Literature shows that SARS-CoV-2 could co-occur in the same microenvironment as a respiratory fungal pathogen. In this context, it is plausible that the two infectious agents may interact. And by extension, it is foreseeable that microbial proteases may activate the spike protein. Therefore, this chapter was concerned with testing whether *Cryptococcus neoformans* could transcribe and secrete proteases into the extracellular environment that may, in theory, activate the spike protein.

The obtained data revealed that the cryptococcal cells could transcribe cryptococcal serine carboxypeptidase *(CNBF4600)*, cryptococcal peptidase *(CNBA1340),* cryptococcal peptidase *(CNAG_00150)*, cryptococcal cerevisin *(CNAG_04625),* and cryptococcal cerevisin *(CNBJ2870)* in *Cryptococcus neoformans* after 6h and 24h of incubation, and these were potentially detected in the supernatant using the Pierce™ colorimetric protease assay kit. In literature, these serine proteases are secreted into the surrounding environment, where they are reported to breach the epithelium as part of their dissemination strategy.

Simulation runs were conducted using the HADDOCK docking programme to test if coronavirus spike protein may be a suitable substrate that may be hydrolysed by cryptococcal serine proteases. In docking, the degree of fitness of an entity at the binding domain of a protein is measured. Here, a high negative score is suggestive of better orientation and high affinity (Aribisala et al., 2022). The higher negative HADDOCK

docking score of cryptococcal serine carboxypeptidase (PDB ID: CNBF4600) and relatively comparable score of cryptococcal peptidase (CNBA1340) with that of furin in this study could be indicative of their better fitness and orientation at the binding pocket of coronavirus spike protein compared to the lower affinity observed with the other investigated proteases. The RMSD measures the degree of stability of a system, and an RMSD value of less than 3 Å is generally good and within an acceptable limit to assess the stability of a resulting protein-ligand/protein complex (Ramirez and Caballero, 2016; Feng et al., 2017; Aribisala et al., 2022). Judging by the observation with RMSD values in this study, it could be logically inferred that the lowest RMSD values observed with both cryptococcal serine carboxypeptidase (PDB ID: CNBF4600) and cryptococcal peptidase (CNBA1340), further supported their stronger affinity with the spike protein, with cryptococcal serine carboxypeptidase being the best of the docked proteases. Moreover, the buried surface area of cryptococcal serine carboxypeptidase formed the best compact macromolecular complex of all the docked proteases, as it had a high-quality association with its HADDOCK score (Venkateswarlu et al., 2023). Again, the latter points to cryptococcal serine carboxypeptidase being a better ligand to interact with the coronavirus spike protein than furin protease or cryptococcal peptidase. The observed amino acid differences highlight that the three proteases had different orientation preferences in the binding site. Similar amino acid residues for the furin protease (to the ones observed in the current study) were reported elsewhere (Vankadari, 2020). As expected, the cryptococcal serine carboxypeptidase-coronavirus spike protein complex had more hydrogen bonds, showing a strong interaction between the protein and the ligand (Rahman et al., 2021). Taken together, these results suggested that cryptococcal

proteases (potentially secreted into the supernatant) could theoretically activate the coronavirus spike protein.

In conclusion, it is important to note that HADDOCK is a computational tool that was used to predict the binding energies of unsolved structures of selected cryptococcal proteases. Therefore, the estimated energies may not correlate with binding energies realised in a solution. Because of this, enzymatic proof is required to test the docking results' veracity.

2.6 REFERENCES

1. Aribisala, J. O., Aruwa, C. E., Uthman, T. O., Nurain, I. O., Idowu, K. and Sabiu, S. (2022). Cheminformatics bioprospection of broad spectrum plant secondary metabolites targeting the spike proteins of Omicron variant and wild-type SARS-CoV-2. *Metabolites.* 12, 982. DOI:10.3390/metabo12100982
2. Bestle, D., Heindl, M. R., Limburg, H., Pilgram, O., Moulton, H., Stein, D. A. and Böttcher-Friebertshäuser, E. (2020). TMPRSS2 and furin are both essential for proteolytic activation of SARS-CoV-2 in human airway cells. *Life Sci Alliance*. 3, 1-14. DOI:10.26508/lsa.202000786
3. Crabtree, J. N., Okagaki, L. H., Wiesner, D. L., Strain, A. K., Nielsen, J. N. and Nielsen, K. (2012). Titan cell production enhances the virulence of *Cryptococcus neoformans*. *Infect Immun.* 80, 3776-85. DOI:10.1128%2FIAI.00507-12
4. Dominguez, C., Boelens, R. and Bonvin, A. M. (2003). HADDOCK: a protein−protein docking approach based on biochemical or biophysical information. *J Am Chem Soc.* 125, 1731-1737. DOI:10.1021/ja026939x
5. Eigenheer, R. A., Lee, Y. J., Blumwald, E., Phinney, B. S. and Gelli, A. (2007). Extracellular glycosylphosphatidylinositol-anchored mannoproteins and proteases of *Cryptococcus neoformans. FEMS Yeast Res*. 7, 499-510. DOI:10.1111/j.1567-1364.2006. 00198.x
6. Ekici, O. D., Paetzel, M. and Dalbey, R. E. (2008). Unconventional serine proteases: variations on the catalytic Ser/His/Asp triad configuration. *Protein Sci*. 17, 2023-2037. DOI:10.1110/ps.035436.108

7. Feng, T., Chen, F., Kang, Y., Sun, H., Liu, H., Li, D., Zhu, F. and Hou, T. (2017). HawkRank: a new scoring function for protein–protein docking based on weighted energy terms. *J Cheminform.* 9, 1-15. DOI:10.1186/s13321-017-0254-7

8. Gutierrez-Gongora, D. and Geddes-McAlister, J. (2022). Peptidases: promising antifungal targets of the human fungal pathogen, *Cryptococcus neoformans*. *FACETS.* 7, 319-342. DOI:10.1139/facets-2021-0157

9. Jaimes, J. A., Millet, J. K., Goldstein, M. E., Whittaker, G. R. and Straus, M. R. (2019). A fluorogenic peptide cleavage assay to screen for proteolytic activity: Applications for coronavirus spike protein activation. *JoVE*. 143, e58892. DOI:10.3791/58892

10. Jaimes, J. A., Millet, J. K. and Whittaker, G. R. (2020). Proteolytic cleavage of the SARS-CoV-2 spike protein and the role of the novel S1/S2 site. *IScience.* 23(6). DOI: 10.1016/j.isci.2020.101212

11. López-Otín, C. and Bond, J. S. (2008). Proteases: multifunctional enzymes in life and disease. *J Biol Chem*. 283, 30433-7. DOI:10.1074%2Fjbc.R800035200

12. Mjokane, N., Maliehe, M., Folorunso, O. S., Ogundeji, A. O., Gcilitshana, O. M., Albertyn, J., Pohl, C. H. and Sebolai, O. M. (2022). Cryptococcal protease (s) and the activation of SARS-CoV-2 spike (S) protein. *Cells.* 11, 437. DOI:10.3390/cells11030437

13. Papa, G., Mallery, D. L., Albecka, A., Welch, L. G., Cattin-Ortolá, J., Luptak, J., Paul, D., McMahon, H. T., Goodfellow, I. G., Carter, A. and Munro, S. and James, L. C. (2021). Furin cleavage of SARS-CoV-2 Spike promotes but is not essential

for infection and cell-cell fusion. *PLoS pathog*. 17, e1009246. DOI: 10.1371/journal.ppat.1009246

14. Peacock, T. P., Goldhill, D. H., Zhou, J., Baillon, L., Frise, R., Swann, O. C., Kugathasan, R., Penn, R., Brown, J. C., Sanchez-David, R. Y., Braga, L. and Barclay, W. S. (2021). The furin cleavage site in the SARS-CoV-2 spike protein is required for transmission in ferrets. *Nat Microbiol*. 6, 899-909. DOI:10.1038/s41564-021-00908-w

15. Rahman, F., Tabrez, S., Ali, R., Alqahtani, A. S., Ahmed, M.Z. and Rub, A. (2021). Molecular docking analysis of rutin reveals possible inhibition of SARS-CoV-2 vital proteins. *J Tradit Complement Med*. 11, 173-179. DOI: 10.1016/j.jtcme.2021.01.006

16. Ramírez, D. and Caballero, J. (2016). Is it reliable to use common molecular docking methods for comparing the binding affinities of enantiomer pairs for their protein target? *Int J Mol Sci*. *1*7, 525. DOI:10.3390/ijms17040525

17. van Dijk, M., van Dijk, A. D., Hsu, V., Boelens, R. and Bonvin, A. M. (2006). Information-driven protein–DNA docking using HADDOCK: it is a matter of flexibility. *Nucleic Acids Res*. 34, 3317-25. DOI:10.1093%2Fnar%2Fgkl412

18. Vankadari, N. (2020). Structure of furin protease binding to SARS-CoV-2 spike glycoprotein and implications for potential targets and virulence. *J Phys Chem Lett.* 11, 6655-6663. DOI: 10.1021/acs.jpclett.0c01698

19. Venkateswarlu, D., Duke, R. E., Perera, L., Darden, T. A. and Pedersen, L. G. (2003). An all-atom solution-equilibrated model for human extrinsic blood coagulation complex (sTF–VIIa–Xa): a protein–protein docking and molecular

dynamics refinement study. *J Thromb Haemost.* 1, 2577-2588. DOI:10.1111/j.1538-7836.2003. 00421.x

20. Villoutreix, B. O., Badiola, I. and Khatib, A. M., 2022. Furin and COVID-19: Structure, function and chemoinformatic analysis of representative active site inhibitors. *Front. Drug Discov*. 74, 425-430. DOI:10.3389/fddsv.2022.899239

CHAPTER 3:

ENZYMATIC EVIDENCE OF CRYPTOCOCCAL SUPERNATANT PROTEOLYTICALLY ACTIVATING THE SARS-COV-2 SPIKE PROTEIN

Parts of this chapter have been submitted to the Journal of Infection and Public Health for consideration.

Manuscript: Mjokane et al. Cryptococcal proteases exhibit binding affinity towards SARS-CoV-2 spike protein and mediate the transduction of HEK-293T cells by SARS-CoV-2 pseudovirions.

Author contribution: Conceptualisation, methodology, software, formal analysis, writing original draft preparation, writing review and editing.

3.1 ABSTRACT

In a priming event of some membrane-enveloped viruses such as the SARS-CoV-2, proteolytic activation by host cell proteases is critical to make the viral fusion peptide competent. Therefore, proteolytic cleavage is a fundamental biochemical process that triggers viral engulfment into the cell in order to deliver the “cargo” (RNA genome). In Chapter 2, it was predicted that cryptococcal serine proteases displayed *in silico* binding affinity to SARS-CoV-2 spike protein. However, does this (predicted binding affinity) translate to biochemical activity in solution? To test this, a fluorogenic mimetic peptide of the SARS-CoV-2 spike protein and a pseudovirion with a full-length SARS-CoV-2 spike protein were used. Both these (mimetic peptide and full-length peptide) contained the furin-like cleavage site with the canonical basic amino acid target sequence **R**-X-**R** or **R**-X-**K**↓, where X can be any amino acid residue. It was theorised that the cleavage of the target sequence would produce a reading signal that can be measured. The biochemical efficiency of cryptococcal protease(s) to mediate cleavage of a potential furin site (underlined, SP**R**RA**R**↓S) at the interface between the S1 and S2 subunit was compared to that of a recombinant furin. It was observed that cryptococcal protease(s) processes this site in a manner comparable to the efficiency of furin ($p > 0.581$). To further confirm this latter, HEK-293T cells were transduced with SARS-CoV-2 pseudovirion in the presence of furin or cryptococcal supernatant. The cryptococcal supernatant showed sufficient proteolytic activity to cleave the spike protein contained in the pseudovirion, and in turn, this was adequate to induce transduction of the pseudovirion into HEK-293T cells. Importantly, this proteolytic activity was comparable ($p < 0.05$) to that recorded for furin.

Thus, it was reasoned that the cryptococcal supernatant might contain furin-like proteases or has a common catalytic mechanistic feature as furin.

Keywords: Cryptococcal supernatant, Full-length peptide, Furin, HEK-293T cells, Mimetic peptide, SARS-CoV-2, Proteolysis, Pseudovirion, Transduction. Spike protein.

3.2 INTRODUCTION

Proteolytic cleavage is a critical biochemical process necessary for viral invasion into the host. To enter a cell, SARS-CoV-2 approaches the host receptor (ACE2) with the spike protein being exposed (Jackson et al., 2020; Zhang et al., 2021; Eslami et al., 2022). Therefore, the latent spike protein should be activated to ensure syncytium formation. This is a function that can be performed by furin, a protease that is enriched in the *trans*-Golgi network and cycles to the cell surface (Mondal et al., 2022).

Furin is a serine endopeptidase made up of 794 amino acids, and its catalysis is mechanised by the canonical catalytic triad made up of Asp153/His194/Ser368 (Thomas, 2002; Osman et al., 2022). Importantly, it cleaves its substrates after dibasic amino acids such as R-R or R-K (Sinha et al., 2023). In SARS-CoV-2 spike protein, it cleaves the amino acid sequence P**R**RA**R**^{685}↓ motif at the interface of S1/S2 and amino acid motif KPS**KR**^{815}↓S**F** in the S2' domain (Essalmani et al., 2020; Sinha et al., 2023). The consequential cleavage of these sites results in an exposed fusion peptide that can merge with the host membrane, leading to endocytosis (Li et al., 2023).

Literature shows that the yeast kexin protease (Kex2p), first identified by Fuller and co-workers, belongs to the same family and is the fungal homologue of furin (Fuller et al., 1989). These two convertases (furin and yeast kexin protease) were shown to share 50% gene sequence similarity (Fuller et al., 1989; Tanaka et al., 2003), and this, as argued by Bresnahan et al. (1990) may translate into significant functional homology. Therefore, it

was not surprising to note in Chapter 2 that selected cryptococcal proteases could theoretically bind the SARS-CoV-2 spike protein. However, as highlighted in the same Chapter, it is critical also to show enzymatic evidence of cryptococcal proteases activating the SARS-CoV-2 spike protein. To this end, this chapter aimed to determine if the cryptococcal supernatant possessed proteolytic activity sufficient to cleave a fluorogenic mimetic peptide of the SARS-CoV-2 spike protein that contained the S1/S2 site, and a full-length spike protein contained in a SARS-CoV-2 pseudovirion.

3.3 MATERIALS AND METHODS

3.3.1 Cultivation of cells

3.3.3.1 Cryptococcal cells and collection of supernatant

The standard cryptococcal reference strain of *Cryptococcus neoformans* H99 was cultivated as detailed in Chapter 2, section 2.3.1. Thereafter, the supernatant was collected likewise.

3.3.3.2 HEK 293T cells

The HEK 293T cells were maintained in Dulbecco′s Modified Eagle′s Medium (DMEM) medium that was supplemented with 10% (v/v) foetal bovine serum (Biochrom,

Germany), 20 U/mL penicillin, and 20 mg/mL streptomycin (Sigma-Aldrich) For each biological repeat, the cells were grown at 37°C and 5% CO_2 until they reached 80% confluence, and their viability was determined using the trypan blue stain. Next, the cells were standardised to reach a final cell concentration of 1 x 10^4 cells/mL in 10 mL of fresh DMEM. A 50 µL suspension of the HEK 293T cells was seeded into wells of a sterile, white disposable 96-well flat-bottom microtitre plate (Greiner Bio-One, Germany) and left overnight in a 5% CO_2 incubator at 37°C.

3.3.2 Activation of the latent SARS-CoV-2 spike protein

3.3.2.1 Fluorogenic assay: proteolytic cleavage of the latent SARS-CoV-2 spike protein

The fluorogenic assay based on the protocol of detailed in Jaimes et al. (2019, 2020), with modifications. For this assay, a synthetic peptide was especially prepared by Biomatik (Ontario, Canada) and was modified to have fluorescence intramolecular quenching capability. Importantly, the peptide contained the amino acid sequence (underlined, SP**R**RA**R**↓S) that is highly susceptible to furin hydrolysis (**Figure 3.1**). A reaction mixture for the synthesised fluorogenic mimetic peptide was carried out in a 100 µL buffer solution (pH 7.5) composed of (1) 100 mM Hepes, (2) 0.5% Triton X-100, (3) 1 mM $CaCl_2$, and (4) 1 mM 2-mercaptoethanol. Furin was diluted to 10 U/mL, and 0.5 µL was added to the reaction mixture. In a separate experiment, 0.5 µL of the cryptococcal supernatant was added. These reaction conditions were reported to activate the hydrolysis of most substrates by furin (Izodoro et al., 2009).

In the end, reactions were performed at 30 °C, and a fluorometer measured fluorescence emission every minute for 45 min. Fluorescence intensity was tracked over this time interval using the wavelength settings, i.e., excitation (λ355 nm) and emission (λ405 nm). Six independent experiments were carried out, and the means Vmax was calculated. Media not inoculated with cryptococcal cells was included as negative control. In the end, the background signal of this negative control was used for normalisation.

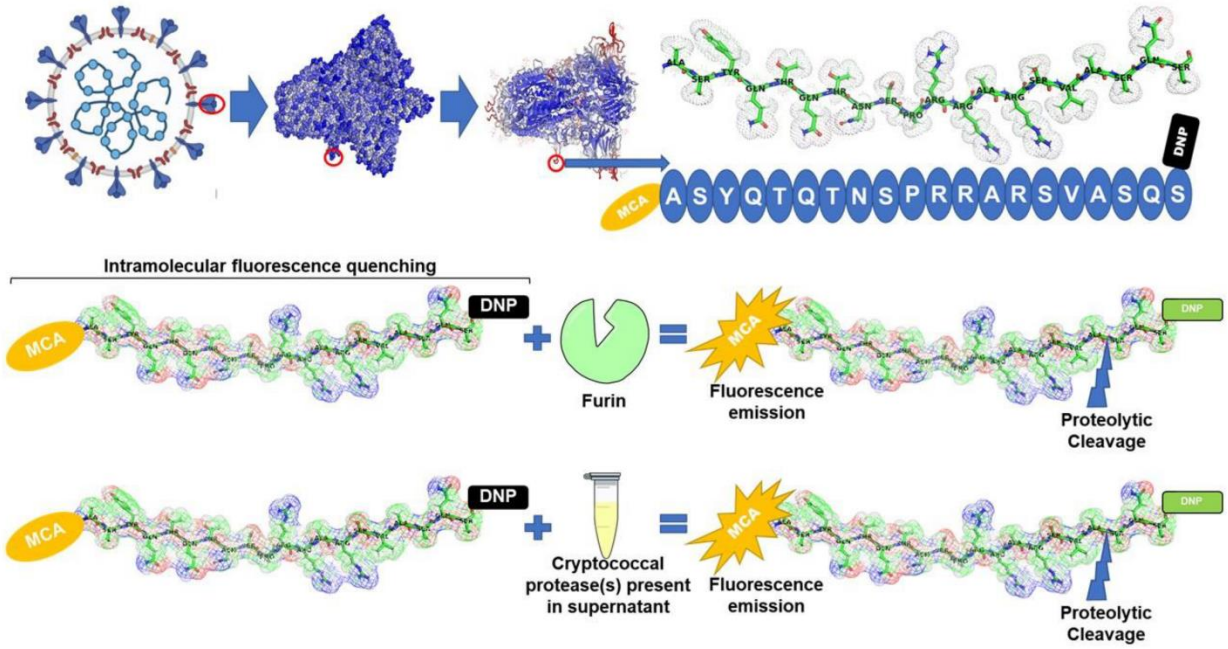

Figure 3.1. The schematic representation of the synthesised fluorogenic mimetic peptide with the unique furin cleavage site (SP**R**RA**R**↓S) that is found at the interface between the S1 and S2 site. Therefore, any mutation to the sequence would impair furin hydrolysis (Jaimes et al., 2019, 2020; Izodoro et al., 2009). The peptide was modified to have intramolecular fluorescence quenching using a FRET pair of 7-methoxycoumarin-4-yl acetyl (MCA) at the N-terminus and N-2,4-dinitrophenyl (DNP) at the C-terminus. Thus, proteolysis by either furin of cryptococcal proteases present in the supernatant would

result in the emission of fluorescence that can be measured. The figure was built using BioRender.com.

3.3.2.2 Transduction assay: proteolytic cleavage of the latent SARS-CoV-2 spike protein

The protocol from BPS Bioscience (San Diego, United States) for transducing HEK-293T cells using the SARS-CoV-2 spike pseudotyped Lentivirus (transfecting vector with all the accessory proteins for viral entry and infectivity - but devoid of the genomic material) was used. This pseudovirion also contains the firefly luciferase gene **(Figure 3.2)**.

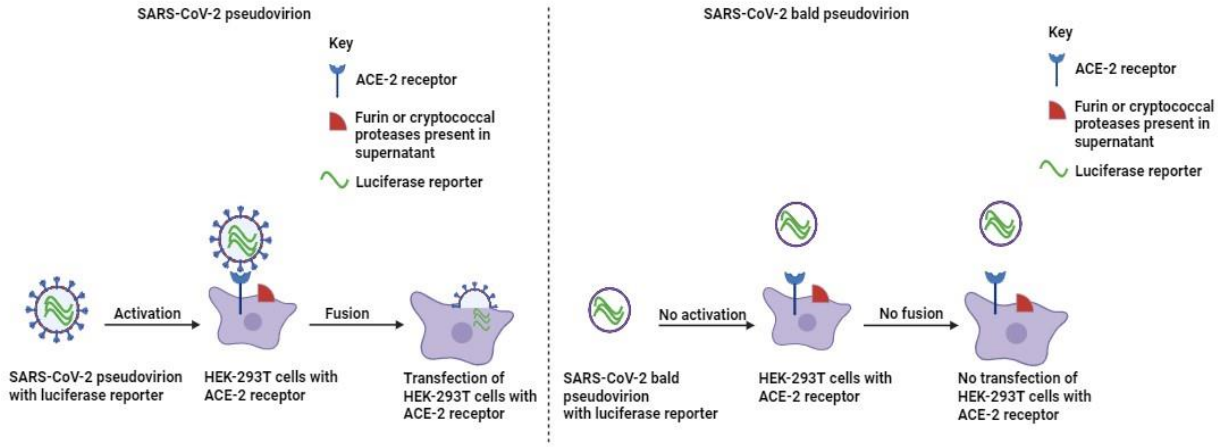

Figure 3.2. The schematic representation of a HEK-293T cell transfection by a SARS-CoV-2 pseudovirion with an intact spike glycoprotein and contains a luciferase reporter instead of the viral genetic material. Transfection could be mediated by the host furin protease or the cryptococcal supernatant, which contains proteases. The figure was built using BioRender.com.

Following overnight incubation, the spent medium was aspirated. A total of 5 µL of the pseudovirion and 44.5 µL of fresh DMEM media were added to the same wells. To initiate pseudovirion entry, 0.5 µL of the recombinant furin (New England Biolabs, Ipswich, United States) or 0.5 µL of the cryptococcal supernatant was added. The plate was incubated overnight at 37°C with 5% CO_2. The next day, the spent media was aspirated, and 50 µL of fresh DMEM media was added. The plate was incubated for 60 h at 37°C with 5% CO_2. A bald pseudovirion that lacks the SARS-CoV-2 spike protein (BPS Bioscience) was included as a control.

3.3.2.3 ONE-Step™ Luciferase assay: Infectivity measurement

The assay was performed according to the manufacturer's protocol (BPS Bioscience). The kit consisted of two components, A (reagent buffer) and B (reagent substrate). In brief, the luciferase reagent buffer (component A) was thawed at room temperature. The components (A + B) were mixed to make a working solution at a 1:100 ratio. The luciferase assay working solution component (A + B) was added directly to the culture medium using an equal volume to the volume of the culture medium, which was 50 µL. The cells were incubated for 30 min while gently rocking at room temperature. After that, luminescence was measured using a Fluoroskan Ascent FL (Thermo-Scientific, United States), which converts logarithmic signals to relative lumuniscence units (RLUs). The luminometer was programmed to perform a 10 sec measurement delay followed by a 20 sec measurement read for luciferase activity. As the DMEM was supplemented with foetal

bovine serum, which may contain proteases, it was included as a negative control. In the end, the background signal of this negative control was used for normalisation.

3.3.2 Statistical analysis

Where applicable, for each study, three independent experiments were performed. No technical repeats were included for each independent experiment. GraphPad Prism 8.0 (GraphPad Software, Inc., United States) was used to calculate the mean values, standard error mean (SEM), and the statistical significance of the data was considered at $p < 0.05$.

3.4 RESULTS

3.4.1 Cryptococcal proteases mediate the cleavage of SARS-CoV-2 mimetic peptide and the HEK-293T transduction by SARS-CoV-2 pseudovirion

Figure 3.3 shows the proteolytic cleavage results of the mimetic SARS-CoV-2 spike protein by furin or cryptococcal supernatant. Analysis of the data shows that both furin and the cryptococcal supernatant could process the unique four-amino-acid sequence (SP**R**RA**R**↓S) contained in the peptide. Importantly, the biochemical efficiency of the supernatant to cleave the target sequence was comparable to the efficiency of furin ($p > 0.581$).

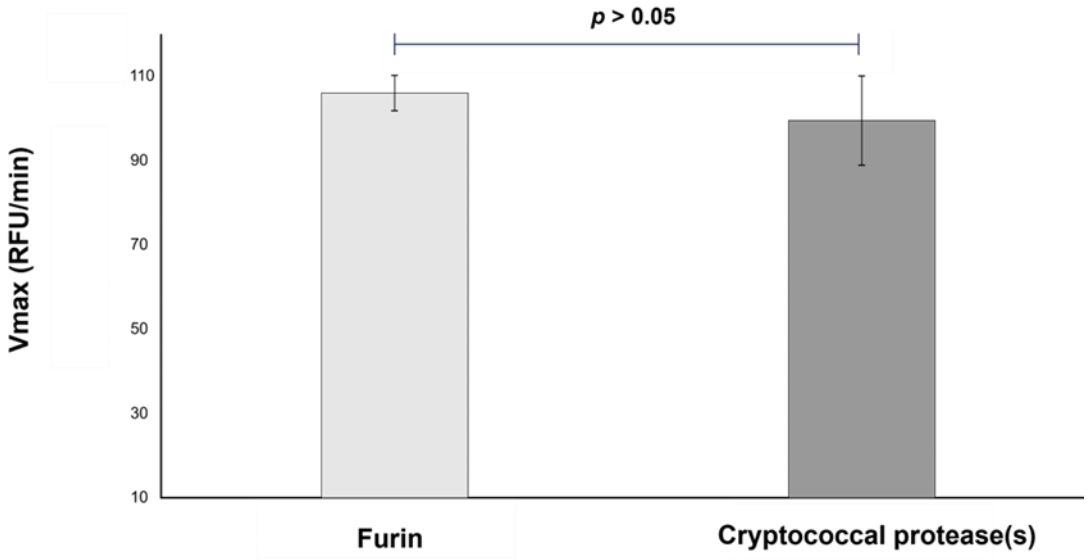

Figure 3.3. A measure of the proteolytic reaction following the cleavage of a fluorescent peptide viz. TNSPR**R**A**R**SVA (SARS-CoV-2 S1/S2), by furin or cryptococcal protease(s) present in the supernatant.

The results of the HEK-293T transduction studies are summarised in **Figure 3.4**. Here, it was noted that the biochemical efficiency of the cryptococcal supernatant (which contains secreted cryptococcal proteases) to transduce HEK-293T cells with SARS-CoV-2 pseudovirions was comparable to the recombinant furin ($p > 0.05$). As expected, zero and close to zero relative luminescence units were obtained when the bald pseudovirion was in the presence of either recombinant furin or cryptococcal supernatant. This data confirms that cryptococcal proteases can activate the SARS-CoV-2 spike protein and thus transduce the HEK-293T cells.

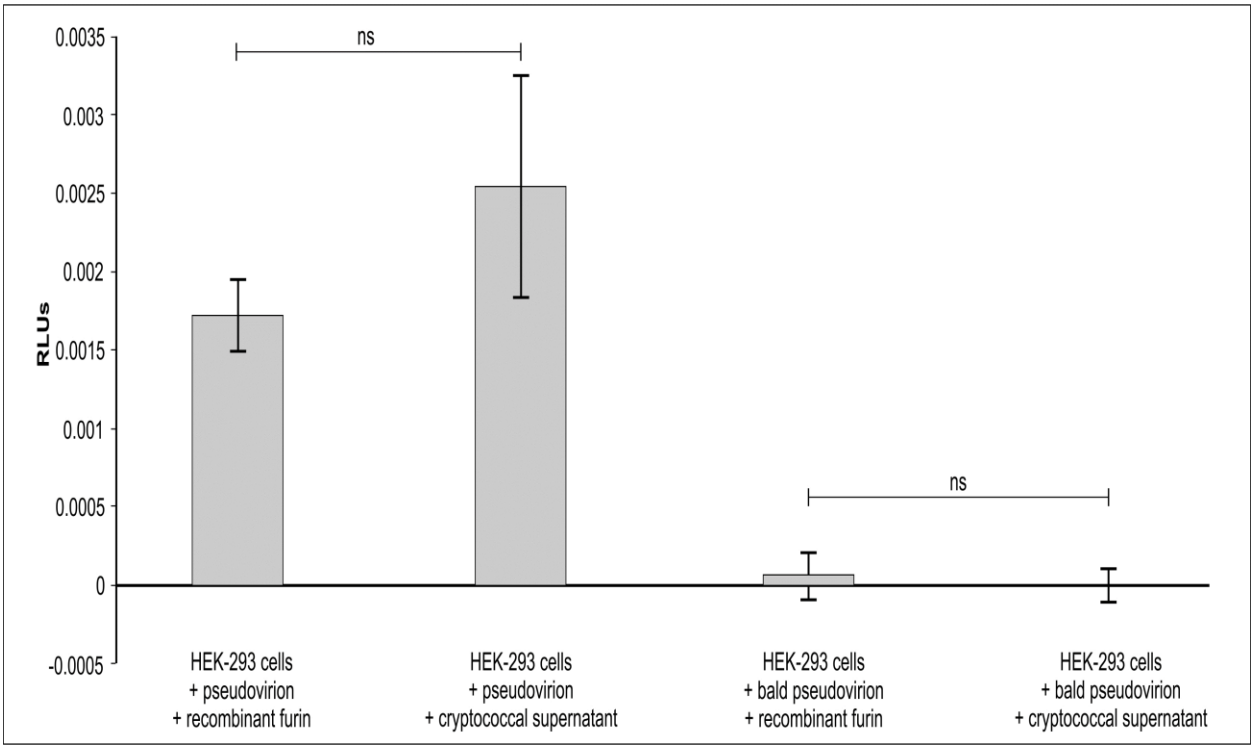

Figure 3.4. The SARS-CoV-2 spike pseudovirion infectivity in HEK-293T cells in the presence of recombinant furin or cryptococcal supernatant. The cells were infected with pseudovirion or bald pseudovirion and assessed for luciferase activity. The SARS-CoV-2 spike pseudovirion contains the luciferase gene and the spike protein. The bald SARS-CoV-2 spike pseudovirion contains the luciferase gene but lacks the spike protein. ns = not significant; RLUs = Relative Luminiscence Units.

3.5 DISCUSSION

Cryptococcus neoformans secretes serine proteases that are essential to its cellular function, including virulence. Importantly, this organism has yeast kexin protease (Kex2p), which has functional homology to the mammalian furin (Bresnahan et al., 1990).

Therefore, these cryptococcal proteases are expected to activate latent protein precursors processed by furin. In the case of the SARS-CoV-2 spike, protein cleavage would occur after dibasic amino acids R-R or R-K, i.e., PR**R**A**R** (Bestle et al., 2020; Essalmani et al., 2022).

To test the above, a biochemical peptide cleavage assay was designed. This assay is well established and has been used to assess the activation of various latent viral glycoproteins. For example, Jaimes et al. (2020) reported that the assay could be modified to screen for the activation of the influenza haemagglutinin Straus and Whittaker, (2017), feline coronavirus spike protein, and MERS-CoV spike protein (Licitra et al., 2013; Millet et al., 2016). In the current study, it was determined that the cryptococcal supernatant could, similarly to furin, activate the SARS-CoV-2 spike protein. An important point to consider is, as highlighted by Jaimes et al. it is conceivable that a purified full-length SARS-CoV-2 spike protein might not be cleaved in a similar manner (due to differences in conformation as it may not resemble the original folding of the full-length protein) to the memetic peptide used in the current study (Jaimes et al., 2020). Therefore, it was prudent to validate the work using a full-length spike protein. Hence the transduction studies.

Successful viral entry requires a number of important components, and these include a host with an ACE-2 receptor to infect and a serine protease for cleavage. To model this, a SARS-CoV-2 pseudovirion was used. The latter is an alternative approach to studying pathogenic viruses, especially highly infectious ones, outside a biosafety level 3 or 4

laboratory. The used pseudovirion had a full-length SARS-CoV-2 spike protein in the correct conformation, including the furin cleavage site. Thus, its processing would result in the delivery of the luciferase RNA into the HEK-293T cells. And it was possible to demonstrate that cryptococcal supernatant could also activate the full-length peptide, thus, in turn, corroborating the results of the mimetic peptide.

In conclusion, altogether these findings suggest that in clinical practice, it is foreseeable that cryptococcal proteases could activate the latent SARS-CoV-2 spike protein during co-infection.

3.6 REFERENCES

1. Bestle, D., Heindl, M. R., Limburg, H., Pilgram, O., Moulton, H., Stein, D. A., Hardes, K., Eickmann, M., Dolnik, O., Rohde, C. and Klenk, H. D. (2020). TMPRSS2 and furin are both essential for proteolytic activation of SARS-CoV-2 in human airway cells. *Life Sci Alliance.* 3, 1-14. DOI:10.26508/lsa.202000786
2. Bresnahan, P. A., Leduc, R., Thomas, L., Thorner, J., Gibson, H. L., Brake, A. J., Barr, P. J. and Thomas, G. (1990). Human fur gene encodes a yeast KEX2-like endoprotease that cleaves pro-beta-NGF *in vivo*. *J Cell Biol.* 111, 2851-2859. DOI:10.1083/jcb.111.6.2851
3. Eslami, N., Aghbash, P. S., Shamekh, A., Entezari-Maleki, T., Nahand, J. S., Sales, A. J. and Baghi, H. B. (2022). SARS-CoV-2: receptor and co-receptor tropism probability. *Curr Microbiol.* 79, 1-13. DOI:10.1007%2Fs00284-022-02807-7
4. Essalmani, R., Jain, J., Susan-Resiga, D., Andréo, U., Evagelidis, A., Derbali, R. M., Huynh, D. N., Dallaire, F., Laporte, M., Delpal, A. and Sutto-Ortiz, P. (2020). SARS-CoV-2 spike-glycoprotein processing at S1/S2 and S2'and shedding of the ACE2 viral receptor: roles of Furin and TMPRSS2 and implications for viral infectivity and cell-to-cell fusion. *J Virol.* 96, 1-24. DOI:10.1128/jvi.00128-22
5. Fuller, R. S., Brake, A. J. and Thorner, J. (1989). Intracellular targeting and structural conservation of a prohormone-processing endoprotease. *Science.* 246, 482-486. DOI:10.1126/science.2683070

6. Izidoro, M. A., Gouvea, I. E., Santos, J. A., Assis, D. M., Oliveira, V., Judice, W. A., Juliano, M. A., Lindberg, I. and Juliano, L. (2009). A study of human furin specificity using synthetic peptides derived from natural substrates, and effects of potassium ions. *Arch Biochem Biophys*. 487, 105-114. DOI: 10.1016/j.abb.2009.05.013

7. Jaimes, J. A., Millet, J. K. and Whittaker, G. R. (2020). Proteolytic cleavage of the SARS-CoV-2 spike protein and the role of the novel S1/S2 site. *IScience,* 23, 1-5. DOI: 10.1016/j.isci.2020.101212

8. Jackson, C. B., Farzan, M., Chen, B. and Choe, H. (2022). Mechanisms of SARS-CoV-2 entry into cells. *Nat Rev Mol Cell Biol.* 23, 3-20. DOI:10.1038/s41580-021-00418-x

9. Li, X., Yuan, H., Li, X. and Wang, H. (2023). Spike protein mediated membrane fusion during SARS-CoV-2 infection. *J Med Virol.* 95, e28212. DOI:10.1002/jmv.28212

10. Licitra, B. N., Millet, J. K., Regan, A. D., Hamilton, B. S., Rinaldi, V. D., Duhamel, G. E. and Whittaker, G. R. (2013). Mutation in spike protein cleavage site and pathogenesis of feline coronavirus*. Emerg Infect Dis.* 19, 1066-1073. DOI:10.3201/eid1907.121094

11. Millet, J. K., Goldstein, M. E., Labitt, R. N., Hsu, H. L., Daniel, S. and Whittaker, G. R. (2016). A camel-derived MERS-CoV with a variant spike protein cleavage site and distinct fusion activation properties. *Emerg Microbes Infect.* 5, 1-9. DOI:10.1038%2Femi.2016.125

12. Mondal, T., Shivange, G., Habieb, A. and Tushir-Singh, J. (2022). A feasible alternative strategy targeting furin disrupts SARS-CoV-2 infection cycle. *Microbiol Spectrum*. 10, e02364-21. DOI:10.1128/spectrum.02364-21

13. Osman, E. E., Rehemtulla, A. and Neamati, N. (2021). Why all the fury over furin? *J Med Chem*. 65, 2747-84. DOI: 10.1021/acs.jmedchem.1c00518

14. Sinha, A., Sangeet, S. and Roy, S. (2023). Evolution of sequence and structure of SARS-CoV-2 spike protein: A dynamic perspective. *ACS Omega.* 8, 23283-23304. DOI:10.1021/acsomega.3c00944

15. Straus, M. R. and Whittaker, G. R. (2017). A peptide-based approach to evaluate the adaptability of influenza A virus to humans based on its hemagglutinin proteolytic cleavage site. *PloS one*. 12, 1-17. DOI: 10.1371/journal.pone.0174827

16. Tanaka, S. (2003). Comparative aspects of intracellular proteolytic processing of peptide hormone precursors: studies of proopiomelanocortin processing. *Zoolog Sci.* 20, 1183-1198. DOI:10.2108/zsj.20.1183

17. Thomas, G. (2002). Furin at the cutting edge: from protein traffic to embryogenesis and disease. *Nat Rev Mol Cell Biol.* 3, 753-66. DOI:10.1038/2Fnrm934

18. Zhang, Q., Xiang, R, Huo, S., Zhou, Y, Jiang, S., Wang, Q. and Yu F. (2021). Molecular mechanism of interaction between SARS-CoV-2 and host cells and interventional therapy. *Signal Transduct Target Ther.* 6, 1-19. DOI:10.1038/s41392-021-00653-w

CHAPTER 4:

GENERAL DISCUSSION AND CONCLUSIONS

4.1 GENERAL DISCUSSION AND CONCLUSIONS

Cryptococcus neoformans is an important fungal pathogen that can cause life-threatening infections in susceptible hosts (Buchanan and Murphy, 1998; Almeida and Casadevall, 2015; Zaragoza, 2019). Its infection, similar to SARS-CoV-2, begins with its inhalation and lodging on the alveolar to cause cryptococcal pneumonia. Therein, in the alveolar space, it can co-occur with other respiratory pathogens and cause co-infections (Ma et al., 2020; Chakravarty et al., 2023). One such pathogen, as documented in this thesis, is SARS-CoV-2. Unfortunately, viral and microbial co-infections are often reported to be severe and result in higher mortality than that of either infection on its own. For example, in a clinical case-control study, it was reported that patients had adverse outcomes, such as dying from sepsis after 10 days of cryptococcemia (Khatib et al., 2021).

Cryptococcal cells are well-endowed with hydrolytic enzymes, such as serine proteases, among other enzymes (Campbell et al., 2015; Mjokane et al., 2021). Pathogenic fungi are said to often use proteases in furtherance of virulence by compromising the host basal membrane; this allows the fungus to invade or escape certain organ systems (Vu et al., 2014; 2019; Chen et al., 2022). Cryptococcal cells, in particular, have been shown to produce a subtilisin-like serine protease belonging to the kexin family, which is also reported to be involved in melanin production, although the exact mechanism is unknown (Clarke et al., 2016; Gutierrez-Gongora and Geddes-McAlister, 2022). Importantly, this yeast kexin protease shares functional homology with the mammalian furin protease (Fuller et al., 1989; Bresnahan et al., 1990; Tanaka, 2003). This implies that cryptococcal

yeast kexin and furin can process latent proteins that display the preferred consensus sequence **R**-X-**R** or **R**-X-**K**↓. This suggests that during a SARS-CoV-2-*Cryptococcus neoformans* co-infection, SARS-CoV-2 can equally pervert cryptococcal yeast kexin protease and use it to activate its latent spike protein. To illustrate this point, in **Figure 4.1**, *Cryptococcus neoformans* is shown colonising the epithelial cells and secreting serine proteases. The secreted proteases could interact with the latent SARS-CoV-2 spike protein and, in turn, activate it, thus allowing for host invasion to take place.

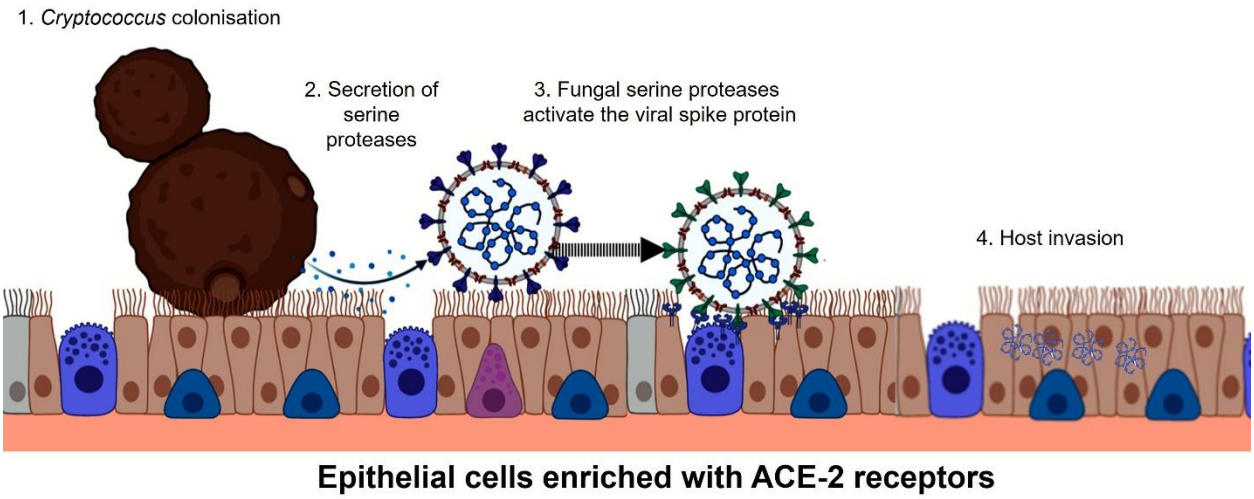

Figure 4.1. A pictogram depicting the involvement of secreted cryptococcal serine proteases in the activation of the SARS-CoV-2 spike protein, ultimately promoting the host invasion. The image was drawn using BioRender.com.

The possible activation of the SARS-CoV-2 spike protein, is observed in the analysis of several experimental outcomes documented in this thesis. This included the confirmation of the HADDOCK docking results via cleavage of the mimetic SARS-CoV-2 peptide and the transduction of HEK 293T cells using SARS-CoV-2 pseudovirion with a full-length spike protein.

Moreover, it is critical to determine if this is a quality limited to *Cryptococcus neoformans* or if it is possible for other respiratory fungal pathogens to also activate latent SARS-CoV-2 spike protein. This is a question addressed in Addendum no. 1. The Addendum shows that *Aspergillus fumigatus* can also activate the SARS-CoV-2 spike protein. Like *Cryptococcus neoformans*, this fungus also produces yeast kexin proteases that are critical for its growth (Jalving et al., 2000; Wang et al., 2015). The versatility of microbial furin-like proteases in activating latent viral glycoproteins extends to processing the influenza haemagglutinin protein and HIV-1 glycoproteins, among other glycoproteins (Stieneke-Gröber et al., 1992; Moulard et al., 1994; Tang et al., 2021).

The above highlights that the control of proteolytic activity could limit the activation of the SARS-CoV-2 spike protein. Here, a protease inhibitor could prove useful in limiting unwanted proteolysis by either fungal or mammalian proteases. This is a question addressed in Addendum no. 2. In the Addendum, it was sought to make the study locally relevant and thus opted to assess the inhibitory effect of the South African-based medicinal plant *Artemisia afra* hot tea infusion extract and its active compound artemisinin in disrupting the activation of the mimetic SARS CoV-2 spike protein by furin and the cryptococcal supernatant. In South Africa, like many other parts of the developing world, a significant portion of the population relies on traditional medicines for their curative qualities. While the hot tea infusion extract and artemisinin could disrupt furin, the same result was not observed for the cryptococcal supernatant. This may be because the supernatant contains a number of molecules. To this end, a future study should consider purifying the supernatant and isolating the cryptococcal yeast kexin protease(s). Here,

showing that the isolated cryptococcal protease could yield similar transduction results or lead to successful invasion in a laboratory animal would be prudent. In the context of the latter, a GFP-labelled model could be an option.

4.2 REFERENCES

1. Almeida, F., Wolf, J. M. and Casadevall, A. (2015). Virulence-associated enzymes of *Cryptococcus neoformans*. *Eukaryot cell.* 14(12), 1173-1185. DOI:10.1128/ec.00103-15
2. Bresnahan, P. A., Leduc, R., Thomas, L., Thorner, J., Gibson, H. L., Brake, A. J., Barr, P. J. and Thomas, G. (1990). Human FUR gene encodes a yeast KEX2-like endoprotease that cleaves pro-beta-NGF *in vivo*. *J Cell Biol.* 111, 2851-2859. DOI:10.1083/jcb.111.6.2851
3. Buchanan, K. L. and Murphy, J. W. (1998). What makes *Cryptococcus neoformans* a pathogen? *Emerg Infect Dis*. 4, 71-83. DOI:10.3201/2Feid0401.980109
4. Campbell, L. T., Simonin, A. R., Chen, C., Ferdous, J., Padula, M. P., Harry, E. and Carter, D. A. (2015). *Cryptococcus* strains with different pathogenic potentials have diverse protein secretomes. *Eukaryot Cell.* 14, 554-563. DOI:10.1128/ec.00052-15
5. Chakravarty, A., Panchagnula, M. V. and Patankar, N. A. (2023). Inhalation of virus-loaded droplets as a clinically plausible pathway to deep lung infection. *Front Physiol.* 14, 1073165. DOI:10.3389/2Ffphys.2023.1073165
6. Chen, Y., Shi, Z. W., Strickland, A. B. and Shi, M. (2022). *Cryptococcus neoformans* infection in the central nervous system: the battle between host and pathogen. *J Fungi.* 8, 1069. DOI:10.3390/jof8101069

7. Clarke, S. C., Dumesic, P. A., Homer, C. M., O'Donoghue, A. J., La Greca, F., Pallova, L., Majer, P., Madhani, H. D. and Craik, C. S. (2016). Integrated activity and genetic profiling of secreted peptidases in *Cryptococcus neoformans* reveals an aspartyl peptidase required for low pH survival and virulence. *PLoS pathog*. 12, e1006051. DOI: 10.1371/journal.ppat.1006051

8. Fuller, R. S., Brake, A. J. and Thorner, J. (1989). Intracellular targeting and structural conservation of a prohormone-processing endoprotease. *Science*. 246, 482-486. DOI:10.1126/science.2683070

9. Gutierrez-Gongora, D. and Geddes-McAlister, J. (2022). Peptidases: promising antifungal targets of the human fungal pathogen, *Cryptococcus neoformans. FACETS.* 7, 319-342. DOI:10.1139/facets-2021-0157

10. Jalving, R., van de Vondervoort, P. J., Visser, J. and Schaap, P. J. (2000). Characterization of the kexin-like maturase of *Aspergillus niger. Appl Environ Microbiol*. 66, 363-368. DOI:10.1128/2Faem.66.1.363-368.2000

11. Khatib, M. Y., Ahmed, A. A., Shaat, S. B., Mohamed, A. S. and Nashwan, A. J. (2021). Cryptococcemia in a patient with COVID-19: A case report. *Clin Case Rep.* 9, 853-855. DOI:10.1002/ccr3.3668

12. Ma, L., Wang, W., Le Grange, J. M., Wang, X., Du, S., Li, C. and Zhang, J. N. (2020). Coinfection of SARS-CoV-2 and other respiratory pathogens*. Infect Drug Resist.* 13, 3045-3053. DOI:10.2147/2FIDR.S267238

13. Mjokane, N., Folorunso, O. S., Ogundeji, A. O. and Sebolai, O. M. (2021). The Possible Role of Microbial Proteases in Facilitating SARS-CoV-2 Brain Invasion. *Biology.* 10, 1-13. DOI:10.3390/2Fbiology10100966

14. Moulard, M., Achstetter, T., Kieny, M. P., Montagnier, L. and Bahraoui, E. (1994). Kex2p: a model for cellular endoprotease processing human immunodeficiency virus type 1 envelope glycoprotein precursor. *Europ J Biochem*. 225, 565-572. DOI:10.1111/j.1432-1033.1994. 00565.x

15. Stieneke-Gröber, A., Vey, M., Angliker, H., Shaw, E., Thomas, G., Roberts, C. and Garten, W. (1992). Influenza virus hemagglutinin with multibasic cleavage site is activated by furin, a subtilisin-like endoprotease. *EMBO J.* 11, 2407-2414. DOI:10.1002/j.1460-2075.1992.tb05305.x

16. Tang, T., Jaimes, J. A., Bidon, M. K., Straus, M. R., Daniel, S. and Whittaker, G. R. (2021). Proteolytic activation of SARS-CoV-2 spike at the S1/S2 boundary: potential role of proteases beyond furin. *ACS Infect Dis*. 7, 264-272. DOI:10.1021/acsinfecdis.0c00701

17. Vu, K., Tham, R., Uhrig, J. P., Thompson III, G. R., Na Pombejra, S., Jamklang, M. and Gelli, A. (2014). Invasion of the central nervous system by *Cryptococcus neoformans* requires a secreted fungal metalloprotease. *MBio.* 5, 10-1128. DOI:10.1128/mbio.01101-14

18. Vu, K., Garcia, J. A. and Gelli, A. (2019). Cryptococcal meningitis and anti-virulence therapeutic strategies. *Front Microbiol.* 10, 353. DOI:10.3389/fmicb.2019.00353

19. Tanaka, S. (2003). Comparative aspects of intracellular proteolytic processing of peptide hormone precursors: studies of proopiomelanocortin processing. *Zoolog Sci*. 20, 1183-1198. DOI:10.2108/zsj.20.1183

20. Wang, J., Zhou, H., Lu, H., Du, T., Luo, Y., Wilson, I. B. and Jin, C. (2015). Kexin-like endoprotease KexB is required for N-glycan processing, morphogenesis and virulence in *Aspergillus fumigatus. Fungal Genet Biol.* 76, 57-69. DOI: 10.1016%2Fj.fgb.2015.02.006

21. Zaragoza, O. (2019). Basic principles of the virulence of *Cryptococcus. Virulence.* 10, 490-501. DOI:10.1080/21505594.2019.1614383

ADDENDUM NO. 1:

ASPERGILLUS FUMIGATUS SECRETES A PROTEASE(S) THAT DISPLAYS *IN SILICO* BINDING AFFINITY TOWARDS THE SARS-COV-2 SPIKE PROTEIN AND MEDIATES SARS-COV-2 PSEUDOVIRION ENTRY INTO HEK 293T CELLS

This addendum is intended to show that other respiratory fungal pathogens can also secrete furin-like proteases. Importantly, these proteases can likewise process the latent SARS-CoV-2 spike protein. Parts of this addendum have been submitted to Virology Journal for consideration.

Author contribution: Conceptualisation, methodology, software, formal analysis, writing original draft preparation, writing review and editing.

Collection of *A. fumigatus* supernatant and detection of protease(s) in the supernatant

A. fumigatus strain was cultured on potato dextrose agar slants (PDA) agar (200 g/L potato infusion, 20 g/L dextrose, 20 g/L agar (Merck, South Africa)) and incubated for 24 h at 30°C. Following this, a loopful of fungal colonies were picked and inoculated into a 250 mL conical flask that contained 100 mL of fresh, sterile YNB (6.7 g/L; Thermo Fisher Scientific, South Africa) broth that was supplemented with glucose (4%; w/v; Merck, South Africa). Next, the flask was then incubated at 30°C for 32 h while agitated at 160 rpm on an orbital shaker (Lasec, South Africa). After 32 h, 25 mL of the culture media was then dispensed into a 50 mL centrifuge tube. The tube was centrifuged at 1000 × *g* for 5 min at 30°C to pellet the cells and mobilise the *Aspergillus* protease(s) into the supernatant. To confirm the mobilisation of the protease(s) into the supernatant, it was tested with a Pierce™ Colorimetric Protease Assay Kit (Thermo Fisher Scientific) in accordance with the manufacturer's protocol. The Kit detects the total protease activity in the tested sample.

Molecular docking studies: protein acquisition, preparation, and molecular docking

The X-ray crystal structures of the solved SARS-CoV-2 spike glycoprotein (PDB ID: 6VXX) and solved *homo sapiens* furin protease (PDB ID: 5JXH) were obtained from the Research Collaboratory for Structural Bioinformatics (RCSB) Protein Data Bank (PDB) (https://www.rcsb.org) while the predicted structure of *A. fumigatus* alkaline protease 1 (PDB ID: AFUA_4G11800) was obtained from UniProt Protein Data Bank (https://www.uniprot.org). **Table 1** shows the proteases used in this study.

Table 1 Furin and *A. fumigatus* alkaline protease 1 and their proposed function in the context of COVID-19 development.

Protease	**Type of protease**	**Source**	**Function(s) in source organism**	**Function in the context of SARS-CoV-2 infection**
Furin protease (PDB ID: 5JXH)	Serine-based	*Homo sapiens*	Activates proprotein substrates (Villoutreix et al., 2022).	Proteolytic cleavage of the viral S1/S2 site (Jaimes et al., 2020; Izidoro et al., 2009; Mjokane et al., 2022)

Table 1 (continued). Furin and *A. fumigatus* alkaline protease 1 and their proposed function in the context of COVID-19 development.

Protease	Type of protease	Source	Function(s) in source organism	Function in the context of SARS-CoV-2 infection
A. fumigatus alkaline protease 1 (PDB ID: AFUA_4G11800)	Serine-based	*Aspergillus fumigatus*	Help to disrupt the host structural barriers (Druey et al., 2020) .	Suggested to act on the furin cleavage site within the S1/S2 site Mjokane et al., 2022).

These structures were optimised *in silico* by removing water molecules and non-standard naming protein residue connectivity (Aribisala et al., 2022). Molecular docking of the structures: SARS-CoV-2 spike protein (target) and furin protease (ligand), or SARS-CoV-2 spike protein (target) and *A. fumigatus* alkaline protease 1 (ligand), were performed using the open-source computational tool known as the high ambiguity driven protein-protein docking (HADDOCK) (https://haddock.science.uu.nl) (Dominguez et al., 2003). This tool was used to analyse the protein-protein interactions through the HADDOCK score, root-mean-square deviation (RMSD), Van der Waals energy, electrostatic energy, desolvation energy, restraints violation energy, and buried surface area.

A. fumigatus supernatant and the proteolytic cleavage of the SARS-CoV-2 mimetic peptide

A reaction mixture for the synthesised fluorogenic mimetic peptide was carried out in a 100 µL buffer solution (pH 7.5) composed of (1) 100 mM Hepes (Merck, South Africa), (2) 0.5% Triton X-100 (Merck, South Africa), (3) 1 mM $CaCl_2$ (Merck, South Africa), and (4) 1 mM 2-mercaptoethanol (Merck, South Africa). Furin was diluted to 10 U/mL, and 0.5 µL was added to the reaction mixture. In a separate experiment, 0.5 µL of the *A. fumigatus* supernatant was added. Reactions were performed at 30 °C, and a fluorometer measured fluorescence emission every minute for 45 min. Fluorescence intensity was tracked over this time interval using the wavelength settings, i.e., excitation (λ355 nm) and emission (λ405 nm). Six independent experiments were carried out, and the means Vmax was calculated.

A. fumigatus supernatant and the transduction of HEK-293T cells by SARS-CoV-2 pseudovirion

Cultivation of HEK-293T cells

The HEK-293T cells were maintained in DMEM medium that was supplemented with 10% (v/v) foetal bovine serum (Biochrom, Germany), 20 U/mL penicillin (Sigma-Aldrich, United States), and 20 mg/mL streptomycin (Sigma-Aldrich). For each biological repeat, the cells

were grown at 37°C and 5% CO_2 until they reached 80% confluence, and their viability was determined using the trypan blue stain (Sigma-Adrich). Next, the cells were standardised to reach a final cell concentration of 1 x 10^4 cells/mL in 10 mL of fresh DMEM (Sigma-Aldrich). A 50 µL suspension of the HEK-293T cells was seeded into wells of a sterile, white disposable 96-well flat-bottom microtitre plate (Greiner Bio-One, Germany) and left overnight in a 5% CO_2 incubator at 37°C.

SARS-CoV-2 pseudovirion entry assay

The protocol from BPS Bioscience for transducing HEK-293T cells using the SARS-CoV-2 spike pseudotyped Lentivirus (transfecting vector with all the accessory proteins for viral entry and infectivity - but devoid of the genomic material) was used (BPS Bioscience, United States). This pseudovirion also contains the firefly luciferase gene. Following overnight incubation, the spent media was aspirated. A total of 5 µL of the pseudovirion and 44.5 µL of fresh DMEM media were added to the same wells. To initiate pseudovirion entry, 0.5 µL of the recombinant furin (New England Biolabs, United States) or 0.5 µL of the *A. fumigatus* supernatant was added. The plate was incubated overnight at 37°C with 5% CO_2. The next day, the spent media was aspirated, and 50 µL of fresh DMEM media was added. The plate was incubated for 60 h at 37°C with 5% CO_2. A bald pseudovirion that lacks the SARS-CoV-2 spike protein (BPS Bioscience) was included as a control.

The use of the ONE-Step™ luciferase assay to measure infectivity

The assay was performed according to the manufacturer's protocol (BPS Bioscience). The kit consisted of two components, A (reagent buffer) and B (reagent substrate). In brief, the luciferase reagent buffer (component A) was thawed at room temperature. The components (A + B) were mixed to make a working solution at a 1:100 ratio. The luciferase assay working solution component (A + B) was added directly to the culture medium using an equal volume to the volume of the culture medium, which was 50 µL. The cells were incubated for 30 min while gently rocking at room temperature. After that, luminescence was measured using a Fluoroskan Ascent FL, which converts logarithmic signals to relative luminescence units (RLUs). The luminometer was programmed to perform a 10-sec measurement delay followed by a 20-sec measurement read for luciferase activity. As the DMEM was supplemented with foetal bovine serum, which may contain proteases, it was included as a negative control. In the end, the background signal of this negative control was used for normalisation.

Statistical analysis

Where applicable, for each study, three independent experiments were performed. No technical repeats were included for each independent experiment. GraphPad Prism 8.0 (GraphPad Software, Inc., United States) was used to calculate the mean values,

standard error mean (SEM), and the statistical significance of the data was considered at $p < 0.05$.

RESULTS

The *A. fumigatus* supernatant contains protease(s) that theoretically activate the SARS-CoV-2 spike protein

The Pierce™ protease assay data are summarised in **Figure 1.** Analyses of the data confirmed that the tested supernatant contained protease activity when compared to absorbance readings obtained against the standard protease provided in the Kit. As a negative control, blank control without the protease and the peptide was included and on separate wells, peptide control without the protease was included. In the end, the background signal of these negative controls was used for normalisation. And by necessary implication, we hypothesised that the *A. fumigatus* alkaline protease 1 is present in the tested supernatant. Therefore, to determine if the observed supernatant activity could translate into activation of the SARS-CoV-2 spike protein, the docking results were considered. Here, the *in silico* comparative analysis data of the docking parameters of SARS-CoV-2 spike protein with furin protease or *A. fumigatus* alkaline protease 1 is detailed in **Table 2.**

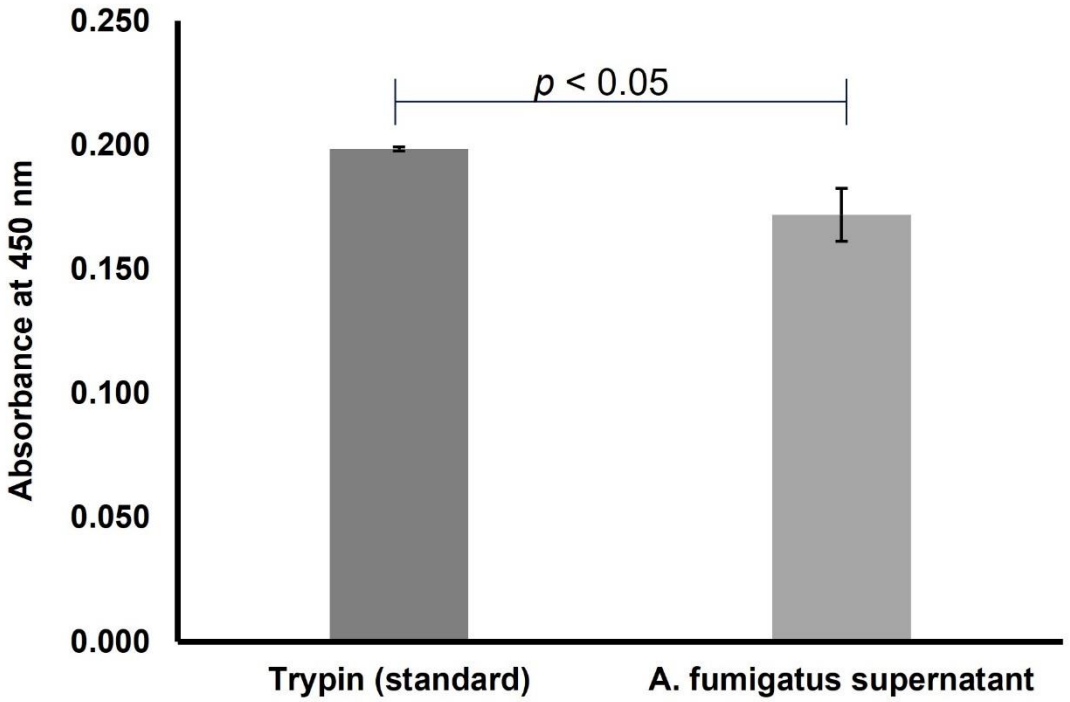

Figure 1. The detection of *A. fumigatus* secreted protease(s) present in the supernatant.

We recorded a HADDOCK score of -79.6 ± 0.1 when furin protease-SARS-CoV-2 spike protein was docked. In contrast, the docking of *A. fumigatus* alkaline protease 1-SARS-CoV-2 spike protein gave a comparable score of -156.2 ± 0.0 ($p < 0.05$) to furin protease. The average RMSD value and Z-score of furin protease in complex with SARS-CoV-2 spike protein were 28.4 ± 0.0 Å and -1.0, and that of *A. fumigatus* alkaline protease 1 were 0.0 ± 0.0 Å and -2.7 ± 0.0 (**Table 2**). The Van der Waals energy and electrostatic energy that contribute to the binding strength for each complex were calculated. For the furin protease-SARS-CoV-2 spike protein complex, the Van der Waals and electrostatic energy values were -50.9 ± 0.1 kcal/mol and -128.1 ± 7.8 kcal/mol, respectively. Compared to these, *A. fumigatus* alkaline protease 1-SARS-CoV-2 spike protein complex

had scores of -77.9 ± 0.0 kcal/mol (Van der Waals energy) and -308.6 ± 0.0 kcal/mol (electrostatic energy).

The buried surface area, i.e., the amount of protein surface not in contact with water upon complexation, data was calculated and analysed. Here, it was noted that the *A. fumigatus* alkaline protease 1 had a score of 3471.7 ± 0.0 $Å^2$ while that of the furin protease (1796.7 ± 18.9 $Å^2$). The furin protease's desolvation energy (-3.6 ± 1.5 kcal/mol) and restraint violation energy (4.9 ± 1.0 kcal/mol) were observed to be far less than the buried surface area score (1796.7 ± 18.9 $Å^2$). Similar readings were obtained for the *A. fumigatus* alkaline protease 1. This protease had a score desolvation energy of -16.5 ± 0.0 kcal/mol and restraint violation energy of 0.0 ± 0.0 kcal/mol (**Table 2**).

In **Figure 2,** we provide information related to the surface representation of the docked complexes, i.e., furin protease-SARS-CoV-2 spike protein and *A. fumigatus* alkaline protease 1-SARS-CoV-2 spike protein – at their respective optimal orientation. We further summarise the characteristic amino acid residues for each protease that were poised to interact with the spike protein cleavage site in the docked complex structures, in **Figure 3**. The furin protease interacted with Q111, E112, P113, T143, H145, G146, N159, H160, P161, D162, L163, A164, G165, N166, D168, P169, G170, V205, A206, N207, N208, G209, V210, Y217, N218, R220, and H246 at the binding pocket of the spike protein.

Table 2 The intermolecular binding energies of the docked furin-SARS-CoV-2 spike protein complex and *A. fumigatus* alkaline protease 1-SARS-CoV-2 spike protein. HADDOCK.

Protease	**Z-score**	**RMSD (Å)**	**HADDOCK score**	**Van der Waals energy (kcal/mol)**	**Electrostatic energy (kcal/mol)**	**Desolvation energy (kcal/mol)**	**Restraints violation energy (kcal/mol)**	**Buried surface area (Å²)**
Furin protease (PDB ID: 5JXH)	-1.0	28.4 ± 0.0	-79.6 ± 0.1	-50.9 ± 0.1	-128.1 ± 7.8	-3.6 ± 1.5	4.9 ± 1.0	1796.7 ± 18.9
A. fumigatus Alkaline protease 1 (PDB ID: AFUA_4G11800)	-2.7± 0.0	0.0 ± 0.0	-156.2 ± 0.0	77.9 ± 0.0	-308.6 ± 0.0	-16.5 ± 0.0	0.0 ± 0.0	3471.7 ± 0.0

Proteases	Surface representation of the interactions
Furin protease (5JXH)	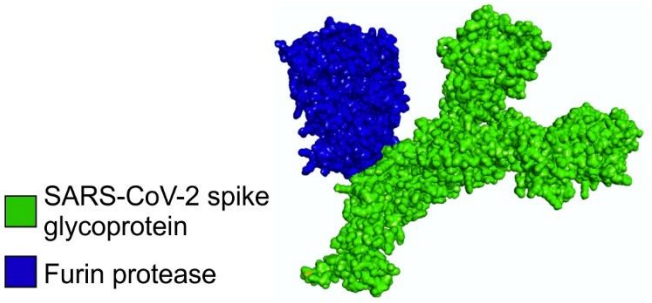
A. fumigatus alkaline protease 1 (AFUA_4G11800)	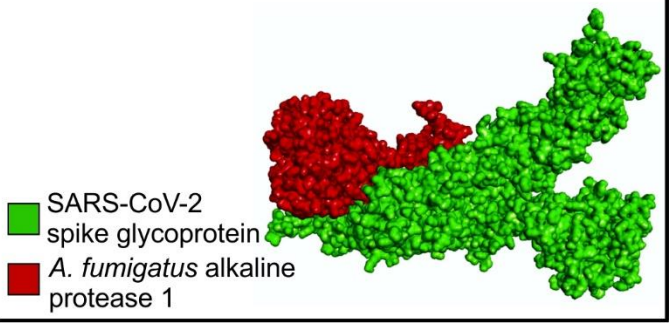

Figure 2. The surface representation of the docked furin protease-SARS-CoV-2 spike protein complex and *A. fumigatus* alkaline protease 1-SARS-CoV-2 spike protein complexes. The Discovery Studio visualiser programme (v21.10.20298) was used for the interactive visualisation and analysis of the molecular structures.

In contrast, *A. fumigatus* alkaline protease 1 interacted with P16, V18, G20, E25, T26, R27, K42, G44, D46, T49, K81, S82, Y83, K84, I85, K86, Q116, W118, L120, D121, L123, H138, K139, Q141, I147, F272, D273, P298, N299, A372, T375, A376, R377, E380, L381, T383, N384, Y399, N402, and A403. In addition, the furin protease-SARS-CoV-2 spike protein complex was linked by 7 hydrogen bonds, while the *A. fumigatus* alkaline protease 1-SARS-CoV-2 spike protein complex had 5 bonds (**Figure 4**).

Proteases	Intermolecular Interactions	Amino acid residues interacting with SARS-CoV-2 spike glycoprotein
Furin protease (5JXH)	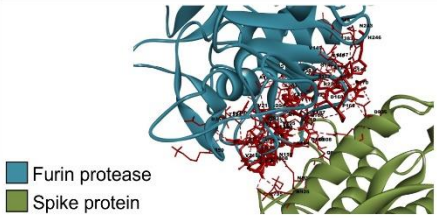	Q111, E112, P113, T143, H145, G146, N159, H160, P161, D162, L163, A164, G165, N166, D168, P169, G170, V205, A206, N207, N208, G209, V210, Y217, N218, R220, H246
A. fumigatus alkaline protease 1 (AFUA_4G11800)	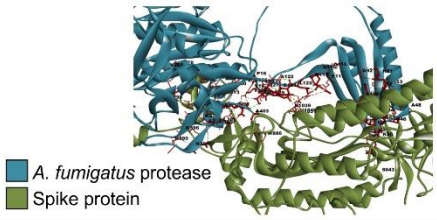	P16, V18, G20, E25, T26, R27, K42, G44, D46, T49, K81, S82, Y83, K84, I85, K86, Q116, W118, L120, D121, L123, H138, K139, Q141, I147, F272, D273, P298, N299, A372, T375, A376, R377, E380, L381, T383, N384, Y399, N402, A403

Figure 3. The intermolecular interactions of the docked furin protease-SARS-CoV-2 spike protein complex and *A. fumigatus* alkaline protease 1-SARS-CoV-2 spike protein showing the amino acid residues of each protease that interacted with the spike protein The Discovery Studio visualiser programme (v21.10.20298) was used for the interactive visualisation and analysis of the molecular structures.

Proteases	Intermolecular Interactions	Number of H-bonds
Furin protease (5JXH)	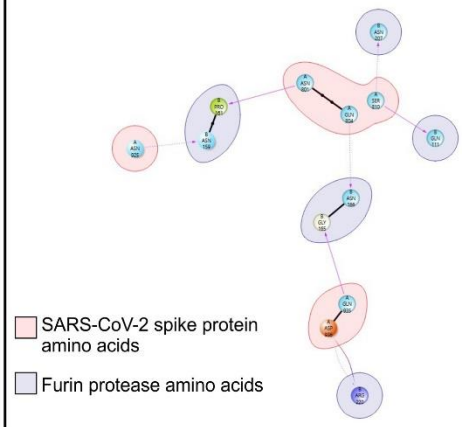	7
A. fumigatus alkaline protease 1 (AFUA_4G11800)	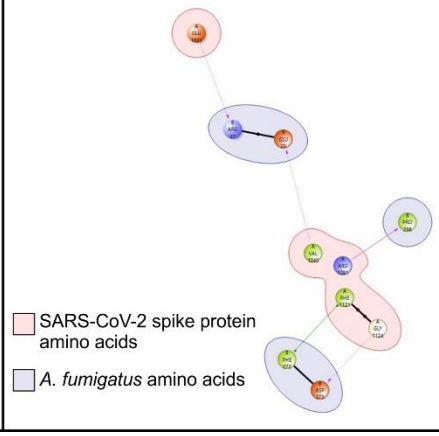	5

Figure 4. The intermolecular interaction of the docked furin protease-SARS-CoV-2 spike protein complex and *A. fumigatus* alkaline protease 1-SARS-CoV-2 spike protein showing the H-bonds for each protease and the SARS-CoV-2 spike protein The Discovery Studio visualiser programme (v21.10.20298) was used for the interactive visualisation and analysis of the molecular structures.

Enzymatic evidence of *A. fumigatus*' supernatant activating the SARS-CoV-2 spike protein

The fluorogenic assay data showing the biochemical efficiency of furin protease or *A. fumigatus* supernatant cleaving a mimetic peptide that contains an amino acid sequence (underlined, SPRRAR↓S) is summarised in **Figure 5**. This unique amino-acid sequence is present at the interface between the S1 and S2 site and serves as a cleavage site for the human furin protease. We determined that the *A. fumigatus* supernatant mediated the proteolytic cleavage of the fluorogenic peptide, however, not in a manner that was comparable to the efficiency of recombinant furin ($p < 0.05$).

A major drawback of using mimetic peptides is that they might not be cleaved in a similar manner as a purified full-length SARS-CoV-2 spike protein - due to differences in conformation; thus, these peptides may not resemble the original folding of the full-length protein as argued by Jaimes and co-workers (2020). Therefore, it was crucial that we validate our findings by using a full-length spike protein present in pseudovirions in a transduction study. To this end, we summarised our infectivity results in **Figure 6**. It was noted that the biochemical efficiency of *A. fumigatus* supernatant to transduce HEK-293T cells with SARS-CoV-2 pseudovirions was more than that of the recombinant furin ($p < 0.05$).

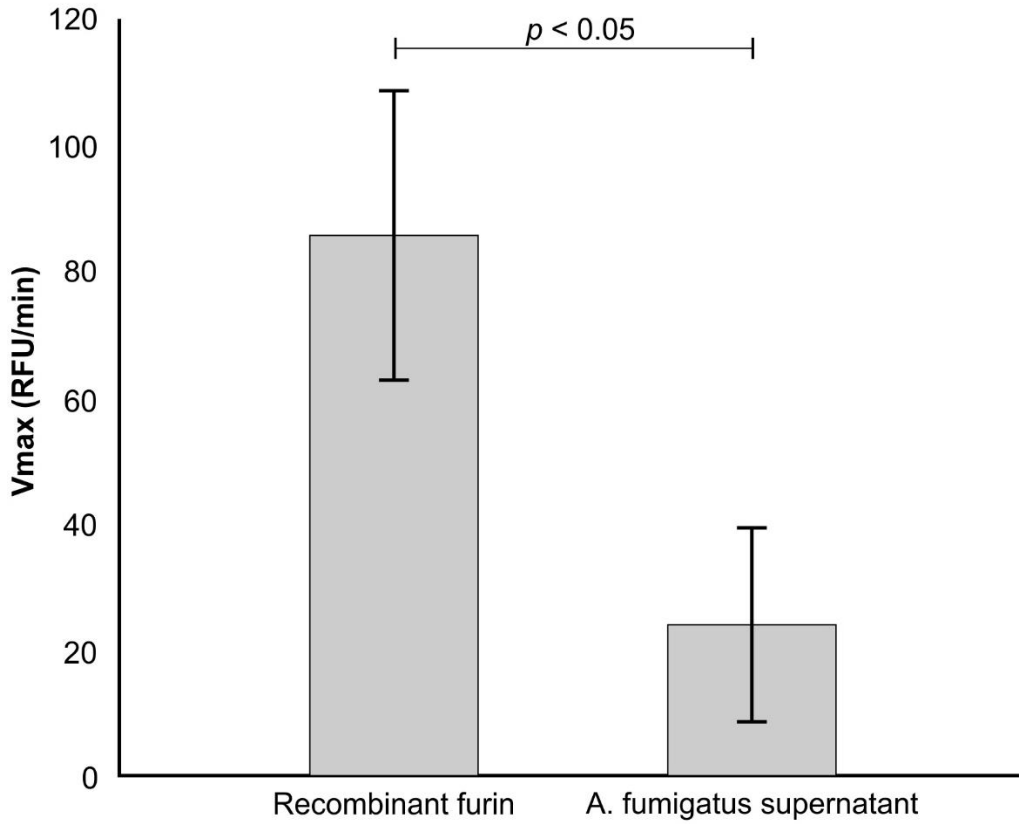

Figure 5. A measure of the proteolytic reaction following the cleavage of a fluorescent peptide viz. viz. TNSPRRARSVA (SARS-CoV-2; S1/S2 site), by the furin protease or *A. fumigatus* supernatant. Vmax = maximum velocity, RFU = Relative Fluorescence Unit

As expected, zero and close to zero relative luminescence units were obtained when the bald pseudovirion was in the presence of either recombinant furin or *A. fumigatus* supernatant. These obtained results confirm that *A. fumigatus* supernatant contains a protease (serine-based) that is able to cleave the fluorogenic peptide and transduce the HEK-293T cells.

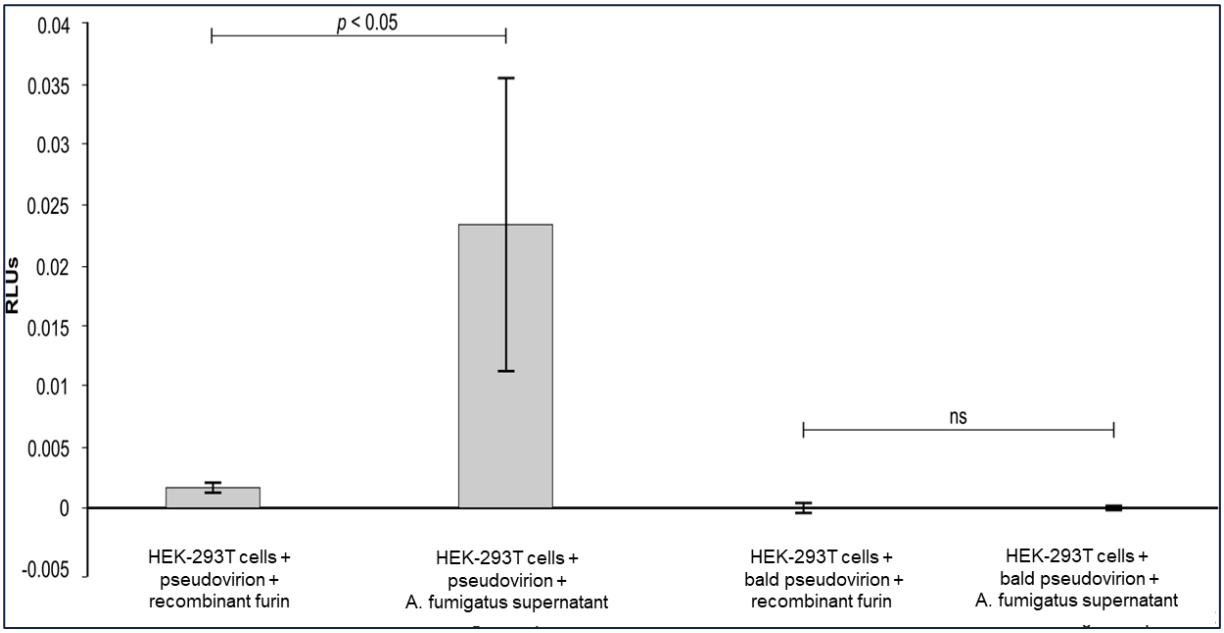

Figure 6. The SARS-CoV-2 spike pseudovirion infectivity in HEK-293T cells in the presence of recombinant furin or *A. fumigatus* supernatant. The cells were infected with pseudovirion or bald pseudovirion, and their luciferase activity was measured. Error bars indicate the standard error measurements of three biological replicates. The SARS-CoV-2 spike pseudovirion contains the luciferase gene and the spike protein. The bald SARS-CoV-2 spike pseudovirion contains the luciferase gene but lacks the spike protein. ns = not significant; RLUs = Relative Luminiscence Units.

CONCLUSION

The presented data show that other fungal pathogens secrete fungal proteases that can also activate the SARS-CoV-2 spike protein. It is envisaged that the co-occurrence of *A.*

fumigatus and SARS-CoV-2 in a patient could see *A. fumigatus* also contributing to the viral invasion.

REFERENCES

1. Aribisala, J. O., Aruwa, C. E., Uthman, T. O., Nurain, I. O., Idowu, K. and Sabiu, S. (2022). Cheminformatics bioprospection of broadspectrum plant secondary metabolites targeting the spike proteins of Omicron variant and Wild-Type SARS-CoV-2. *Metabolites.* 12, 1-26. DOI:10.3390/metabo12100982
2. Dominguez, C., Boelens, R. and Bonvin, A. M. (2003). HADDOCK: a protein− protein docking approach based on biochemical or biophysical information. *J Am Chem Soc.* 125, 1731-1737. DOI:10.1021/ja026939x
3. Druey, K. M., McCullough, M. and Krishnan, R. (2020). *Aspergillus fumigatus* protease alkaline protease 1 (Alp1): a new therapeutic target for fungal asthma. *J Fungi.* 6, 1-9. DOI:10.3390/jof6020088
4. Izidoro, M. A., Gouvea, I. E., Santos, J. A., Assis, D. M., Oliveira, V., Judice, W. A., Juliano, M. A., Lindberg, I. and Juliano, L. (2009). A study of human furin specificity using synthetic peptides derived from natural substrates, and effects of potassium ions. *Arch Biochem Biophys*. 487, 105-114. DOI: 10.1016/j.abb.2009.05.013
5. Jaimes, J. A., Millet, J. K. and Whittaker, G. R. (2020). Proteolytic cleavage of the SARS-CoV-2 spike protein and the role of the novel S1/S2 site. *IScience,* 23, 1-5. DOI: 10.1016/j.isci.2020.101212
6. Mjokane, N., Maliehe, M., Folorunso, O. S., Ogundeji, A. O., Gcilitshana, O. M., Albertyn, J., Pohl, C. H. and Sebolai, O. M. (2022). Cryptococcal protease (s) and the activation of SARS-CoV-2 spike (S) protein. *Cells.* 11, 1-8. DOI:10.3390/cells11030437

7. Villoutreix, B. O., Badiola, I. and Khatib, A. M. (2022). Furin and COVID-19: Structure, function and chemoinformatic analysis of representative active site inhibitors. *Front Drug Discov*. 74, 425-430. DOI:10.3389/fddsv.2022.899239

ADDENDUM NO. 2:

THE USE OF THE SOUTH AFRICAN-BASED MEDICINAL PLANT, *ARTEMISIA AFRA*, IN LIMITING THE ACTIVATION OF THE MIMETIC SARS-COV-2 SPIKE PROTEIN

This addendum is intended to show that the tea extract of the *Artemisia* plant contains bioactive molecules that inhibit the proteolytic cleavage of the SARS-CoV-2 spike protein

Mjokane's contribution: Developed the methodology, carried out the experiments, wrote the manuscript.

INTRODUCTION

Since time immemorial, man has always looked to nature for answers. Through the harnessing of indigenous knowledge, it was possible to fashion medicines from plants believed to be imbued with curative properties (Bagwana, 2015; Eshete and Molla, 2021; Mwaka et al., 2023). In South Africa, these medicines are referred to as umuthi, meaning 'tree' (Du Toit, 1998; Grace et al., 2003; Byrne et al., 2017).

The landmark drug artemisinin is fashioned from the plant *Artemisia* annua (Krishna et al., 2008; Weathers et al., 2011; Elfawal et al., 2012). Ancient Chinese texts show that Chinese folk used to extract this compound using low temperature water. Importantly, the seminal work of Tu Youyou that earned her the 2015 Novel Prize in Physiology or Medicine, demonstrated that artemisinin could be purposed to cure malaria (Su and Miller, 2015). While the World Health Organization (WHO) has not advocated for the use of the *Artemisia*, traditional health practitioners (THPs) have continuously prescribed its plant material for its anti-pneumonia properties (Fuzimoto, 2021). This has extended to control viral infections. For example, in countries like Kenya and Uganda, *Artemisia* tea is used to treat viral infections such as HIV/AIDS (Lubbe et al., 2012; Salehi et al., 2018). And recently, the advent of COVID-19 saw THPs prescribing the *Artemisia* plant material also to control the deadly SARS-CoV-2 (Kapepula et al., 2020; WHO, 2020). The president of Madagascar also authorised the use of *Artemisia* extracts and COVID-19 patients were encouraged to drink the so-called “COVID-Organics” (Nie, 2021). The

COVID-Organics were exported to other many African countries with the hope of preventing and treating COVID-19 infections (Nie, 2021).

While the WHO discourages the overuse of the *Artemisia* plant material, as it may lead to artemisinin resistance, there is value in establishing if it can control SARS-CoV-2. And in particular, if it can prevent proteolytic cleavage of the SARS-CoV-2 spike protein.

MATERIALS AND METHODS

Extraction of *Artemisia* tea

The artemisinin was extracted as part of the plant material using the extraction protocol of Nie et al. (2021), with minor modifications. Briefly, 10 mL of distilled water was heated to 90 °C in a 100 mL Erlenmeyer flask. A gram of store-bought *Artemisia afra* herbal tea was weighed and infused into the hot distilled water. The tea infusion was maintained for 2 min at 90 °C before allowing it to cool down for 20 min at ambient room temperature (25°C). Following this, the tea infusion was filtered with the use of a filter paper and washed with (20×2 mL) of fresh distilled water. Next, the solvent (i.e. water) was then eliminated by rotary evaporation, and the dried tea extract (solid material) was stored at −20 °C before sample preparation.

Sample preparation

From the dried tea extract, ~135 mg was weighed and allowed to thaw at room temperature. Thereafter, 3 mL of DMSO was added to the dried tea extract, and the solution was heated at 40 °C for solvation. Using filter paper, the solution was filtered into a 1.5 mL centrifuge tube and stored at -20°C. The final concentration estimation was 45 mg/mL.

Proteolytic cleavage of the mimetic SARS-CoV-2 spike protein in the presence of *Artemisia afra* tea infusion extract and artemisinin

The fluorogenic assay based on the protocol of detailed in Jaimes et al. (2019, 2020), with modifications. For this assay, a synthetic peptide was especially prepared by Biomatik (Ontario, Canada) and was modified to have fluorescence intramolecular quenching capability. Importantly, the peptide contained the amino acid sequence (underlined, SP**R**RA**R**↓S) that is highly susceptible to furin hydrolysis (**Figure 3.1**).

A reaction mixture for the synthesised fluorogenic mimetic peptide was carried out in a 100 µL buffer solution (pH 7.5) composed of (1) 100 mM Hepes, (2) 0.5% Triton X-100, (3) 1 mM $CaCl_2$, and (4) 1 mM 2-mercaptoethanol. Furin was diluted to 10 U/mL, and 0.5 µL was added to the reaction mixture. In a separate experiment, 0.5 µL of the cryptococcal supernatant was added. These reaction conditions were reported to activate the hydrolysis of most substrates by furin (Izodoro et al., 2009). The protease inhibitors that

were used were the *Artemisia afra* tea infusion, artemisinin (Glentham Life Sciences, United Kingdom), artesunate (a derivative of artemisinin; Glentham Life Sciences, United Kingdom) and the traditional furin inhibitor, decanoyl-RVKR-CMK (Merck, United States). *Artemisia afra* tea extract was tested at 10 mg/mL, artemisinin at 10 mg/mL, artesunate at 10 mg/mL, and decanoyl-RVKR-CMK at 1 mg/mL.

In the end, reactions were performed at 30 °C, and a fluorometer measured fluorescence emission every minute for 45 min. Fluorescence intensity was tracked over this time interval using the wavelength settings, i.e., excitation (λ355 nm) and emission (λ405 nm). Three independent experiments were carried out, and the means Vmax was calculated. Media not inoculated with cryptococcal cells was included as negative control. In the end, the background signal of this negative control was used for normalisation.

RESULTS

The results of cryptococcal supernatant proteolysis cleavage of the SARS CoV-2 mimetic peptide are summarised in **Figure 1**. The data further confirms that the supernatant possesses proteolytic activity; however, all the inhibitors ($p > 0.05$) except for artesunate ($p < 0.05$) could not disrupt or inhibit proteolysis cleavage of the mimetic SARS-CoV-2 spike protein. It is possible that as the supernatant may contain other ingredients, they may have interfered. Therefore, it is ideal to first isolate the cryptococcal yeast kexin protease(s) and repeat this study before concrete conclusions can be made.

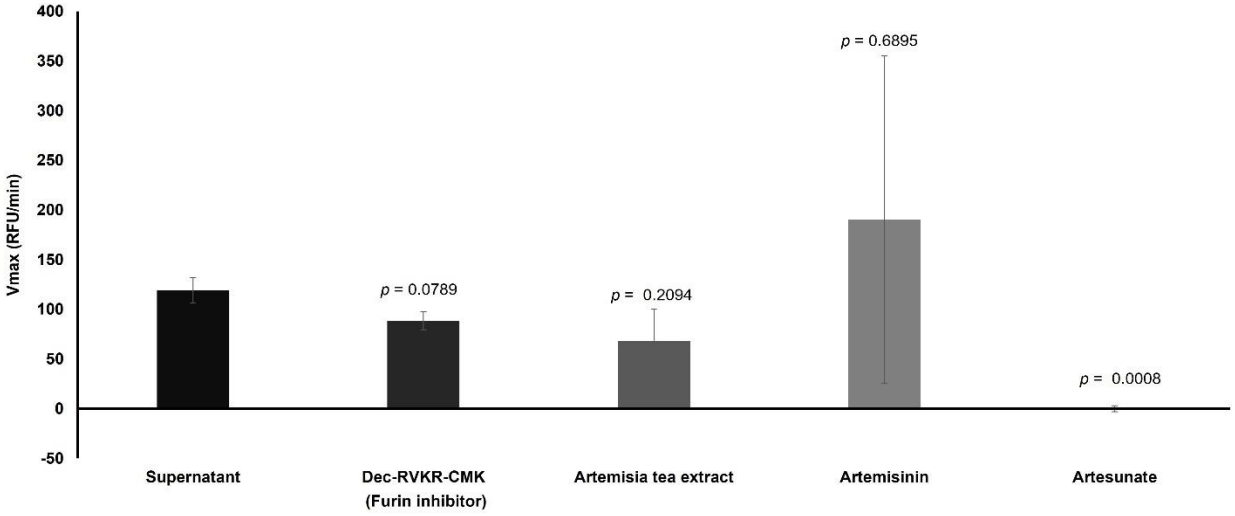

Figure 1. Inhibition of supernatant SARS-CoV-2 spike protein activation by *Artemisia* plant extract.

Concerning the disruption/inhibition of the furin proteolysis activity, success was achieved (**Figure 2**). Here, it was noted that compared to non-treated condition, i.e. proteolysis in the absence of inhibitors, all the conditions with protease inhibitors resulted in the inhibition of furin proteolysis. In fact, there was no difference in the potency of *Artemisia* tea extract, artemisinin and artesunate when compared to decanoyl-RVKR-CMK, the traditional inhibitor of furin.

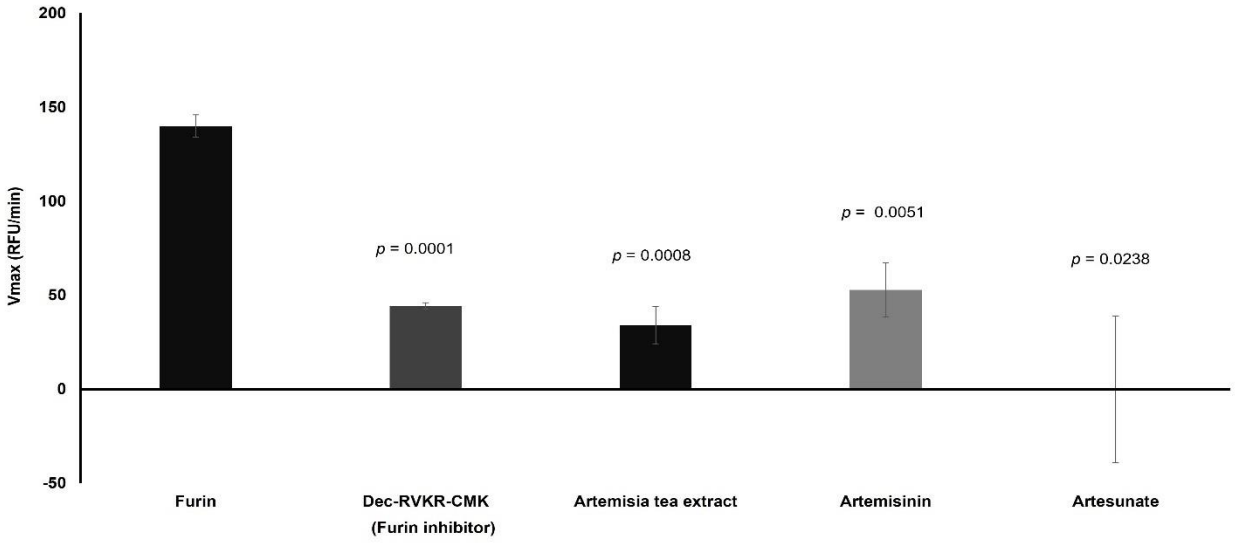

Figure 2. Inhibition of furin SARS-CoV-2 spike protein activation by *Artemisia* plant extract.

CONCLUSION

The presented data show there is value in exploring the anti-COVID-19 properties of *Artemisia afra* and its active compound. This preliminary data set up a motivation for pilot a study assessing if *Artemisia afra* extract and its active compound, artemisinin, can control unwanted proteolysis during a systemic co-infection in a mammalian host.

REFERENCES

1. Bagwana, P. (2015). Indigenous knowledge of traditional medicine: answering the question of knowledge acquisition and transmission among the traditional health practitioners in Uganda. *Antropoloji.* 30, 13-32. DOI:10.1501/antro_0000000318
2. Byrne, M. J., Williams, V. L. and Wojtasik, E. M. (2017). The viability of propagules of alien plant species sold for traditional medicine in South Africa. *S Afr J Bot.* 109, 281-287. DOI: 10.1016/j.sajb.2017.01.206
3. Du Toit, B. M. (1998). Modern folk medicine in South Africa. *S Afr J Ethnol*. 21, 145-152. DOI:10.10520/AJA02580144_15
4. Elfawal, M. A., Towler, M. J., Reich, N. G., Golenbock, D., Weathers, P. J. and Rich, S. M. (2012). Dried whole plant *Artemisia annua* as an antimalarial therapy. *PloS One*. 7, e52746. DOI: 10.1371/journal.pone.0052746
5. Eshete, M. A. and Molla, E. L. (2021). Cultural significance of medicinal plants in healing human ailments among Guji semi-pastoralist people, Suro Barguda District. *Ethiopia. J Ethnobiol Ethnomed.*17(1), 1-18. DOI:10.1186/s13002-021-00487-4
6. Fuzimoto, A. D. (2021). An overview of the anti-SARS-CoV-2 properties of *Artemisia annua,* its antiviral action, protein-associated mechanisms, and repurposing for COVID-19 treatment. *J Integr Med*.19, 375-388. DOI: 10.1016/j.joim.2021.07.003

7. Grace, O. M., Prendergast, H. D. V., Jäger, A. K., Van Staden, J. and Van Wyk, A. E. (2003). Bark medicines used in traditional healthcare in KwaZulu-Natal, South Africa: An inventory. *S Afr J Bot*. 69, 301-363. DOI:10.1016/S0254-6299(15)30318-5

8. Kapepula, P. M., Kabengele, J. K., Kingombe, M., Van Bambeke, F., Tulkens, P. M., Kishabongo, A. S. and Nachega, J. B. (2020). *Artemisia Spp.* derivatives for COVID-19 treatment: anecdotal use, political hype, treatment potential, challenges, and road map to randomized clinical trials. *Am J Trop Med Hyg.*103, 960. DOI:10.4269/ajtmh.20-0820

9. Krishna, S., Bustamante, L., Haynes, R. K. and Staines, H. M. (2008). Artemisinins: their growing importance in medicine. *Trends Pharmacol Sci.* 29, 520-527. DOI: 10.1016/2Fj.tips.2008.07.004

10. Lubbe, A., Seibert, I., Klimkait, T. and Van der Kooy, F. (2012). Ethnopharmacology in overdrive: the remarkable anti-HIV activity of *Artemisia annua. J Ethnopharmacol*. 141, 854-859. DOI: 10.1016/j.jep.2012.03.024

11. Mwaka, A. D., Achan, J. and Orach, C. G. (2023). Traditional health practices: A qualitative inquiry among traditional health practitioners in northern Uganda on becoming a healer, perceived causes of illnesses, and diagnostic approaches. *Plos One*. 18, e0282491. DOI: 10.1371/2Fjournal.pone.0282491

12. Nie, C., Trimpert, J., Moon, S., Haag, R., Gilmore, K., Kaufer, B. B. and Seeberger, P. H. (2021). *In vitro* efficacy of *Artemisia* extracts against SARS-CoV-2. *Virol J.* 18, 1-7. DOI:10.1186/s12985-021-01651-8

13. Salehi, B., Kumar, N. V. A., Şener, B., Sharifi-Rad, M., Kılıç, M., Mahady, G. B. and Sharifi-Rad, J. (2018). Medicinal plants used in the treatment of human immunodeficiency virus. *Int. J. Mol. Sci*. 19, 1459. DOI:10.3390/ijms19051459

14. Su, X. Z. and Miller, L. H. (2015). The discovery of artemisinin and the Nobel Prize in Physiology or Medicine. *Sci China Life Sci.* 58, 1175–1179. DOI:10.1007/2Fs11427-015-4948-7

15. Weathers, P. J., Arsenault, P. R., Covello, P. S., McMickle, A., Teoh, K. H. and Reed, D. W. (2011). Artemisinin production in *Artemisia annua*: studies in planta and results of a novel delivery method for treating malaria and other neglected diseases. *Phytochem Rev.* 10, 173-183. DOI:10.1007/2Fs11101-010-9166-0

16. World Health Organisation. WHO supports scientifically proven traditional medicine (2020). https://www.afro.who.int/news/who-supports-scientifically-proven-traditional-medicine